SPECTRAL AND TEMPORAL WEIGHTING OF SOUND LOCALIZATION: EFFECTS OF COMPETING NOISE AND HEARING IMPAIRMENT

By

Monica Lenore Folkerts

Dissertation

Submitted to the Faculty of the

Graduate School of Vanderbilt University

in partial fulfillment of the requirements

for the degree of

DOCTOR OF PHILOSOPHY

in Hearing and Speech Sciences

June 30, 2022

Nashville, Tennessee

Erin M. Picou, Au.D., Ph.D.

Marc Brennan, Ph.D.

René H. Gifford, Ph.D.

Todd A. Ricketts, Ph.D.

G. Christopher Stecker, Ph.D.

To my other half, Jacob Schwartz,
and to my family

ACKNOWLEDGMENTS

I want to thank my advisors, Dr. Chris Stecker and Dr. Erin Picou. Chris, you expanded my knowledge of spatial hearing, gave me the freedom to trust my scientific ideas, and provided an exciting environment to accomplish this work. Erin, you expanded my knowledge of hearing impairment, helped me become a more confident scientific communicator, and helped me through the most challenging moments during this process. I want also to thank my committee members who pushed me academically early on and helped make this work relevant to the clinical population. I would also like to thank Catherine Xu for recruiting participants and data collection assistance. I would also like to thank our funding: Grant No. R01 DC011548 (to G.C.S.) from the National Institute on Deafness and Other Communication Disorders (NIDCD) and additional support from the Vanderbilt University Medical Center and the Department of Hearing and Speech Sciences.

TABLE OF CONTENTS

DEDICATION iii
ACKNOWLEDGMENTS iv

1. Introduction: Observer Weighting of Sound Localization Cues 1
1.1. Binaural Cues 2
1.2. Binaural Cues Across Frequency 3
1.3. Binaural Cues Across Time 6
1.4. Experimental Chapters 7
REFERENCES 9

2. Spectral Weighting Functions for Localization of Complex Sound: Effects of Competing Noise 12
2.1. Introduction 12
2.2. Methods 15
2.2.1. Participants 16
2.2.2. Stimuli 16
2.2.3. Procedure 17
2.2.4. Analysis 19
2.3. Results and Discussion 21
2.3.1. Spectral Weighting Functions 21
2.3.2. Localization Performance in Competing Noise 25
2.3.3. Relating Spectral Weighting to Interaural Sensitivity in Competing Noise 31
2.3.4. Relating Spectral Weighting to Interaural Cue Availability in Competing Noise 33
2.3.5. Limitations 39
2.4. Summary and Conclusions 40
REFERENCES 42

3. Temporal Weighting Functions for Localization: Effects of Competing Noise 47
3.1. Introduction 47
3.2. Methods 51
3.2.1. Participants 51
3.2.2. Stimuli 51
3.2.3. Procedure 52
3.2.4. Analysis 53
3.3. Results and Discussion 55
3.3.1. Temporal Weighting Functions 55
3.3.2. Localization Performance in Competing Noise 60
3.3.3. Suggestions for the Reduction of Onset Dominance in Competing Noise 63
3.4. Summary and Conclusions 65
REFERENCES 67

4. Spectral Weighting Functions for Localization of Complex Sound: Effects of Hearing Impairment **70**

4.1. Introduction 70

4.2. Methods 73
4.2.1. Participants 74
4.2.2. Target Stimuli 75
4.2.3. Masking Noise for Hearing Loss Simulation 76
4.2.4. Procedure 77
4.2.5. Analysis 80

4.3. Results and Discussion 83
4.3.1. Free-field Detection Thresholds 83
4.3.2. Spectral Weighting Functions 86
4.3.3. Localization Performance 96
4.3.4. Measured Interaural Cues 99
4.3.5. The Effect of Free-field Threshold and Age 102

4.4. Summary and Conclusions 106
REFERENCES 108

5. Temporal weighting functions for localization of complex sound: Effects of Hearing Impairment **115**

5.1. Introduction 115

5.2. Methods 118
5.2.1. Participants 118
5.2.2. Target Stimuli 119
5.2.3. Procedure 120
5.2.4. Analysis 121

5.3. Results and Discussion 123
5.3.1. Temporal Weighting Functions 123
5.3.2. Localization Performance 131
5.3.3. The Effect of Free-field Threshold and Age 136

5.4. Summary and Conclusions 139
REFERENCES 141

6. Concluding Remarks **148**

6.1. Chapter 2: Spectral Weighting in Competing Noise 148

6.2. Chapter 3: Temporal Weighting in Competing Noise 150

6.3. Chapter 4: Spectral Weighting for Simulated and Real SNHL 151

6.4. Chapter 5: Temporal Weighting for Simulated and Real SNHL 154

6.5. Conclusion 155
REFERENCES 157

LIST OF FIGURES

FIG. 1.1. Mean SWFs for five stimulus conditions in quiet. 5
FIG. 2.1. Schematic used to record localization responses (180° arc). 18
FIG. 2.2. Mean SWFs obtained in various levels of competing noise. 22
FIG. 2.3. Individual-participant SWFs found in various levels of competing noise. 23
FIG. 2.4. Violin plots of AR_{800} values found in various levels of competing noise. 24
FIG. 2.5. Localization response values as a function of base loudspeaker for participant 2103. 27
FIG. 2.6. Localization response values as a function of base loudspeaker for participant 2109. 28
FIG. 2.7. Mean RMS error and mean R^2 value found in various levels of competing noise. 29
FIG. 2.8. Diagram of binaural cue analysis. 34
FIG. 2.9. Average ITD, IAC, and ITD cues found in quiet and various levels of noise. 36
FIG. 3.1. Mean TWFs obtained in quiet various levels of competing noise. 57
FIG. 3.2. Violin plots of AR_{onset} values found in various levels of competing noise. 58
FIG. 3.3. Individual-participant TWFs found quiet and in various levels of competing noise. 60
FIG. 3.4. Mean RMS error and mean R^2 value found in various levels of competing noise. 61
FIG. 3.5. Localization response values as a function of base loudspeaker for participant 2108. 63
FIG. 4.1. Schematic used to record localization responses (360° arc). 79
FIG. 4.2. Localization response values as a function of base loudspeaker for participant 2207. 80
FIG. 4.3. Individual-participant free-field hearing thresholds. 84
FIG. 4.4. Mean SWFs obtained in quiet (NH and SNHL) and threshold elevating noise (NH). 87
FIG. 4.5. Individual-participant SWFs found in quiet and threshold elevating noise. 91
FIG. 4.6. Individual-participant (SNHL) SWFs and free-feild thresholds. 93
FIG. 4.7. Violin plots of AR_{800} values found in quiet and threshold elevating noise. 96
FIG. 4.8. Mean RMS error and mean R^2 value found in quiet and threshold elevating noise. 97
FIG. 4.9. Average ITD, IAC, and ITD cues found in quiet and threshold elevating noise. 101
FIG. 4.10. 800-Hz weight plotted as a function free-field threshold and age (SNHL). 103
FIG. 5.1. Mean TWFs obtained in quiet (NH and SNHL) and threshold elevating noise (NH). 124
FIG. 5.2. Individual-participant TWFs found in quiet and threshold elevating noise. 127
FIG. 5.3. Individual-participant (SNHL) SWFs and free-feild thresholds. 128
FIG. 5.4. Violin plots of AR_{onset} values found in quiet and threshold elevating noise. 130
FIG. 5.5. Mean RMS error and mean R2 value found in quiet and threshold elevating noise. 132
FIG. 5.6. Localization response values as a function of base loudspeaker for participant 2107. 133
FIG. 5.7. Localization response values as a function of base loudspeaker for participant 2216. 135
FIG. 5.8. AR_{onset} plotted as a function free-field threshold and age (SNHL). 137

CHAPTER 1

Introduction: Observer Weighting of Sound Localization Cues

Sound localization is the ability to determine the direction of a sound source, such as a bird chirping in a tree or a loudspeaker in an experimental environment. For localization in the horizontal plane (azimuth), the auditory system relies primarily on binaural cues which arise from interaural differences between the sound arriving at each ear. Binaural cues vary in availability and reliability across frequency and time, and their utility changes across the spectrotemporal components of the signal. Observer weighting methods have been used to determine the relative influence or weight of spectral or temporal components of a stimulus during sound localization and lateralization (where binaural cues are presented over headphones). These utility patterns or weighting functions reveal a relative dominance of some components over others. In other words, only a portion of those components are relied upon during localization across the spectrotemporal components of a complex signal.

Understanding the salient components across frequency and time can provide the scientific and clinical field with a better understanding of localization strategies used in noise-filled listening environments and when the auditory system is impaired. Although these weighting patterns have been established for listeners with normal hearing (NH) in the free field (quiet) or in (simulated) reverberation, they have not been measured in the presence of competing noise or for listeners with sensorineural hearing loss (SNHL). Both interfering noise and SNHL can change the availability, reliability, and sensitivity of binaural cues. In four separate experiments, I measured weighting patterns across frequency and time for listeners with

NH in the presence of competing noise, for listeners with NH with a simulated hearing loss, and for listeners with SNHL in quiet.

In the remainder of this chapter, I review the binaural cues available for sound localization across frequency and time, specifically focusing on the salient components across each dimension. Then, the following four chapters (Chapters 2-5) formally describe the experiments. Each chapter includes a brief introduction section, some of which is repeated in this chapter. Finally, Chapter 6 summarizes the primary findings of the experiments and describes future work that will be required to understand observer weighting during auditory localization fully.

1.1. Binaural Cues

When a sound is presented from an angle azimuth (other than 0° or 180°), the resultant waveform reaches each ear with slight differences, providing the listener with binaural cues. The waveform takes less time to arrive at the ipsilateral ear (closest to the signal) than the contralateral ear (further from the signal). The difference in microseconds (μs) is measured as the time the sound takes to reach the contralateral ear after it has reached the ipsilateral ear. This binaural cue is the interaural time difference (ITD). The interaural phase difference (IPD) cue is directly related to the ITD cue. The IPD cue arises from the difference in the instantaneous phase of the stimuli between the two ears. The IPD in degrees could be calculated using the formula: *360 x frequency x ITD (in seconds)* for pure tone stimuli. There are two types of ITD cues: the interaural time difference in the fine structure of the signal (ITD_{fs}) and the interaural time difference carried by the envelope of the signal (ITD_{env}). The head also attenuates the waveform, creating an "acoustic shadow" that leads to a reduced sound level pressure at the ear contralateral from the sound source. The difference in decibels (dB) is measured as the sound level at the

contralateral ear subtracted from the sound level at the ipsilateral ear. This binaural cue is the interaural level difference cue (ILD). The ITD and ILD cue values increase systematically with increasing azimuth (away from 0°) up to 90° on the left and right. From 90° to 180° on the left and right, the cue values systematically decrease.

1.2. Binaural Cues Across Frequency

The availability of ITD and ILD cues is dependent on the stimulus frequency. The ITD_{fs} or the IPD cue is limited to frequencies below about 1500 Hz (e.g., Klumpp and Eady, 1956, Yost and Dye, 1988). This is due to the relationship of the ITD cue with the IPD cue. When a signal has an ITD larger than the frequency cycle, the ITD cue becomes ambiguous. The frequency limit of the ITD_{env} cue is dependent on the shape of the envelope, and as the frequency of the envelope decreases, the cue becomes ambiguous (Schubert and Wernick, 1969; Blauert, 1997). The availability of the ILD cue is limited to higher frequencies (Feddersen et al., 1957; Wightman and Kistler, 1989; Brungart and Rabinowitz, 1999). This limitation is due to high-frequency waveforms being attenuated more than low-frequency waveforms, which can wrap around the head.

The "Duplex Theory" of Lord Rayleigh (Strutt, 1907) posits that the ITD_{fs} cue is utilized during the localization of low-frequency stimuli while the ILD cue is utilized during the localization of high-frequency stimuli. Also, when listeners are presented with all available binaural cues across broadband stimuli, they rely primarily on the low-frequency ITD_{fs} cue (Wightman and Kistler, 1992; Macpherson and Middlebrooks, 2002). To determine this, Wightman and Kistler (1992) measured the binaural cues available to each listener and presented them back to the listener in opposition, i.e., a leftward ITD and a rightward ILD. Wightman and

Kistler (1992) found that localization of broadband stimuli was in the direction of the imposed ITD_{fs} cue while localization of high-pass stimuli followed the ILD cue, but not ITD_{env} cues. Macpherson and Middlebrooks (2002) measured the binaural cues available to each listener; however, only one binaural cue was manipulated at a time during the presentation, while the other remained "natural." The response location (i.e., how much the response changed) as a function of the amount of cue manipulation (away from the natural stimulus) was used to derive a perceptual weight employing linear regression. The weight described the manipulated cue's influence on the response location; 0 being no influence and 1 being a total influence. The ITD_{fs} cue received greater perceptual weight than the ILD cue when listeners localized broadband and low-pass stimuli. The ILD cue received a larger perceptual weight than the ITD_{env} when listeners localized high-pass stimuli.

Observing weighting methods have been used to determine the perceptual weighting of frequency components during sound localization (Folkerts and Stecker, 2022) and lateralization (Ahrens et al., 2020; Baltzell et al., 2020; Folkerts and Stecker, 2022). Similar to Macpherson and Middlebrooks (2002), the goal is to determine the perceptual influence of each component on the overall lateralization or localization response. However, instead of one binaural cue serving as the manipulated component, multiple frequency components with small differences in binaural cue value or degree azimuth serve as the independent variables. Dependent variables are then the overall perceived lateralization or localization. Regression methods (Ahumada and Lovell, 1971) are used to determine the influence of each independent variable (e.g., the frequency components' location in degrees azimuth) on the dependent variable (the response in degrees azimuth). The influence of each component across frequency is the normalized weight (summing to 1) which, when plotted together, constitute the spectral weighting functions (SWF),

which are displayed for various stimulus conditions (legend) in Figure. 1.1 for localization in quiet (i.e., the free field; data from Folkerts and Stecker, 2022).

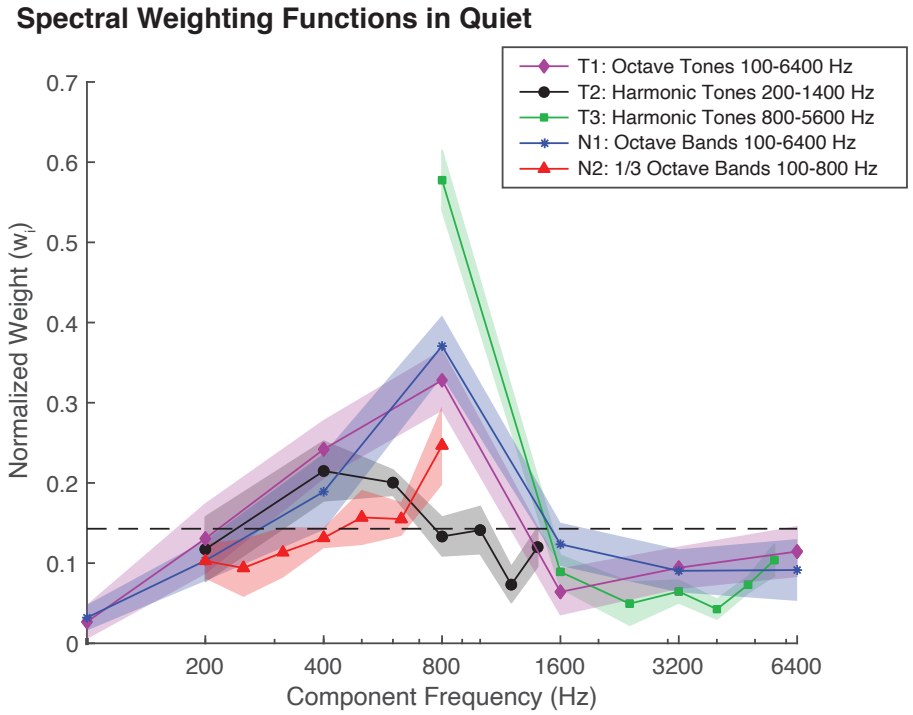

FIG. 1.1. Across-listener SWFs for five stimulus conditions in quiet: T1 (magenta diamonds); T2 (black circles), T3 (green squares), N1 (blue asterisks), and N2 (red triangles). Symbols and thick lines plot cross-participant (n = 10) mean normalized weight as a function of component frequency. Shaded regions indicate bootstrapped ±95% confidence intervals on each mean weight. Dashed lines indicate the expected value (1/7) for uniform weighting across components. Data derived from Folkerts and Stecker (2022).

The SWFs for localization in quiet measured by Folkerts and Stecker (2022; Fig. 1.1) display the maximum weight placed on the 800-Hz component except for stimulus condition T2,

harmonic tones from 200-1400 Hz. This upweighting of the 800 Hz is referred to as the peak of the ITD dominance region. However, the overall range of the ITD dominance region may encompass frequencies above and below that exact frequency. Participants weigh components within this range equally (i.e., frequency components from 400 to 1000 Hz for stimulus condition T2). Overall, the SWFs confirm that listeners with NH rely primarily on a specific range of low-frequency ITD cues encompassing the ITD dominance region (Ahrens et al., 2020; Baltzell et al., 2020; Folkerts and Stecker, 2022).

1.3. Binaural Cues Across Time

Across time, listeners tend to utilize the binaural cues available at the onset portion of the stimulus. For example, listeners localize the stimulus towards the first click when two clicks are presented in succession. This perceptual effect has been termed the law of the first wavefront, the Haas effect, or the precedence effect, which is most commonly used now (Gardner, 1968; Zurek, 1987; Litovsky et al., 1999; Brown et al., 2015). Both localization (or lateralization) towards the first stimulus and the fusion of the two stimuli as one perceptual image is dependent on the time interval between the two stimuli.

When a sound is presented in a room with reflective surfaces, the first arriving echo, early reflections, and reverberation combine with the signal milliseconds after the sound onset. These reflections distort the original stimulus, including a reduction of the binaural cues available (Rakerd and Hartmann, 1985; Shinn-Cunningham et al., 2005), which tend to reduce towards values of 0 (dB and ms). However, the onset is free of such distortions as only the direct sound reaches the two ears. The precedence effect, a form of onset dominance, is thought to be taken advantage of by listeners due to their experience in reverberant environments.

Studies of binaural adaptation similarly reveal that listeners take advantage of the onset portion of the stimulus. Integration of binaural information across time was expected to increase binaural sensitivity with the increase of the stimulus duration (Houtgast and Plomp, 1968). Hafter and Dye (1983) measured ITD_{env} thresholds for click trains presented with various inter-click-intervals (ICIs). As the ICI became shorter than 5 ms, the integration of binaural information was reduced across time. They concluded that high-rate, short ICI stimuli were lateralized based on the ITD_{env} cue at the onset of the stimulus. Hafter and colleagues (1983) found similar results for the ILD cue, while Bibee and Stecker (2016) found similar results for the ITD_{fs} cue.

Like SWFs, temporal weighting functions (TWFs) are measured using observer weighting methods. The response location serves as the dependent variable. Components of the stimulus over time [such as clicks in a click train (Stecker and Hafter, 2002)] are presented with small differences in binaural cue value or degrees azimuth. The locations of clicks or components serve as the independent variables. TWFs measured in quiet (i.e., the free field) by Stecker and Hafter (2002) reveal large relative weights compared to remaining clicks for ICIs less than or equal to 5 ms, similar to the rate limitation found in studies of binaural adaption. Onset dominance is prevalent when the stimulus is presented over headphones as an ITD_{fs} cue (Diedesch and Stecker, 2015), an ITD_{env} cue (e.g., Saberi 1996; Brown and Stecker, 2010; Stecker et al., 2013), or an ILD cue (e.g., Brown and Stecker, 2010; Stecker et al., 2013), with the same rate limitation found in the free field.

1.4. Experimental Chapters

Observer weighting methods were used to measure SWFs and TWFs as described here. The first two Chapters report SWFs (Chapter 2) and TWFs (Chapter 3) in the presence of competing noise for participants with NH. The hypotheses were that SWFs would reveal a shift in the peak of the ITD dominance region toward higher frequencies, while TWFs would reveal a reduction in onset dominance. The last two experimental Chapters report SWFs (Chapter 4) and TWFs (Chapter 5) for participants with SNHL and in presence of a threshold elevating noise masker (simulating SNHL) for participants with NH. The hypotheses were that SWFs would reveal a shift in the ITD dominance region toward lower frequencies while TWFs would reveal a reduction in onset dominance for participants with real and simulated SNHL. The final chapter, Chapter 6, finishes with concluding remarks about the experimental chapters and highlights future directions for the field.

REFERENCES

Ahrens, A., Joshi, S. N., and Epp, B. (**2020**). "Perceptual Weighting of Binaural Lateralization Cues across Frequency Bands," J. Asso. Res. Otolryn., **21**, 485–496. doi:10.1007/s10162-020-00770-3

Ahumada, A., and Lovell, J. (**1971**). "Stimulus Features in Signal Detection," J. Acoust. Soc. Am., **49**, 1751–1756. doi:10.1121/1.1912577

Baltzell, L. S., Cho, A. Y., Swaminathan, J., and Best, V. (**2020**). "Spectro-temporal weighting of interaural time differences in speech," J. Acoust. Soc. Am., **147**, 3883–3894. doi:10.1121/10.0001418

Bibee, J. M., and Stecker, G. C. (**2016**). "Spectrotemporal weighting of binaural cues: Effects of a diotic interferer on discrimination of dynamic interaural differences," J. Acoust. Soc. Am., **140**, 2584–2592. doi:10.1121/1.4964708

Blauert, J. (**1997**). *Spatial Hearing: The Psychophysics of Human Sound Localization*, MIT Press, 514 pages.

Brown, A. D., and Stecker, G. C. (**2010**). "Temporal weighting of interaural time and level differences in high-rate click trains," J. Acoust. Soc. Am., **128**, 332–341. doi:10.1121/1.3436540

Brungart, D. S., and Rabinowitz, W. M. (**1999**). "Auditory localization of nearby sources. Head-related transfer functions," J. Acoust. Soc. Am., **106**, 1465–1479. doi:10.1121/1.427180

Diedesch, A. C., and Stecker, G. C. (**2015**). "Temporal weighting of binaural information at low frequencies: Discrimination of dynamic interaural time and level differences," J. Acoust. Soc. Am., **138**, 125–133. doi:10.1121/1.4922327

Feddersen, W. E., Sandel, T. T., Teas, D. C., and Jeffress, L. A. (**1957**). "Localization of High-Frequency Tones," J. Acoust. Soc. Am., **29**, 988–991. doi:10.1121/1.1909356

Folkerts, M.L., and Stecker, G. C. (**2022**). "Spectral weighting functions for lateralization and localization of complex," J. Acoust. Soc. Am., **151**, 3409–3425. doi:10.1121/10.00011469

Gardner, M. B. (**1968**). "Historical Background of the Haas and/or Precedence Effect," J. Acoust. Soc. Am., **43**, 1243–1248. doi:10.1121/1.1910974

Hafter, E. R., and Dye, R. H. (**1983**). "Detection of interaural differences of time in trains of high-frequency clicks as a function of interclick interval and number," J. Acoust. Soc. Am., **73**, 644–651. doi:10.1121/1.388956

Houtgast, T., and Plomp, R. (**1968**). "Lateralization Threshold of a Signal in Noise," J. Acoust. Soc. Am., **44**, 807–812. doi:10.1121/1.1911178

Klumpp, R. G., and Eady, H. R. (**1956**). "Some Measurements of Interaural Time Difference Thresholds," J. Acoust. Soc. Am., **28**, 859–860. doi:10.1121/1.1908493

Litovsky, R. Y., Colburn, H. S., Yost, W. A., and Guzman, S. J. (**1999**). "The precedence effect," J. Acoust. Soc. Am., **106**, 1633–1654.

Macpherson, E. A., and Middlebrooks, J. C. (**2002**). "Listener weighting of cues for lateral angle: The duplex theory of sound localization revisited," J. Acoust. Soc. Am., **111**, 2219. doi:10.1121/1.1471898

P. M. Zurek (**1987**). "The precedence effect," Directional Hearing, Springer, New York, NY, pp. 85–105.

Rakerd, B., and Hartmann, W. M. (**1985**). "Localization of sound in rooms, II: The effects of a single reflecting surface," J. Acoust. Soc. Am., **78**, 524–533. doi:10.1121/1.392474

Saberi, K. (**1996**). "Observer weighting of interaural delays in filtered impulses," Percep. and Psych., **58**, 1037–1046. doi:10.3758/BF03206831

Schubert, E. D., and Wernick, J. (**1969**). "Envelope versus Microstructure in the Fusion of Dichotic Signals," J. Acoust. Soc. Am., **45**, 1525–1531. doi:10.1121/1.1911633

Shinn-Cunningham, B. G., Kopco, N., and Martin, T. J. (**2005**). "Localizing nearby sound sources in a classroom: Binaural room impulse responses," J. Acoust. Soc. Am., **117**, 3100–3115. doi:10.1121/1.1872572

Stecker, G. C., and Hafter, E. R. (**2002**). "Temporal weighting in sound localization," J. Acoust. Soc. Am., **112**, 1046–1057. doi:10.1121/1.1497366

Stecker, G. C., Ostreicher, J. D., and Brown, A. D. (**2013**). "Temporal weighting functions for interaural time and level differences. III. Temporal weighting for lateral position judgments," J. Acoust. Soc. Am., **134**, 1242–1252. doi:10.1121/1.4812857

Strutt, J. W. (**1907**). "XII. On our perception of sound direction," Philosophical Magazine, **13**, 214–232. doi:10.1080/14786440709463595

Wightman, F. L., and Kistler, D. J. (**1989**). "Headphone simulation of free-field listening. I: Stimulus synthesis," J. Acoust. Soc. Am., **85**, 858–867. doi:10.1121/1.397557

Wightman, F. L., and Kistler, D. J. (**1992**). "The dominant role of low-frequency interaural time differences in sound localization," J. Acoust. Soc. Am., **91**, 1648–1661. doi:10.1121/1.402445

Yost, W. A., and Dye, R. H. (**1988**). "Discrimination of interaural differences of level as a function of frequency," J. Acoust. Soc. Am., **83**, 1846–1851. doi:10.1121/1.396520

CHAPTER 2

Spectral Weighting Functions for Localization of Complex Sound: The Effect of Competing Noise

2.1. Introduction

In a natural environment, noise reaches the two ears, and listeners can detect and localize a signal embedded in the noise, such as a voice in a crowd. Monaural and binaural spatial hearing cues support a listener's ability to perform sound localization as well as to segregate talkers from competing noise (Bronkhorst and Plomp, 1988, 1989, 1992). Monaural cues arise from the shape of the pinnae, head, and torso. Binaural cues arise from interaural differences between the two ears, which include interaural level differences (ILDs), from attenuation of the sound by the head, and interaural time differences (ITDs), from the delay between the sound arriving at each ear. In the presence of a competing noise, both the ability to detect and lateralize a signal degrades as the signal-to-noise ratio (SNR) decreases (Hirsh, 1948; Houtgast and Plomp, 1968; Good and Gilkey, 1996; Lorenzi et al., 1999; Brungart and Simpson, 2009). However, the spatial configuration which best aids in signal detection does not directly correspond to the spatial configuration which best aids lateralization and localization (Cohen, 1981). Signal detection performance improves when the signal is spatially separated from the competing sound (Houtgast and Plomp,1968), whereas lateralization and localization performance improve when the signal and competing sound are in close proximity (Good et al., 1997; Lorenzi et al., 1999).

During localization, broadband competing sounds are more disruptive for low-frequency target signals than for high-frequency or broadband target signals, an effect that has been demonstrated for competing sounds presented from lateral angles (Lorenzi et al., 1999), behind

the listener (Abel and Hay, 1996), or from random locations (Brungart and Simpson, 2009). These data demonstrate that high-frequency information contained in the target is important for precise localization in the presence of an interferer. High-frequency stimuli provide informative monaural cues.

Monaural cues are mainly used to localize sound in elevation (Hebrank and Wright, 1974) but may also be involved in resolving conflicting binaural cues in azimuth. A signal is presented to a listener in the free field, such as through a loudspeaker; the sound either directly enters the ear canal or is reflected off the listener's torso, head, and pinna surfaces. Across frequency components, the reflections either add together and increase the amplitude or cancel and decrease in amplitude. The result of these reflections is a filter that describes the transformation of the source spectrum at the eardrum. This filter is the head-related transfer function (HRTF) which can be measured using microphones placed inside the ear canal of either the listener, such as in Wightman and Kistler (1989), or using a head and torso model, such as Knowles Electronics Manikin for Acoustic Research (KEMAR; Burkhard and Sachs, 1975). Measurements using a model of just one ear (e.g., Shaw and Teranishi, 1968) display changes in the spectrum depending on the sound source angle in azimuth and elevation, especially at high frequencies. The high-frequency directional dependent changes of the HRTF have been suggested to be useful to resolve front-back confusions when binaural cues become ambiguous (Musicant and Butler, 1984). High-frequency stimuli also provide informative binaural cues.

Early experiments on the frequency-dependence of binaural cues for localization by Lord Rayleigh (Strutt, 1907) led to the "Duplex Theory," which posits that the ITD cue is utilized during the localization of low-frequency tones while the ILD cue is utilized during the localization of high-frequency tones. The limit of the ITD cue up to about 1500 Hz is partly due

to the relationship of ITD with the interaural phase difference (IPD), which becomes ambiguous as frequency increases. The ILD, on the other hand, is impacted by the head shadow, which attenuates high frequencies more than low frequencies because low frequencies have larger wavelengths that could wrap around the head. Thus, although listeners are sensitive to ILD cues across a broad range of frequencies (e.g., Yost, 1981), ILD cues are more reliable for high frequencies due to the physical properties of sound and the head. Consistent with the Duplex Theory, the extant literature demonstrates that ITD cues are perceptually dominant in the localization of broadband stimuli, while ILD cues (and sometimes ITD cues provided by the envelope of the signal) dominate the localization of high-frequency stimuli in quiet (i.e., without the presence of an interferer; Wightman and Kistler, 1992; Macpherson and Middlebrooks, 2002).

More recently, observer weighting methods have been used to determine perceptual weighting across frequency components during sound lateralization and quiet localization (Folkerts and Stecker, 2022). The stimulus components are randomly distributed across slight spatial variations of binaural cues or sound source location to disentangle the influence of frequency components composing complex sounds. Listeners then make spatial judgments (perceived sound source lateralization or localization) on the unified percept formed by the stimulus components. The influence of each component across frequency on perceived source lateralization/location is derived as a weight from the continuous spatial judgment (e.g., Fig. 2.2) using regression methods (Ahumada and Lovell, 1971). Spectral weighting functions (SWFs) display the weighting as a function of frequency. Aherens et al. (2020) measured lateralization SWFs for a noise complex comprised of 11 bands of noise, each 1-ERB wide and with center frequencies ranging from 442 to 5544 Hz (a 1-ERB gap separated adjacent bands). This resulted

in an elevated weight for the 442-Hz centered band of noise during ITD lateralization and the 5544-Hz band of noise during ILD lateralization when cues were presented independently. For SWFs measured during lateralization by Folkerts and Stecker (2022), with cues in agreement and with more broadband stimuli (100 to 6400 Hz), listeners placed the greatest weight on the 800-Hz ITD component. They also measured SWFs during localization, resulting in listeners placing the greatest weight on the 800-Hz component. The elevated weight at 800 Hz is consistent with the ITD dominance region during the lateralization of filtered clicks, peaking around 600 to 800 Hz (Bilsen and Raatgever, 1973; Tollin and Henning, 1999). SWFs have also been measured for more "real world" stimuli, including noise and tone complexes presented with simulated reverberation (Folkerts and Stecker, 2022) and speech (Baltzell et al., 2020). However, SWFs have yet to be measured in the presence of competing noise, which is common in real-world environments.

The current study aimed to measure SWFs for the localization of complex tones in the presence of competing noise. Two independent Gaussian noises were presented laterally to the listener. Based on previous work demonstrating the importance of high-frequency information for localization in noise (Abel and Hay, 1996; Lorenzi et al., 1999; Brungart and Simpson, 2009), it was expected that the dominance region in the SWFs would shift to a higher frequency range when measured in the presence of the competing noise. Therefore, the target complex tones were comprised of tones within the ITD dominance region and across a range of high frequencies.

2.2. Methods

SWFs were measured in the presence of competing noise for participants with normal hearing. Two stimulus conditions from Folkerts and Stecker (2022) containing high frequencies (T1 and T3) were utilized. SWFs were measured (and analyzed) in a similar manner to Folkerts and Stecker (2022), with the exception that Gaussian noise was presented in three SNR conditions (+9, 0, and -6 dB) for each stimulus condition. SWFs in competing noise were compared to established SWFs in quiet (from Folkerts and Stecker, 2022).

2.2.1. Participants

Participants were ten adults (8 females) aged 21 – 28 years that were recruited from the Vanderbilt University community. One participant (0515) is the author. Normal hearing was confirmed with pure tone audiometric thresholds less than 20 dB HL that differed less than 15 dB between left and right ears for octave frequencies from 250 to 8000 Hz. Participants were monetarily compensated. Approval was obtained for experimental procedures from Vanderbilt University Medical Center Institutional Review Board (IRB #191952).

2.2.2. Stimuli

All stimuli were generated in MATLAB (Mathworks, Natick, MA) and synthesized at 48 kHz. Stimuli were presented through the Dante audio-over-ethernet network (Focusrite Rednet, El Segundo, CA) with digital amplification (Ashly ne820PE, Webster, NY) for playback to a 64-loudspeaker array (Meyer MM-4, Berkeley, CA) in in the Vanderbilt Bill Wilkerson Anechoic Chamber Laboratory (ACL; 4.6 x 6.4 x 6.7 m; Eckel Industries, Cambridge, MA). The loudspeakers in the ACL are at ear height, spanning 360° (5.625° of separation) with a 2-meter radius.

Stimuli included the target tone complexes participants localized (used to measure SWFs) and the competing noise. The target signals were tone complexes, each consisting of seven pure-tone components presented at equal amplitude. The duration of the tone complex was 100 ms with 10-ms $\cos^2$ onset/offset ramps. The component configuration was octave frequencies from 100 to 6400 Hz for stimulus condition T1 and harmonics of 800 Hz spanning 800 to 5600 Hz for stimulus condition T3. The overall level of the target signal was held constant, at 60 dB SPL, across SNR conditions. The spatial configuration of each of the seven frequency components was manipulated from trial to trial to introduce spatial jitter. On each trial, a "base" azimuth was chosen from 11 possible locations; -56.26° to +56.26° in 11.25° steps. Five adjacent loudspeakers centered on the base azimuth [-11.25°, -5.625°, 0°, +5.625°, and +11.25° (relative to the base)] constituted the set of source loudspeakers from which individual components of the stimulus were presented on a given trial. Each component was randomly and independently assigned to one of the five source loudspeakers.

The competing noises were two 200-ms Gaussian noises independently generated for the left and right lateral loudspeakers (-90° and +90°) and presented simultaneously, 50 ms before the target signal. The level of the competing noise was dependent on the SNR condition: -6 dB SNR (66 dB SPL), 0 SNR (60 dB SPL), and +9 SNR (51 dB SPL).

2.2.3. Procedure

A touch-sensitive display (Apple iPad Air, Cupertino, CA) was mounted at a comfortable distance (~0.5 m in front and ~0.5 m below ear level) from the listener. This was used to record localization responses aligned to a top-down schematic of the room and loudspeaker array displayed on the screen (Fig. 2.1). On each trial, participants were instructed to sit upright and

face directly forward (toward the loudspeaker at 0°) before and during each stimulus presentation. These instructions helped to ensure participants received expected spatial cues. Immediately following each single presentation of the stimulus, participants were instructed to make an eye movement to the target signal's perceived location and then record that location on the schematic diagram by touching the iPad screen. Participants were asked to indicate the leftmost edge or leftmost image on any trial in which the lateral percept appeared "wide" or "split." The response azimuth was computed from the touch screen response and recorded as the localization judgment.

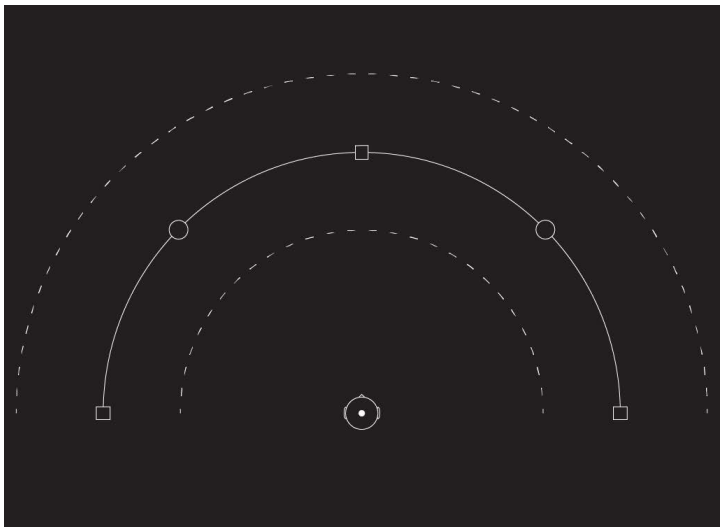

FIG. 2.1. Schematic used to record localization responses. The head marks the participant with a centered white dot at the middle bottom portion of the 180° arc. The solid white line of the arc indicates the loudspeaker array. Landmarks are included along the solid line indicating 0° (top empty square), -90° and +90° (empty bottom squares), and -45° and +45° (empty middle circles). In the sound field, -45° and +45° were marked by unused circular loudspeakers. Dashed lines were used to indicate the distance (if necessary), either in front or behind the loudspeaker array.

The base loudspeaker was selected pseudorandomly from 11 possible locations (± 56.25°) across trials, with each base value presented six times per run of 66 trials. Participants completed six runs (396 trials) for each of the six conditions (i.e., two stimulus conditions, T1 and T3, in three SNR conditions).

2.2.4. Analysis

SWFs were calculated separately for each listener and condition. Within each 66-trial run, the localization judgment was normalized by rank transform across each 66-trial run. Perceptual weights for each of the seven frequency components were estimated by multiple linear regression of the rank-transformed responses θ_R onto the azimuth values of each component θ_i.

$$\theta_R = \sum_{i=1}^{7} \beta_i \, \theta_i + k \tag{1}$$

Weights were computed by normalizing regression coefficients β_i so that absolute values summed to 1 across weights.

$$w_i = \beta_i \, / \sum_{j=1}^{7} |\beta_j| \tag{2}$$

The normalized weights w_i indicate the relative influence of the frequency component i on participants' localization judgments. Plotted together, the normalized weights constitute the SWF for each listener in each condition. Group average SWFs were calculated by taking the arithmetic mean normalized weight across participants, for each component.

Folkerts and Stecker (2022) computed the "average ratio" (AR) as a univariate measure of non-uniformity, specifically with an emphasis on the 800-Hz component in the ITD dominance region (AR_{800}). The AR_{800} was used to interpret the prominence of the 800-Hz component across quiet and SNR conditions. The AR_{800} was defined as the ratio of weight on the 800-Hz component to the mean of other weights:

$$AR_{800} = \mathrm{w}_{800Hz} / (\sum_{j \neq 800Hz} w_j / 6) \quad (3)$$

The AR_{800} was calculated for each listener in each condition, and the group average was the arithmetic mean across participants.

As in Folkerts and Stecker (2022), the current study computed the SWF confidence intervals and evaluated planned comparisons of weight and AR_{800} by non-parametric bootstrap tests. Bootstrapped confidence intervals on mean weight values were computed by resampling weights, with replacement, across subjects to generate 2000 bootstrap replicates. The mean weight was computed for each replicate to estimate the sampling distribution of mean weights. Confidence intervals were computed at the 95% level by taking the 2.5 and 97.5 percentile points from this sampling distribution.

Null-hypothesis significance tests used a similar approach. Each measure (e.g., AR_{800}) was resampled across participants to generate 2000 bootstrap replicates. A statistic of interest (e.g., mean or difference between two means) was then computed for each bootstrap replicate to estimate the corresponding sampling distribution. The proportion of bootstrap replicates falling at or below the null-hypothesis prediction (e.g., AR <= 1) defines the (one-sided) p-value, which is expressed to one significant digit. For two-sided statistical tests, the p-value was computed as

the minimum of proportions falling on either side of the prediction doubled. When any proportion was zero (i.e., the bootstrap sampling distribution did not overlap the null-hypothesis prediction), p-values are listed at the resolution of the bootstrap test itself (i.e., $p <$. 0005 for 2000-fold bootstrap).

2.3. Results and Discussion

2.3.1. Spectral Weighting Functions

Figure 2.2 displays the mean SWF obtained in each of the six conditions (i.e., two stimulus conditions in three competing noise conditions) and included for comparison SWFs measured in quiet (leftmost column) for the two stimulus conditions, previously reported in Folkerts and Stecker (2022; see also in Fig. 1.1). For reference, the SWFs measured in quiet are plotted as thin lines on each competing noise panel. Significant differences between component weights in quiet and competing noise are indicated with asterisks. In the presence of various levels of noise, the overall shape of the SWFs generally appears consistent with SWFs found in quiet. There were no significant differences between the weight placed on the 800-Hz component in quiet and in the presence of competing noise. However, in condition T1 (octave tones 100-6400 Hz), the 400-Hz component received a greater weight in the -6 dB SNR condition ($p < .05$) and in the +9 dB SNR condition ($p < .001$) than in quiet, resulting in a slight "widening" of the ITD dominance region peak toward lower frequencies. These results are contrary to the hypothesized result of a weight maxima shift to higher frequencies. Across most conditions, the highest frequency components in both stimulus conditions (6400 Hz and 5600 Hz for T1 and T3, respectively) were weighted lower in competing noise than in the quiet ($p < .02$ across all SNRs).

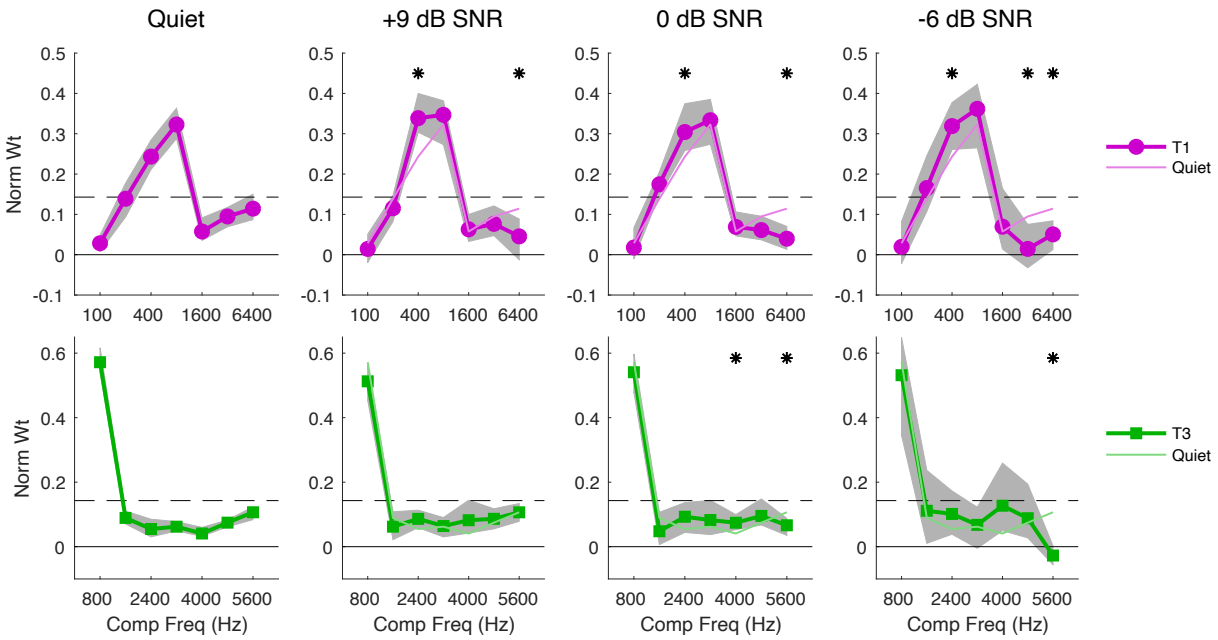

FIG. 2.2. Mean SWFs obtained in various levels of competing noise (columns: +9 dB SNR, 0 dB SNR, and -6 dB SNR) including no noise (leftmost column: "Quiet") adapted from Folkerts and Stecker (2022; Fig. 1.1). Top and bottom panels plot SWF data for stimulus conditions T1 (octave tones 100-6400 Hz; magenta circles) and T3 (harmonic tones 800-5600 Hz; green squares), respectively. Symbols and thick lines plot cross-participant mean normalized weight as a function of component frequency. Shaded regions indicate bootstrapped ±95% confidence intervals on each mean weight. Dashed lines indicate the expected value (1/7) for uniform weighting across components. Quiet SWFs are replotted as thin colored lines in competing noise panels for purposes of comparison. Bootstrapped, two-tailed, significant differences ($p < .05$) between weights in the quiet and competing noise weights are indicated with asterisks (*) at the top of each panel.

Individual SWFs for each participant, including SWFs reported in quiet by Folkerts and Stecker (2022), are displayed in Fig. 2.3. The overall trend of SWF shapes is consistent with the

results found in the mean data. That is, a consistent weight maximum in the ITD dominance region (the 800-Hz component), with a possible shift of the peak region toward lower regions (stimulus condition T1; top row).

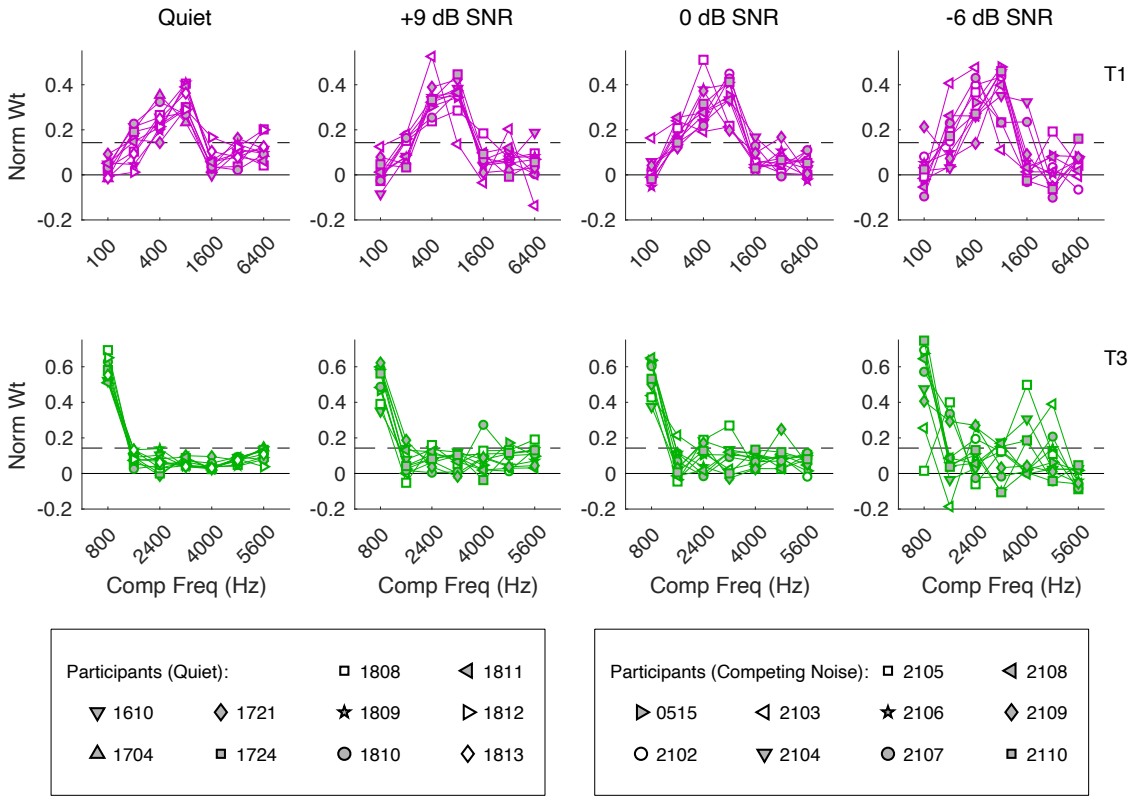

FIG. 2.3. Individual-participant SWFs found in various levels of competing noise (columns: +9 dB SNR, 0 dB SNR, and -6 dB SNR), including no noise (leftmost column: "Quiet") adapted from Folkerts and Stecker (2022). Panels, arranged identically to Fig. 1, plot SWFs obtained for individual participants (symbols; legend at bottom). Note that one group of participants completed the competing noise conditions; a non-identical group of participants completed the quiet experiment.

AR_{800} distributions are displayed in Fig. 2.4 as violin plots (Hintze and Nelson, 1998; Bechtold, 2016), including the AR_{800} distributions in the same target stimulus conditions in quiet (Folkerts and Stecker, 2022) for comparison purposes. The AR_{800} was used in the current analysis because the AR_{800} in quiet focused on the peak of the dominance region at 800 Hz. There were no significant differences in AR_{800} across quiet and SNR conditions. All AR_{800} values across SNR conditions were significantly greater than 1, indicated by asterisks. The consistent non-uniformity across SNR conditions indicates that participants continue to utilize the cues in the ITD dominance region, even in the presence of competing noise. However, this measurement may not capture the "broadening" of the peak in stimulus condition T1 (octave tones 100-6400 Hz), which seemed to occur as an increase in the 400-Hz component for the +9 and -6 dB SNR conditions.

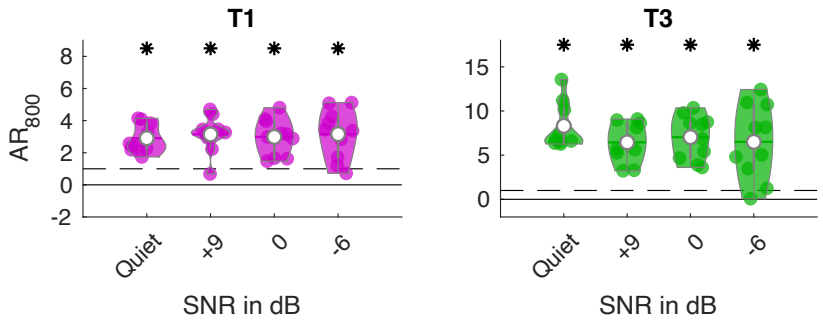

FIG. 2.4. Violin plots (Hintze and Nelson, 1998; Bechtold, 2016) of AR_{800} values (vertical axis) are shown for each stimulus condition (panels), plotted across SNR conditions (-6, 0, and +9 dB SNR; horizontal axis) including in quiet (adapted from Folkerts and Stecker, 2022). Colored circles in each panel plot AR_{800} for individual participants; violin plots indicate the density (width of each violin) and mean (white circle) of obtained values. Dashed lines indicate the

expectation for uniform spectral weighting AR = 1. Asterisks (*) indicate conditions in which AR_{800} significantly exceeded this value ($AR_{800} > 1$, $p < .01$ by 2000-fold bootstrap test).

The SWFs in all SNR conditions reveal a decrease in the relative weight for high-frequency components, contrary to the expectation that the maxima of 800-Hz component found in quiet would shift towards high-frequency components in the presence of competing noise. The largest weights were found to remain within the ITD dominance region (with a slight expansion of the peak toward lower frequencies), even in the least favorable SNR conditions (-6 dB). SWFs continue to reveal elevated weights for components within the dominance region. The data support a persistent ITD dominance region in the presence of competing noise. The down-weighting of the high-frequency cues is surprising and inconsistent with previous studies, which suggested high-frequency information to be particularly important for localization in noise (Abel and Hay, 1996; Lorenzi et al., 1999; Brungart and Simpson, 2009).

2.3.2. Localization Performance in Competing Noise

The shapes of SWFs across SNR conditions are similar; however, the variability in weighting across participants increases as the SNR decreases. This variability is evident in Fig. 2.2, where the confidence interval (grey shaded region) widens in the -6 dB SNR condition, Fig. 2.3, where the variability of SWF shapes across participants increases in the -6 dB SNR condition, and Fig. 2.4, where the range of individual AR_{800} values (colored circles) increases. A possible explanation may be the degradation of localization performance in the presence of competing noise, especially as the SNR becomes less favorable (Good et al., 1997; Lorenzi et al.,

1999; Brungart and Simpson, 2009). To explore this possibility, localization performance was examined for the current data.

Recall that, to measure SWFs, spatial jitter was introduced so that the multiple linear regression model (function 1) could be utilized. Therefore, perfect localization would mean a listener's response is within the five adjacent loudspeakers spanning a 22.5° range. Localization responses outside of that range are "errors". When a competing sound is present during localization, errors can be due to a bias. These biases have been observed as a "pulling" of the perception of the source angle toward the competing noise angle (Butler and Naunton, 1964; Good and Gilkey, 1996) or as a "pushing" of the perception of the source angle away from the competing noise angle (Best et al., 2007). Response azimuths as a function of the base loudspeaker are plotted in Fig. 2.5 and 2.6 for individual participants' who had a pulling and pushing bias, respectively. Participant 2103 (Fig. 2.5) demonstrated a high localization response density for the lateral angles at all stimulus and SNR values (i.e., responses were outside of the two dark grey lines indicating the 22.5° range). Most of the responses for negative base values fell below the 22.5° range, and most of the responses for positive base values fell above the 22.5° range. As the SNR unfavorably decreased to -6 dB, participant 2103 had little to no responses near 0° (when statistically, the range of component loudspeakers center around 0° for 9.1% of the trials). A pulling bias is said to have occurred for participant 2103. A similar bias was recognized for participant 2105 in the -6 dB SNR condition, though only for stimulus condition T3 (which consists of mostly high-frequency tones; harmonic tones 800-5600 Hz). Participant 2109 (Fig. 2.6) had a pushing bias, where the density of responses generally flattened and fell closer to 0° in the -6 dB SNR condition (i.e., responses were outside of the 22.5° range; however, responses for negative base values fell above the range and responses for positive base values

fell below the range). As in Lorenzi et al. (1999), both pulling and pushing biases were observed across a small set of participants in the current study.

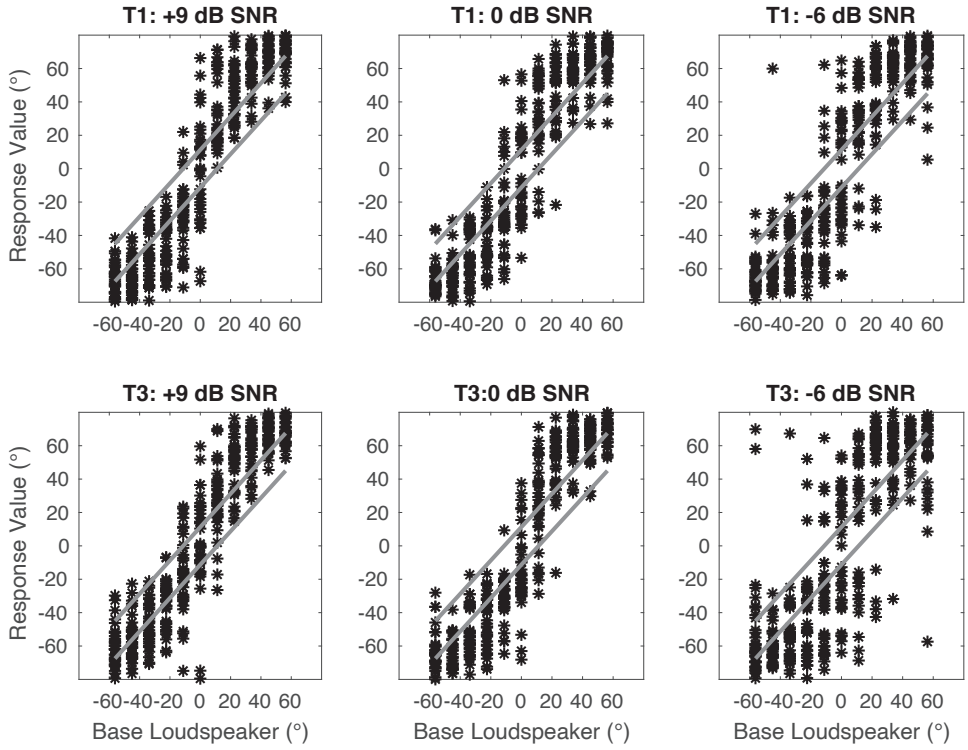

FIG. 2.5. Each panel plots individual response values (in degrees; before rank-transformation) as a function of base loudspeaker (as asterisks) for participant 2103. Thick grey lines indicate the 22.5° range of responses around the base azimuth. Top panels indicate stimulus condition T1 (octave tones 100-6400 Hz), and bottom panels indicate stimulus condition T3 (harmonic tones 800-5600 Hz). Columns from left to right indicate the SNR conditions +9 dB, 0 dB, and -6 dB, respectively.

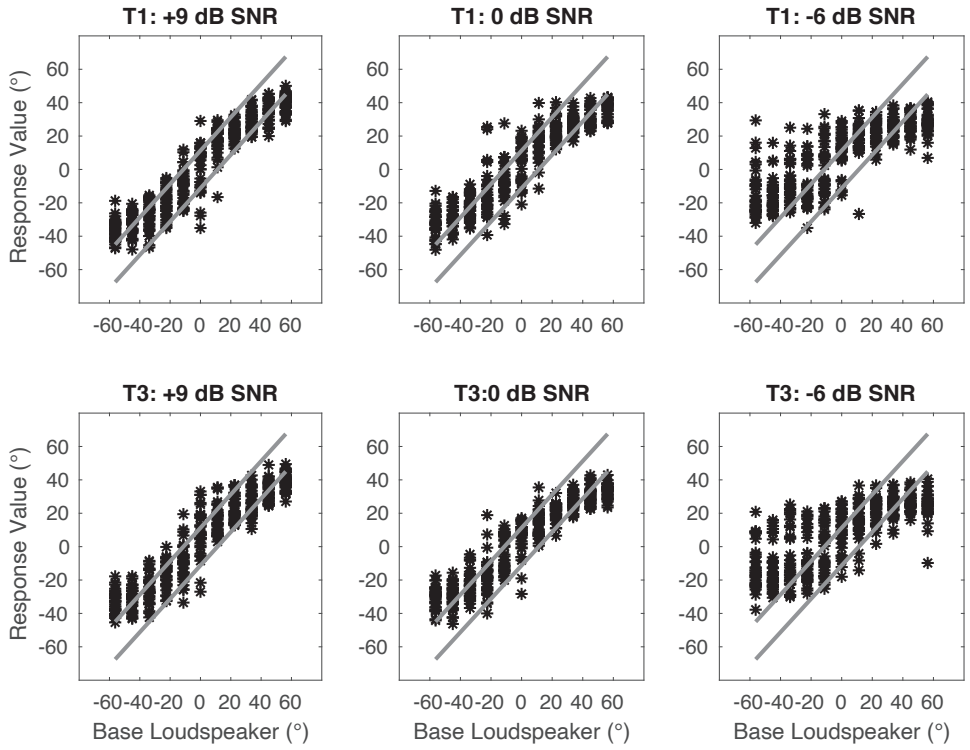

FIG. 2.6. The same as Fig. 2.5, except for participant 2109.

The root mean square (RMS) error is a statistic used by both Good and Gilkey (1995) and Lorenzi et al. (1999) to calculate a participant's average error, in degrees, during localization in noise. This metric was used due to its ability to account for both variance and bias in localization responses. In their tasks, localization was based on the perception of the sound source emitting from one loudspeaker. In the current study, the RMS error indicates errors made outside of the 22.5° range of spatial jitter. The left panel of Fig. 2.7 displays the mean RMS error (across participants), in degrees, as a function of SNR condition for each frequency stimulus. Bootstrapped difference tests at each SNR value were calculated between stimulus conditions T1 and T3 and between SNR conditions (within stimulus conditions). The RMS error in both stimulus conditions (T1 and T3) are relatively similar at +9 and 0 dB SNR as opposed to -6 dB

SNR, where stimulus condition T3 has a higher degree of error than T1. However, the difference at the low SNR did not reach significance. For both stimulus conditions (T1 and T3), the RMS error was significantly larger in the -6 dB SNR condition than in the +9 dB and 0 dB conditions (lines with asterisks).

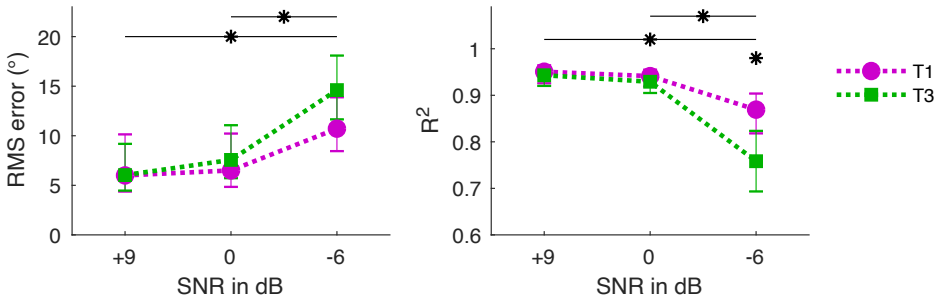

FIG. 2.7. The left panel plots mean RMS error (in degrees) across participants as a function of SNR in dB for stimulus conditions T1 (magenta circles; octave tones 100-6400 Hz) and T3 (green squares; harmonic tones 800-5600 Hz; legend to the right of panels). The right panel plots the mean R^2 value across participants as a function of SNR in dB for stimulus conditions T1 and T3. Error bars indicate bootstrapped ±95% confidence intervals on each mean value (RMS error or R^2). Asterisks (*) indicate bootstrapped, two-tailed, significant differences ($p < .05$) between (RMS error or R^2) values in stimulus condition T1 versus T3. Asterisks with lines indicate significant differences across SNR conditions (for both stimulus conditions, calculated separately).

Another way to measure the variability (or errors) in localization responses is by fitting a line to their localization responses as a function of the sound source. The R^2 statistic indicates the proportion of variance accounted for by the line. Gilkey and Good (1996) and Lorenzi et al.

(1999) measured the R^2 statistic using regression with one predictor variable because the sound source was emitted from one loudspeaker. However, in the current study, the sound source was emitted from five adjacent loudspeakers. Therefore, the R^2 statistic is calculated from the multiple linear regression model (function 1; with seven predictor variables) used to calculate weights (Stecker and Hafter, 2009). The R^2 statistic was derived from each SWF measurement (for each participant in each condition). The right panel of Fig. 2.7 displays the mean R^2 value across participants as a function of SNR condition for each frequency stimulus. Bootstrapped difference tests at each SNR value were calculated between stimulus conditions T1 and T3 and between SNR conditions (within stimulus conditions). Similar to the differences in RMS error across stimulus conditions, the R^2 values are similar for T1 and T3 at +9 and 0 dB SNR. At -6 dB SNR, the R^2 values are significantly different between stimulus conditions T1 and T3 (asterisk). For both stimulus conditions (T1 and T3), the R^2 value was significantly smaller in the -6 dB SNR condition than the +9 dB and 0 dB conditions (lines with asterisks).

Across both stimulus conditions, T1 (octave tones 100-6400 Hz) and T3 (harmonic tones 800-5600 Hz), the RMS errors and R^2 values display an increase in localization response error when the SNR is below 0 dB. These data are consistent with the RMS errors and R^2 values reported by Lorenzi et al. (1999) when using broadband and high-pass click stimuli. However, Lorenzi et al. (1999) found that for low-pass stimuli (1600 Hz cutoff), response error rates increased, more so than for broadband and high-pass click stimuli (with no differences found between broadband and high-pass stimuli). With these results, Lorenzi et al. (1999) concluded that listeners localize signals (in the presence of a lateral masker) using cues available high-frequency components (i.e. the ILD or ITD in the envelope) (since there were more errors found for low-pass stimuli). In the current experiment, results based on localization error (Fig. 2.7)

reveal differences between stimuli that were broadband (T1; octave tones 100-6400 Hz) and stimuli that encompassed mostly high frequencies (T3; harmonic tones 800-5600 Hz), the latter producing more errors. These results don't align with those of Lorenzi et al. (1999) who found less errors when high frequency components were available. However, there are differences in the stimuli utilized (clicks versus tone complexes), competing noise configuration (one lateral noise versus two lateral noises), and localization error statistic derivation (see above). It should also be noted, as stated in the previous section, the results of the SWFs measured in the presence of competing noise are inconsistent with the conclusion by previous studies that listeners utilized the cues in the high-frequency portions of the stimulus over low-frequency portions.

2.3.3. Relating Spectral Weighting to Interaural Sensitivity in Competing Noise

One potential explanation for the spectral dominance around 800 Hz is that the auditory system is most sensitive to binaural cues across the sound spectrum in that frequency region. Folkerts and Stecker (2022) found that the ITD SWFs generally follow the inverse proportion squared of ITD thresholds below 1250 Hz. The SWFs found in the presence of competing noise reflect a continued use of the ITD dominance region; therefore, it would be expected that ITD sensitivity within the dominance region is less affected by competing noise than higher frequencies. Yost et al. (1971) measured the ITD sensitivity of filtered click stimuli in the presence of continuous Gaussian noise. ITD thresholds remained low for click stimuli whose spectrum contained low-frequency information, while thresholds increased when the click stimuli's spectrum only contained frequencies above 1000 Hz. Thresholds slightly decreased for low frequency clicks bandpass filtered from 4 Hz to 500 Hz compared to clicks filtered from 4 Hz to 800 Hz and above. ITD sensitivity in noise was the least altered when the click stimuli

contained frequencies within the dominance region. This effect is apparent even if high-frequency stimuli contain ITD cues within the envelope. Yost (1975) measured the lateralization accuracy of a low-frequency tone (600 Hz), high-frequency bandpass noise (3900 Hz centered, 600 Hz wide), and a high-frequency amplitude modulated (AM) tone (3900 Hz tone, 600 Hz AM) in quiet and in the presence of continuous, uncorrelated Gaussian noise low-pass filtered at 5000 Hz. Lateralization accuracy for an ITD value of 100 ms was close to 100% for all three stimuli in quiet; however, accuracy decreased for the high-frequency bandpass noise and AM tone in the competing noise, while accuracy was only slightly reduced for the low-frequency tone. Yost's (1971) results indicate that the tone within the dominance region is less disrupted in the presence of competing noise. Leading to the assumption that in quiet (the free field), the ITD cue in the components with higher weights are less disrupted and, in the current study, participants continue to utilize cues within the dominance region.

In quiet, Mills (1958) measured the minimum audible angle (MAA), the just noticeable differences (JND) a listener could detect between two horizontal plane locations. The MAA is about 1° at 0° azimuth and increases monotonically as the lateral angle is increased and is dependent on the frequency of the tone, with the smallest MAA found around 750 Hz (Mills, 1960), following the elevated weight at 800 Hz found for SWFs during localization in quiet. In competing noise, the MAA of a high-frequency tone (2000 Hz) increases from 3° in quiet to 6° in noise; however, the MAA does not change for a low-frequency tone (500 Hz; Jacobsen, 1976). The disruption of JNDs for high-frequency stimuli but not for low-frequency stimuli in quiet are consistent with the disruptions found for ITD lateralization across frequency. The SWFs found in the current study display the salience of undisrupted cues within the dominance region.

2.3.4. Relating Spectral Weighting to Interaural Cue Availability in Competing Noise

One aspect of perceptual weighting is the availability of cues. To explore the degree to which ITD and ILD cues are distorted or reduced, the T1 (octave tones 100-6400 Hz) stimuli in quiet and the three SNR conditions (+9, 0, -6 dB) were recorded using KEMAR. All stimulus components were distributed to base loudspeakers during the recording, and each recording consisted of a presentation of the components from one base loudspeaker location (-56.26° to +56.26° in 11.25° steps). A 50-ms sliding window beginning at the stimulus onset was shifted by 10 ms for a total of 6 windows encompassing the 100-ms duration of the signal. For each window, the Binaural Toolbox (Akeroyd, 2001) was utilized to calculate the average ITD, interaural correlation (IAC), and ILD across windows (see diagram; Fig. 2.8). Binaural cues were analyzed separately for each component frequency by filtering using equivalent rectangular bandwidths (ERBs) centered at each nominal component frequency. The peak of the cross-correlation function (between the left and right ERB filtered window after modeling for neural transduction) served as the IAC and the location of the peak of the ITD for each ERB-centered component. The ILD was measured by dividing the left and right ERB filtered window's RMS value of intensity and transforming that divided value to dB.

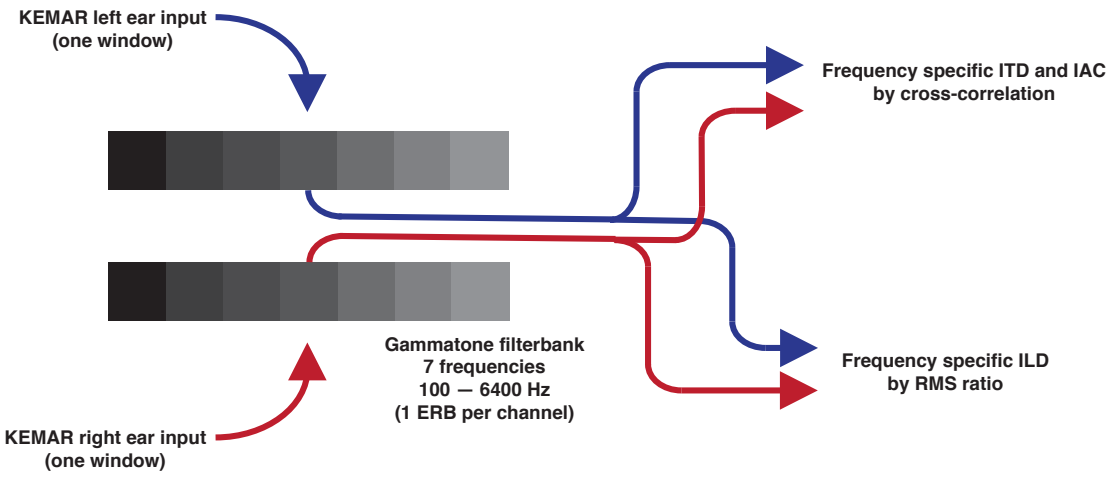

FIG. 2.8. Diagram of binaural cue analysis utilizing the Binaural Toolbox (Akeroyd, 2001). Each 10 ms windowed KEMAR recording for the left (blue arrows) and right ear inputs (red arrows) of the KEMAR was separately filtered by the gammatone filterbank. Each of the ERB-wide, filtered signals were compared across ears (left and right channels) by means of cross-correlation (to calculate ITD and IAC) and RMS ratio (to calculate ILD).

In Fig. 2.9, color plots are utilized to display average cue values across windows; each panel is a color plot with each row of panels displaying the average ITD, IAC, and ILD values and each column of panels indicating the quiet and SNR conditions (+9, 0, and -6 dB). Within each panel, colored values are plotted for each ERB centered at each frequency component (x-axis) as a function of the base loudspeaker location (i.e., the component location in degrees).

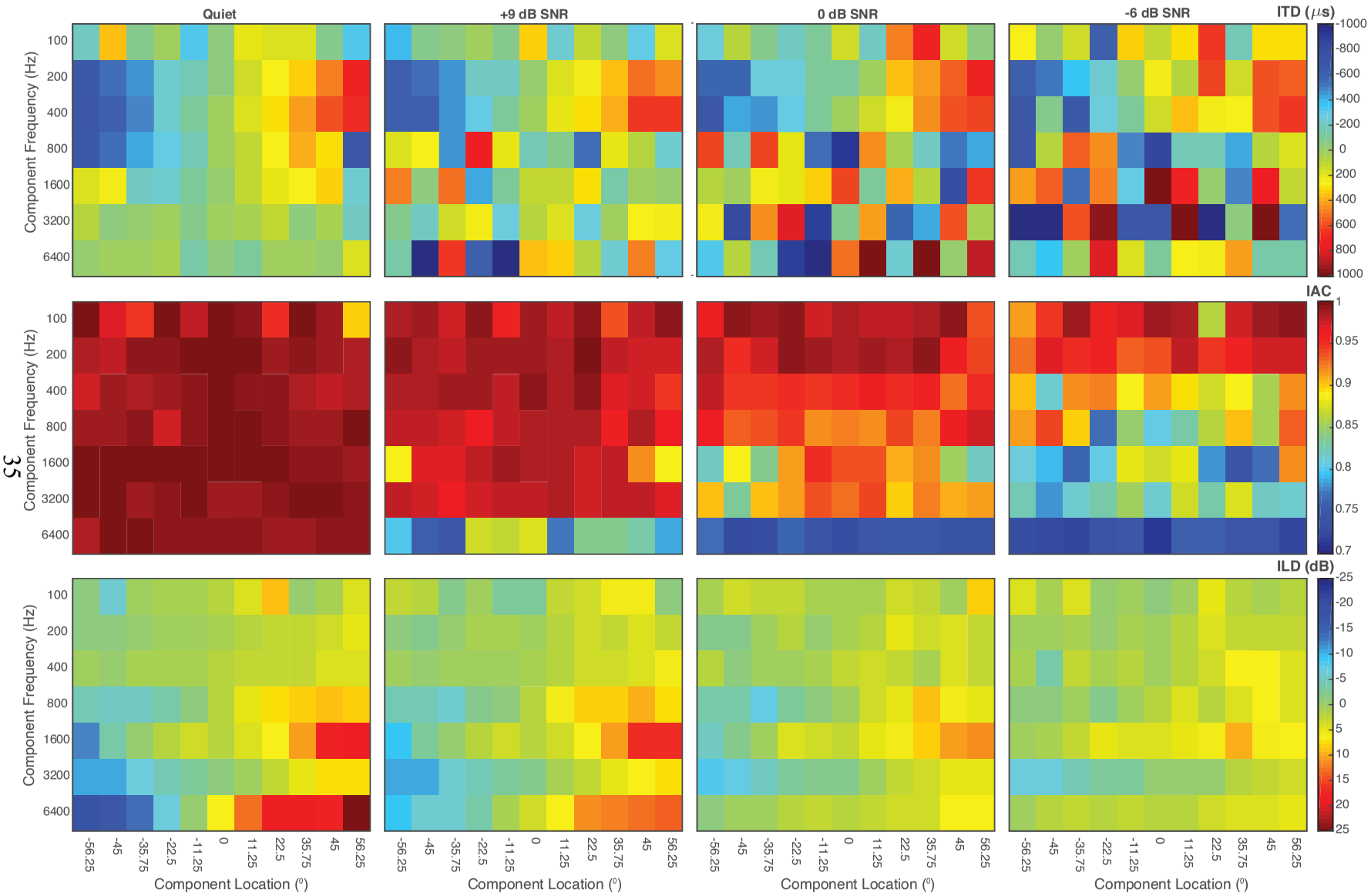
Quiet
+9 dB SNR
0 dB SNR
-6 dB SNR
ITD (μs)
IAC
ILD (dB)
Component Frequency (Hz)
100
200
400
800
1600
3200
6400
Component Location (°)
-56.25
-45
-35.75
-22.5
-11.25
0
11.25
22.5
35.75
45
56.25
-1000
-800
-600
-400
-200
0
200
400
600
800
1000
1
0.95
0.9
0.85
0.8
0.75
0.7
-25
-20
-15
-10
-5
0
5
10
15
20
25

FIG. 2.9. Average ITD, IAC, and ITD cues (rows) calculated across 50 ms windows shifted by 10 ms for a total duration of the stimulus (100 ms) for quiet and SNR conditions (+9, 0, and -6 dB; columns). Each panel plots the cue values for each ERB centered at the component (Hz; x-axis) as a function of component location (°; y-axis). The cue values are plotted as colored values indicated by the color bar to the right of the last column for each row. The ITD values range from blue, indicating a -1000-μs ITD, to red, indicating a 1000-μs ITD. The IAC values range from blue, indicating an IAC value of 1, to red, indicating an IAC value of .7. The ILD values range from blue, indicating a -25 dB ILD to red, indicating a 25 dB ILD.

Visual inspection of Fig. 2.9 reveals that, in quiet, the average ITD cue value (Fig. 2.9; first row and column) systematically and reliably changed with azimuth for frequency components 200, 400, and 800 Hz; that is, at the most negative azimuthal (leftward) component locations, the cue value is between -1000- and -400-μs ITD (blue to light blue). As the components move to more positive azimuthal (rightward) locations, the average ITD cue value monotonically increases until the values are between 400- and 1000-μs ITD (orange to red) for the rightward component locations. The average ITD at all component locations is less reliable at higher frequencies as the ITD values are near 0 μs. When the competing noise is present (remaining columns), the average ITD values from the 800-Hz component to the 6400-Hz component become erratic as the cue values become random. At the 200- and 400-Hz components, the ITD cue values are less monotonic. The average ITD cue value at 800 Hz in each of the SNR conditions is less monotonic and reliable; therefore, one may assume that participants should increase their relative perceptual weight for lower frequencies. Indeed, the behavioral data, displayed in Fig. 2.2 (top panels), depicts this shift in SWFs across all SNR

values compared to SWF in quiet. That is, the 800-Hz component remains relatively highly weighted, and there is an upweighting of lower frequencies (400 Hz) in competing noise.

The average IAC in quiet (Fig. 2.9; second row, first column) remains high across all frequencies, ranging from .9 to 1 (orange to red), with most values being near 1 (dark red). When the competing noise is present at a +9 dB SNR (Fig. 2.9; second row, second column), the average IAC fall below .9 at the highest component frequency, 6400 Hz. When the competing noise is present at a 0 dB SNR (Fig. 2.9; second row, third column), the average IAC falls for lower frequencies, i.e., 1600 and 3200 Hz. This trend continues for the competing noise is presented at a -6 dB SNR (Fig. 2.9; second row, fourth column), where the IAC is reduced, even down to the 800-Hz component. Therefore, systematically, the IAC is reduced from high to low frequencies as the level of the competing noise increases.

To understand these systematic changes, the IAC was measured for the competing noise only (SNR $-\infty$), using the same methods described above for the three levels of competing noise. At 3200 and 6400 Hz the IAC is between .72 and .76, at 1600 Hz the IAC is between .8 and .87, at 800 Hz the IAC is between .83 and .89, at 400 Hz the IAC is between .79 and .82, at 400 Hz, the IAC is between .88 and .94, and at 200 Hz the IAC is between .99 and .96. For two independent Gaussian noise maskers presented at lateral angles, one may assume that the IAC should be similar and close to 0 across low and high frequencies. However, the IAC for one independent Gaussian noise is 1 since the signal reaches both ears. Therefore, two Gaussian noises may decrease the correlation but most likely will not reduce to correlation to 0. Cross-correlation measurements of noise made in reverberant environments also display frequency-dependent IAC values; that is, as the frequency decreases below 500 Hz, the IAC value increases toward 1 (Lindevald and Benade, 1986; Hartmann et al., 2005; Rakerd and Hartmann, 2010).

The authors of these studies indicate that a high coherence at low frequencies is due to the wavelengths, which are longer at low frequencies and therefore similar across ears. Rakerd and Hartmann (2010) also measured the ITD lateralization performance of a noise band centered at 225, 715, and 2850 Hz at various IAC values. Lateralization degrades faster with decreasing IAC for the lower- and higher-frequency noise bands. For the noise band centered at 715 Hz, a coherence above .5 resulted in fairly accurate lateralization. That is, even with low IAC values, the sensitivity remains within the ITD dominance region. Therefore, although the coherence is higher at lower frequencies, participants most likely continue to have a higher perceptual weight for the frequencies near 800 Hz.

As expected, the average ILD in quiet (Fig. 2.9; third row, first column) is more reliable for higher-frequency components. Like the ITD values at low frequencies, the ILD at mid to high frequencies (800 to 6400 Hz) systematically increases from negative values (between -25 to -10 dB; blue) at negative azimuthal (leftward) component locations to positive values (between 10 to 25 dB; red). As the frequency of the component decreases, the ILD range of values becomes compressed, as is expected due to the properties of head attenuation. At 200 and 400 Hz, the ILD values across component locations are low; however, systematic changes from left to right are not as apparent as those found for higher frequencies. As the SNR decreases from +9 dB to -6 dB (Fig. 2.9; third row, second to the fourth column), the ILD range is compressed, more so for the 6400-Hz component. Because the competing noise comprises two laterally projecting maskers presented at equal levels, the reduction of the ILD range is most likely due to the physical masking of the ILD value of the target components. The physical masking is most likely more apparent in high frequencies because the energy of white noise is higher at higher-frequency ERBs because the bandwidth increases. Although the ILD range is reduced, the ILD cue may

still be available. Therefore, one assumption that has been made in the section relating SWFs to ITD sensitivity may not account for the weighting of the ILD cue in competing noise. Rakerd and Hartmann (2010) measured trading ratios, that is, the relative weight between ITD and ILD cues, for ITD stimuli with various coherence levels. As the coherence decreased, the trading ratios increased, resulting in an increased relative weight for the ILD cue. To understand if such weighting changes are also apparent for competing noise (which reduces the IAC value), lateralization SWFs where the ITD and ILD are presented with small cue variations, as in Folkerts and Stecker (2022), should be measured in the presence of competing noise.

2.3.5. Limitations

The competing noise spatial configuration used in the current study was designed to simulate a real-world environment where uncorrelated noises arise from various locations. The lateral most angles (-90° and +90°) were chosen as they have been shown to produce more localization errors (Good et al., 1997; Lorenzi et al., 1999). However, an important feature of the current study compared to Lorenzi et al. (1999), who found the degradation of localization to be higher for low-frequency stimuli than high-frequency stimuli, is that one competing noise was used in their study. Suzuki et al. (1993) demonstrated localization degradation for a 2000 Hz tone in a competing pink noise presented at -30, 0, and +30 with a -10 dB SNR but intact localization for a 500 Hz and 1000 Hz tone. Suzuki et al. (1993) also presented the competing pink noise as six independent noise channels (±30°, ±90°, and ±150°) and found similar results, that is, degradation of localization performance for the 2000 Hz tone. Therefore, it is assumed that one competing noise would have a similar effect on SWFs as found in the current study.

Another significant difference between the experiments which exhibit degradation of localization performance of low-frequency stimuli versus high-frequency stimuli (Good et al., 1997; Lorenzi et al., 1999) or versus broadband stimuli (Brungart and Simpson, 2009) and the current study is the use of filtered click trains versus complex tones. The presence of competing noise may affect the lateralization of click trains and tonal stimuli differently; however, the SWFs found for octave bands of noise with the same center frequencies as stimulus condition T1 were similar in shape to the SWF for T1. Therefore, a change in the weighting function may be expected if the stimuli were filtered clicks.

2.4. Summary and Conclusions

The purpose of the current study was to explore the effects of competing noise on SWFs. The SWFs of the current participants were compared to participants tested in quiet (Folkerts and Stecker, 2022). The results of this study revealed three main findings:

1) SWFs measured in the presence of competing noise revealed the greatest weight on the 800-Hz component of complex tones across all SNRs (+9, 0, and -6 dB). Compared to SWFs measured in quiet, the 400-Hz component revealed an elevated weight, and the highest frequency components revealed a reduced weight. These results are consistent with frequency-dependent ITD sensitivity in the presence of competing noise.

2) Although no systematic differences in the salience of the dominance region were found across SNRs, localization performance and consequentially the performance of the model used to measure SWFs degraded when the SNR was -6 dB SNR. The degradation was more apparent for stimulus condition T3, which contained primarily high frequencies, than stimulus condition T1,

which contained a broad range of frequencies. Therefore, the current results do not align with earlier work that noise least affects high-frequency stimuli (e.g., Lorenzi et al., 1999).

3) The ITD cue measured for the T1 stimulus components in noise reveals unreliable or sporadic ITD values across azimuth for the 800-Hz component in noise, leading to a possible explanation of the increase in perceptual weight to the 400-Hz component, which remains more intact.

REFERENCES

Abel, S. M., and Hay, V. H. (**1996**). "Sound Localization the Interaction of Aging, Hearing Loss and Hearing Protection," Scand. Aud., **25**, 3–12. doi:10.3109/01050399609047549

Ahrens, A., Joshi, S. N., and Epp, B. (**2020**). "Perceptual Weighting of Binaural Lateralization Cues across Frequency Bands," J. Assoc. Res. Oto., **21**, 485–496. doi:10.1007/s10162-020-00770-3

Ahumada, A., and Lovell, J. (**1971**). "Stimulus Features in Signal Detection," J. Acoust. Soc. Am., **49**, 1751–1756. doi:10.1121/1.1912577

Akeroyd, M. A. (**2001**). "A binaural cross-correlogram toolbox for MATLAB," Technical Report, University of Connecticut Health Center/ University of Sussex, software downloadable from http://www.ihr.mrc.ac.uk/projects/matlab/binaural_toolbox (Last viewed 10 Oct. 2014).

Baltzell, L. S., Cho, A. Y., Swaminathan, J., and Best, V. (**2020**). "Spectro-temporal weighting of interaural time differences in speech," J. Acoust. Soc. Am., **147**, 3883–3894. doi:10.1121/10.0001418

Bechtold, B. (**2016**). "Violin Plots for Matlab", Github Project. doi: 10.5281/zenodo.4559847

Best, V., Gallun, F. J., Carlile, S., and Shinn-Cunningham, B. G. (**2007**). "Binaural interference and auditory grouping," J. Acoust. Soc. Am., **121**, 1070–1076. doi:10.1121/1.2407738

Bilsen, F. A., and Raatgever, J. (**1973**). "Spectral Dominance in Binaural Lateralization," Acoustica, **28**, 131–132.

Bronkhorst, A. W., and Plomp, R. (**1988**). "The effect of head-induced interaural time and level differences on speech intelligibility in noise," J. Acoust. Soc. Am., **83**, 1508–1516. doi: 10.1121/1.395906

Bronkhorst, A. W., and Plomp, R. (**1989**). "Binaural speech intelligibility in noise for hearing-impaired listeners," J. Acoust. Soc. Am., **86**, 1374–1383. doi:10.1121/1.398697

Bronkhorst, A. W., and Plomp, R. (**1992**). "Effect of multiple speechlike maskers on binaural speech recognition in normal and impaired hearing," J. Acoust. Soc. Am., **92**, 3132–3139. doi:10.1121/1.404209

Brughera, A., Dunai, L., and Hartmann, W. M. (**2013**). "Human interaural time difference thresholds for sine tones: The high-frequency limit," J. Acoust. Soc. Am., **133**, 2839–2855. doi:10.1121/1.4795778

Brungart, D. S., and Simpson, B. D. (**2009**). "Effects of bandwidth on auditory localization with a noise masker," J. Acoust. Soc. Am.,, **126**, 3199–3208. doi:10.1121/1.3243309

Burkhard, M. D., and Sachs, R. M. (**1975**). "Anthropometric manikin for acoustic research," J. Acoust. Soc. Am., **58**, 214–222. doi:10.1121/1.380648

Cohen, M. F. (**1981**). "Interaural time discrimination in noise," J. Acoust. Soc. Am., **70**, 1289–1293.

Folkerts, M.L., and Stecker, G. C. (**2022**). "Spectral weighting functions for lateralization and localization of complex," J. Acoust. Soc. Am., **151**, 3409–3425. doi:10.1121/10.00011469

Gilkey, R. H., and Good, M. D. (**1995**). "Effects of Frequency on Free-Field Masking," Hum. Factors, **37**, 835–843. doi:10.1518/001872095778995580

Good, M. D., and Gilkey, R. H. (**1996**). "Sound localization in noise: The effect of signal-to-noise ratio," J. Acoust. Soc. Am., **99**, 1108–1117. doi:10.1121/1.415233

Good, M., Gilkey, R. H., and Ball, J. M. (**1997**). "The relation between detection in noise and localization in noise in the free field," Binaural and Spatial Hearing in Real and Virtual Environments, Laurence Erlbaum Associates, Inc, Erlbaum, Hillsdale, NJ, pp. 349–376.

Hartmann, W. M., Rakerd, B., and Koller, A. (**2005**). "Binaural Coherence in Rooms," Acta. Acust. Acoust., **91**, 451-462.

Hebrank, J., and Wright, D. (**1974**). "Spectral cues used in the localization of sound sources on the median plane," J. Acoust. Soc. Am., **56**, 1829–1834. doi:10.1121/1.1903520

Hintze, J. L., and Nelson, R. D. (**1998**). "Violin Plots: A Box Plot-Density Trace Synergism," Am. Stat., **52**, 181–184. doi:10.1080/00031305.1998.10480559

Hirsh, I. J. (**1948**). "The Influence of Interaural Phase on Interaural Summation and Inhibition," J. Acoust. Soc. Am., **20**, 536–544. doi:10.1121/1.1906407

Houtgast, T., and Plomp, R. (**1968**). "Lateralization Threshold of a Signal in Noise," J. Acoust. Soc. Am., **44**, 807–812. doi:10.1121/1.1911178

Jacobsen, T. (**1976**). "Localization in noise," (Technical Report No. 10). (Technical University of Denmark Acoustics Laboratory, Denmark).

Lindevald, I. M., and Benade, A. H. (**1986**). "Two-ear correlation in the statistical sound fields of rooms," J. Acoust. Soc. Am., **80**, 661–664. doi:10.1121/1.394061

Lorenzi, C., Gatehouse, S., and Lever, C. (**1999**). "Sound localization in noise in normal-hearing listeners," J. Acoust. Soc. Am., **105**, 1810–1820. doi:10.1121/1.426719

Macpherson, E. A., and Middlebrooks, J. C. (**2002**). "Listener weighting of cues for lateral angle: The duplex theory of sound localization revisited," J. Acoust. Soc. Am., **111**, 2219. doi:10.1121/1.1471898

Mills, A. W. (**1958**). "On the Minimum Audible Angle," J. Acoust. Soc. Am., **30**, 237–246. doi:10.1121/1.1909553

Musicant, A. D., and Butler, R. A. (**1984**). "The influence of pinnae-based spectral cues on sound localization," J. Acoust. Soc. Am., **75**, 1195–1200. doi:10.1121/1.390770

Rakerd, B., and Hartmann, W. M. (**2010**). "Localization of sound in rooms. V. Binaural coherence and human sensitivity to interaural time differences in noise," J. Acoust. Soc. Am., **128**, 3052–3063. doi:10.1121/1.3493447

Shaw, E. A. G., and Teranishi, R. (**1968**). "Sound Pressure Generated in an External-Ear Replica and Real Human Ears by a Nearby Point Source," J. Acoust. Soc. Am., **44**, 240–249. doi:10.1121/1.1911059

Stecker, G. C., and Hafter, E. R. (**2009**). "A recency effect in sound localization?," J. Acoust. Soc. Am., **125**, 3914–3924. doi:10.1121/1.3124776

Strutt, J. W. (**1907**). "XII. On our perception of sound direction," Phil. Mag., **13**, 214–232. doi:10.1080/14786440709463595

Suzuki, Y., Yokoyama, T., and Sone, T. (**1993**). "Influence of interfering noise on the sound localization of a pure tone," J. Acoust. Soc. Jpn., **14**, 327–339. doi: 10.1250/ast.14.327

Tollin, D. J., and Henning, G. B. (**1999**). "Some aspects of the lateralization of echoed sound in man. II. The role of the stimulus spectrum," J. Acoust. Soc. Am., **105**, 838–849. doi:10.1121/1.426273

Wightman, F. L., and Kistler, D. J. (**1989**). "Headphone simulation of free-field listening. I: Stimulus synthesis," J. Acoust. Soc. Am., **85**, 858–867. doi:10.1121/1.397557

Wightman, F. L., and Kistler, D. J. (**1992**). "The dominant role of low-frequency interaural time differences in sound localization," J. Acoust. Soc. Am., **91**, 1648–1661. doi:10.1121/1.402445

Yost, W. A. (**1975**). "Comments on ''Lateralization and the binaural masking-level difference'' [G. B. Henning, J. Acoust. Soc. Am. 55, 1259–1263, (1974)]," J. Acoust. Soc. Am., **57**, 1214–1215. doi:10.1121/1.380548

Yost, W. A. (**1981**). “Lateral position of sinusoids presented with interaural intensive and temporal differences,” J. Acoust. Soc. Am., **70**, 397–409. doi:10.1121/1.386775

Yost, W. A., and Dye, R. H. (**1988**). “Discrimination of interaural differences of level as a function of frequency,” J. Acoust. Soc. Am., **83**, 1846–1851. doi:10.1121/1.396520

Yost, W. A., Wightman, F. L., and Green, D. M. (**1971**). “Lateralization of Filtered Clicks,” J. Acoust. Soc. Am., **50**, 1526–1531.

CHAPTER 3

Temporal Weighting Functions for Localization:

Effects of competing noise

3.1. Introduction

In complex, reverberant environments, the binaural cues supporting auditory localization vary in time. The information provided by the onset of the signal is known to contribute more so to location perception than the ongoing information. This is evidenced by phenomena known as the precedence effect and onset dominance. The precedence effect (also known as the "law of the first wavefront" or the "Haas effect"; Gardner, 1968; Zurek, 1987; Litovsky et al., 1999; Brown et al., 2015) is the perception that two spatially separated signals (the "lead" and the "lag") are fused as a single spatial percept when the delay between them is below the echo threshold. The echo threshold is the smallest delay in which both the lead and the lag signals are perceived as one stimulus toward the lead; the values range between 2 to 50 ms for click or speech stimuli, respectively (Litovsky et al., 1999; Brown et al., 2015). When the two signals are perceptually fused, with inter-stimulus intervals below the echo threshold, listeners perceive the fused signal at or towards the location of the leading signal.

Onset dominance is evident in studies of binaural adaptation as the failure of fusion of the spatial information provided by post-onset stimuli. Hafter and colleagues (Hafter and Dye, 1983; Hafter et al., 1983) provided listeners with trains of click stimuli with varying inter-click-intervals (ICIs) between click trains. It was expected that discrimination performance would improve with increasing duration of the click train if the binaural system integrated all temporal information in the stimulus. However, for ICIs less than or equal to 5 ms, performance did not improve as expected with additional post-onset information when the duration of the stimuli

increased, suggesting a lack of integration of the post-onset information. That is, for short ICIs or high modulation rates, listeners relied upon the binaural information at the onset of the stimulus. Similar to stimuli presented within the echo threshold during the precedence effect, clicks presented with short ICIs are onset-dependent. Conversely, with long ICIs or low modulation rates, the characteristics of each individual click are similar to stimulus onsets. The clicks occur slowly enough that the repeated clicks are outside the echo threshold, and each click provides distinct onset cues. Therefore, multiple clicks at low rates serve as consistent envelope onsets.

The direct measurement of onset dominance is possible with observer weighting methods. A temporal weighting function (TWF) measures the perceptual weighting across temporal epochs for localization (e.g., Stecker and Hafter, 2002) or lateralization [for interaural time difference (ITD) stimuli: e.g., Saberi, 1996; Freyman et al., 1997; Stecker and Brown, 2010; for interaural level difference (ILD) stimuli: Stecker and Brown, 2010]. For example, using click train stimuli, Stecker and Hafter (2002) measured TWFs in an anechoic chamber; their results revealed more onset dominance for shorter ICIs (e.g., 3 ms) than for longer ICIs (e.g., 8 and 14 ms). At longer ICIs, the onset and ongoing clicks similarly contributed to the perceived location of the click trains. At shorter ICIs, the onset click contributed most to the perceived location. The perceptual dominance of the onset is thought to aid in localization in reverberant environments where echoes can interfere with the ongoing stimuli by providing irrelevant cues, while the onset contains no such interference. However, most studies have been employed over headphones or in anechoic environments where reverberation is nonexistent.

To understand the effects of reverberation on onset dominance, Stecker and Moore (2018) measured TWFs in quiet and with the presence of simulated reverberation. For 5-ms ICI stimuli, onset dominance was more prevalent in reverberation than in anechoic conditions. Onset

dominance, therefore, is more evident in the presence of interfering echoes, consistent with the theorized importance of onset cues for auditory localization. These data demonstrate the importance of the stimulus onset for localization in quiet and in the presence of reverberation. However, less is known about how other complex, real-world environment factors, such as competing noise, affect onset dominance.

In natural environments, interference may arise from competing sound sources that occur before the target stimulus onset. Leakey and Cherry (1957) demonstrated a reduction of the salience of the onset in competing noise during a precedence effect task. In their task, they presented listeners with a lead and lag stimulus. The level of the lag stimulus was increased until the localized percept of the stimulus pair was no longer towards the lead, essentially overcoming the onset dominance. The amount of level increase to the lag needed to overcome onset dominance was dependent on the level of the competing noise. As the level of the competing noise increased, less of a level increase to the lag was needed to overcome onset dominance. When onset dominance was specifically measured with observer weighting methods during localization in competing noise, two studies revealed inconsistent results. When the target stimuli were Gaussian noise bursts, and the competing sound was Gaussian noise presented directly behind the listener, onset dominance was slightly but not significantly different in the presence of the competing sound when compared to onset dominance in quiet across various SNRs (Chiang and Freyman, 1998). For target speech stimuli presented with spatially diffuse babble as the competing noise, listeners (including listeners with hearing impairment) assigned to low SNR conditions (0 and +6 dB) had reduced onset dominance in the presence of competing noise when compared to onset dominance in quiet (Akeroyd and Guy, 2011).

The discrepancy between the results obtained by Chiang and Freyman (1998) and Akeroyd and Guy (2011) can stem from many factors. First, the location of the competing noise presented behind the listener by Chiang and Freyman (1998) may have reduced the deleterious effect of the competing noise on onset dominance. It has been found that competing sounds are more disruptive to localization when they are positioned at more lateral angles (-90° or +90°) than when positioned directly in front or behind (0° or 180°) the listener (Good et al., 1997; Lorenzi et al., 1999). Second, the study of Akeroyd and Guy (2011) included listeners with hearing impairment, and it is difficult to discern if a reduction in onset dominance was found specifically in listeners with normal hearing. Therefore, the current study measured the prevalence of onset dominance in the presence of competing noise presented at lateral angles (-90° and +90°) in participants with normal hearing. As in Chapter 2, the influence of the competing noise on localization performance was addressed as a secondary assessment of the data.

The current study aimed to measure TWFs in quiet and in the presence of competing noise at various SNRs. The current methods measure the relative weighting of individual clicks in a click train (as in Stecker and Moore, 2018), allowing to calculate not only the influence of stimulus pairs on location perception (as in Chiang and Freyman, 1998 and Akeroyd and Guy, 2011) but the influence of individual informative clicks (or events). Also, clicks were presented within a smaller degree of separation (22.5°) than stimulus pairs presented in Chiang and Freyman (1998) and Akeroyd and Guy (2011; 60° up to 120° azimuth, across midline). We tested the hypothesis that onset dominance would be reduced monotonically with the unfavorable decrease in SNR. The competing hypothesis is that the relative weight of the first click in the click train will be similar in quiet and in various levels of competing noise, revealing similar onset dominance across conditions.

3.2. Methods

TWFs were measured in quiet and in the presence of competing noise for participants with normal hearing. A 2-ms ICI was utilized as a high-rate stimulus known to elicit onset dominance (e.g., Stecker and Brown, 2010). TWFs were measured (and analyzed) similar to Stecker and Moore (2018), with the exception that Gaussian noise was presented in three SNR conditions (+9, 0, and -6 dB) for each stimulus condition.

3.2.1. Participants

The participants in the current study are the same participants from Chapter 2. Participants were ten adults (8 females) aged 21 – 28 years that were recruited from the Vanderbilt University community. Normal hearing was confirmed with pure tone audiometric thresholds of less than 20 dB HL that differed by less than 15 dB between left and right ears for octave frequencies from 250 to 8000 Hz. Participants were monetarily compensated. Approval was obtained for experimental procedures from Vanderbilt University Medical Center Institutional Review Board (IRB #191952). All participants in the current study also participated in the Chapter 2 study, including the author (0515).

3.2.2. Stimuli

All stimuli were generated in MATLAB (Mathworks, Natick, MA) and synthesized at 48 kHz. Stimuli were presented through the Dante audio-over-ethernet network (Focusrite Rednet, El Segundo, CA) with digital amplification (Ashly ne820PE, Webster, NY) for playback to a 64-loudspeaker array (Meyer MM-4, Berkeley, CA) in in the Vanderbilt Bill Wilkerson Anechoic Chamber Laboratory (ACL; 4.6 x 6.4 x 6.7 m; Eckel Industries, Cambridge, MA). The

loudspeakers in the ACL are at ear height, spanning 360° (5.625° of separation) with a 2-meter radius.

Stimuli include the target click trains participants localized (used to measure TWFs) and the competing noise. Target signals were trains of 16 4-kHz Gabor clicks (with a nominal duration of 2 ms) as in Stecker and Hafter (2002; 2009) and Stecker and Moore (2018). The inter-click-interval (ICI) of 2 ms was utilized. The overall level of the target signal was held constant, at 60 dB SPL, across SNR conditions. The spatial configuration of each click in the click train was manipulated from trial to trial to introduce spatial jitter, similar to Chapter 2. On each trial, a "base" azimuth was chosen from 11 possible locations; -56.26° to +56.26° in 11.25° steps. Five adjacent loudspeakers centered on the base azimuth [-11.25°, -5.625°, 0°, +5.625°, and +11.25° (relative to the base)] constituted the set of source loudspeakers from which individual components of the stimulus were presented on a given trial. Each click was randomly and independently assigned to one of the five source loudspeakers.

The competing noises were two 200-ms Gaussian noises independently generated for the left and right lateral loudspeakers (-90° and +90°) and presented simultaneously, 84 ms before the target signal. The level of the competing noise was dependent on the SNR condition: -6 dB SNR (66 dB SPL), 0 SNR (60 dB SPL), and +9 SNR (51 dB SPL).

3.2.3. Procedure

A touch-sensitive display (Apple iPad Air, Cupertino, CA) was mounted at a comfortable distance (~0.5 m in front and ~0.5 m below ear level) from the listener. This was used to record localization responses aligned to a top-down schematic of the room and loudspeaker array displayed on the screen (Fig. 2.1; a 180° arc with minimal reference points such as 0°). On each

trial, participants were instructed to sit upright and face directly forward (toward the loudspeaker at 0°) before and during each stimulus presentation. These instructions helped to ensure participants received expected spatial cues. Immediately following each single presentation of the stimulus, participants were instructed to make an eye movement to the target signal's perceived location and then record that location on the schematic diagram by touching the iPad screen. Participants were asked to indicate the leftmost edge or leftmost image on any trial in which the lateral percept appeared "wide" or "split." The response azimuth was computed from the touch screen response and recorded as the localization judgment. The base loudspeaker was selected pseudorandomly from 11 possible locations (± 56.25°) across trials, with each base value presented six times per run of 66 trials. Participants completed six runs (66 trials each) for each of the four conditions (quiet and three SNR conditions).

3.2.4. Analysis

TWFs were calculated separately for each listener and condition. Within each 66-trial run, the localization judgment was normalized by rank transform across each 66-trial run. Perceptual weights for each of the 16 clicks were estimated by multiple linear regression of the rank-transformed responses θ_R onto the azimuth values of each component θ_i.

$$\theta_R = \sum_{i=1}^{16} \beta_i \, \theta_i + k \tag{1}$$

Weights were computed by normalizing regression coefficients β_i so that absolute values summed to 1 across weights.

$$w_i = \beta_i \,/\, \sum_{j=1}^{16} |\beta_j| \tag{2}$$

The normalized weights w_i indicate the relative influence of the click i on participants' localization judgments. Plotted together, the normalized weights constitute the TWF for each listener in each condition. Group average TWFs were calculated by taking the arithmetic mean normalized weight across participants, for each click.

Stecker and Moore (2018) computed the "average ratio" (AR) as a univariate measure of non-uniformity, specifically with an emphasis on the first (onset). The AR_{onset} was used to interpret the prominence of onset dominance quiet and SNR conditions. The AR_{onset} was defined as the ratio of weight on the first click to the mean of the remaining clicks:

$$AR_{\text{onset}} = w_{\text{click 1}} \,/\, (\sum_{j \neq \text{click 1}} w_j / 15) \tag{3}$$

As in Stecker and Moore (2018), the current study computed the TWF confidence intervals and evaluated planned comparisons of weight and AR_{onset} by non-parametric bootstrap tests. Bootstrapped confidence intervals on mean weight values were computed by resampling weights, with replacement, across subjects to generate 2000 bootstrap replicates. The mean weight was computed for each replicate to estimate the sampling distribution of mean weights. Confidence intervals were computed at the 95% level by taking the 2.5 and 97.5 percentile points from this sampling distribution.

Null-hypothesis significance tests used a similar approach. Each measure (e.g., AR_{onset}) was resampled across participants to generate 2000 bootstrap replicates. A statistic of interest (e.g., mean or difference between two means) was then computed for each bootstrap replicate to

estimate the corresponding sampling distribution. The proportion of bootstrap replicates falling at or below the null-hypothesis prediction (e.g., AR <= 1) defines the (one-sided) p-value, which is expressed to one significant digit. For two-sided statistical tests, the p-value was computed as the minimum of proportions falling on either side of the prediction, doubled. When any proportion was zero (i.e., the bootstrap sampling distribution did not overlap the null-hypothesis prediction), p-values are listed at the resolution of the bootstrap test itself (i.e., $p < .0005$ for 2000-fold bootstrap).

When spectral weighting functions (SWFs) were measured in Chapter 2 in the same competing noise configuration, localization performance was degraded at low SNRs (see also: Abel and Hay, 1996; Lorenzi et al., 1999; Brungart and Simpson, 2009). SWF localization performance and TWF preliminary data suggested that some participants may experience error biases as a "pushing" or "pulling" of the target signal away or towards the competing noise in degrees azimuth during localization. Both phenomena have been experienced by listeners in Chapter 2 and in previous localization in noise experiments (Butler and Naunton, 1964; Good and Gilkey, 1996; Lorenzi et al., 1999; Best et al., 2007). To evaluate biases, the response values versus the base loudspeaker were plotted for individual participants (see Fig. 3.5). To further evaluate localization performance, root mean square (RMS) error (indicating errors made outside of the 22.5° range of spatial jitter) and the R^2 were calculated for each listener in each condition.

3.3. Results and Discussion

3.3.1. Temporal Weighting Functions

As in Stecker and Moore (2018), the current study computed the TWF confidence intervals and evaluated planned comparisons of weight and AR_{onset} by non-parametric bootstrap

tests. Bootstrapped confidence intervals on mean weight values were computed by resampling weights, with replacement, across subjects to generate 2000 bootstrap replicates. The mean weight was computed for each replicate to estimate the sampling distribution of mean weights. Confidence intervals were computed at the 95% level by taking the 2.5 and 97.5 percentile points from this sampling distribution.

Figure 3.1 displays the mean TWF obtained in quiet (left panel) and in the various levels of competing noise (remaining panels). For reference, the mean TWF found in quiet is replotted as a thin line in each competing noise panel. When measured in competing noise, the weight placed on the first click of the TWFs was significantly smaller across all SNR conditions ($p < .05$ indicated by asterisks). These results are consistent with those of Leakey and Cherry (1957) and Akeroyd and Guy (2011), in which onset dominance was reduced in the presence of competing noise. However, contrary to expectations from the results found by Leakey and Cherry (1957), there is no obvious pattern of onset dominance decreasing with decreasing SNR [see Chiang and Freyman (1999) on why the level adjustment methods in noise may represent loudness recruitment and not localization-specific onset dominance]. Any monotonic decrease in onset dominance with decreasing SNR should be apparent in Fig. 2.2, which displays AR_{onset} across quiet and competing noise conditions as violin plots.

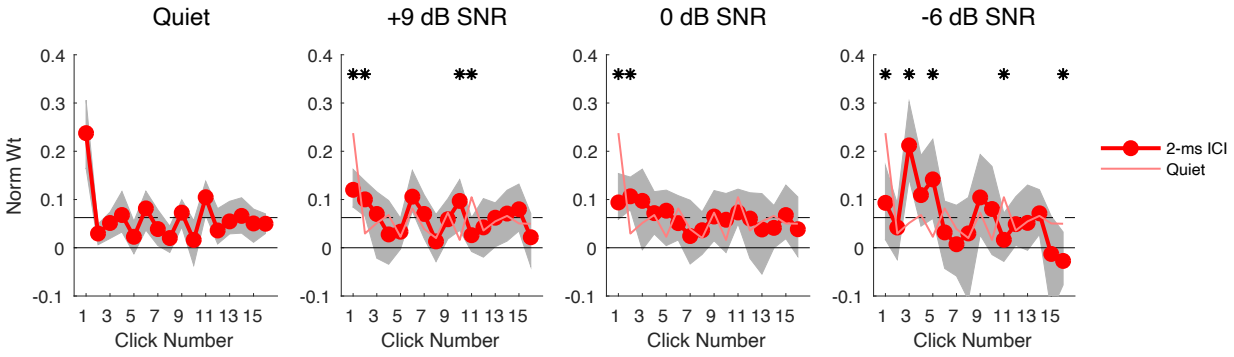

FIG. 3.1. Mean TWFs obtained in quiet and various levels of competing noise (columns: Quiet, +9 dB SNR, 0 dB SNR, and -6 dB SNR). Symbols and solid lines plot cross-participant mean normalized weight as a function of click number. Shaded regions indicate bootstrapped ±95% confidence intervals on each mean weight. Dashed lines indicate the expected value (1/16) for uniform weighting across components. Quiet TWFs are replotted as thin colored lines in competing noise panels for purposes of comparison. Bootstrapped, two-tailed, significant differences ($p < .05$) between click weights in quiet and competing noise are indicated with asterisks (*) at the top of each panel.

The mean AR_{onset} values, which indicate the degree of onset dominance relative to the remaining clicks, are displayed in Figure 2.2 (open circles). Analysis revealed that the quiet and +9 dB SNR conditions are significantly greater than 1, indicating non-uniform temporal weighting across clicks. However, the mean AR_{onset} value is significantly larger in quiet than in the +9 dB SNR condition, indicating a reduction in onset dominance with the introduction of competing noise. The mean AR_{onset} value in quiet is also significantly greater than all other noise conditions, with no significant differences between noise conditions. The mean AR_{onset} values are 2.1, 1.7, and 1.9 for +9, 0, and -6 dB SNR conditions, respectively. Indicating no pattern of

decreasing onset dominance with decreasing SNR. There may, however, be patterns of changes of the weighting function that the AR_{onset} values could not capture, such as an increase in weighting to later clicks.

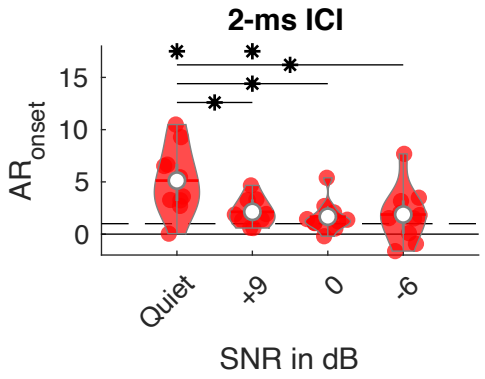

FIG. 3.2. Violin plots (Hintze and Nelson, 1998; Bechtold, 2016) of AR_{onset} values (vertical axis) are plotted for quiet and across SNR conditions (-6, 0, and +9 dB SNR; horizontal axis). Red circles plot AR_{onset} for individual participants; violin plots indicate the density (width of each violin) and mean (white circle) of obtained values. Dashed lines indicate the expectation for uniform temporal weighting AR = 1. Asterisks (*) indicate conditions in which AR_{onset} significantly exceeded this value ($AR_{onset} > 1$, $p < .01$ by 2000-fold bootstrap test). Asterisks with a line indicate bootstrapped significant differences between conditions ($p < .05$, two-tailed).

In competing noise, the weights to the second or later clicks were elevated. When the level of the noise was at or below the level of the target stimuli (+9 and 0 dB SNR; middle panels of Fig. 3.1), the weight given to the second click was significantly greater than in quiet. Similarly, when the noise increased beyond the level of the target (-6 dB SNR; right panel of Fig. 3.1), it was the third and fifth click in the click train that received a greater weight than in quiet.

Because the two competing noise sources were independently and randomly generated on each trial, there should be no such fluctuation in the envelope of the competing noise participants could rely on that would lead to a dominant weight later in the stimulus (as seen in the -6 dB SNR condition; click three). These patterns in a possible "shift" of the dominant weight from the onset in quiet (the first click) may be evident in Fig. 3, which plots the independent participant TWFs. For most participants, TWFs in quiet perceptually weigh the onset (click one) above the line of equity (dashed line: 1/16). Most of the remaining 15 clicks receive a weight less than .1. With a low level of noise added (+9 dB SNR), the onset is no longer above the line of equity for all participants; however, it is above zero. The remaining weights increase in range across participants compared to the range of weights in quiet, now all weighing less than .25. The range of weights continues to expand, both negatively and positively. This pattern is also evident in the confidence intervals of TWFs (Fig. 3.1) and the range of AR_{onset} values (Fig. 3.2), which increase with decreasing SNR. This phenomenon is most likely due to the decrease in localization performance with decreasing SNR, as found in the same competing noise configuration as Chapter 2. Along with the possible effects of localization degradation, with the increase in the range of weighting function patterns, it is difficult to assess any specific pattern change in the individual participant data (Fig. 3.1) evident in the cross-participant mean data (Fig. 3.1). Except for some ranges of weights across clicks, where all participants weighted the click above 0; for example, click three in the -6 dB SNR condition (Fig. 3.3 right panel).

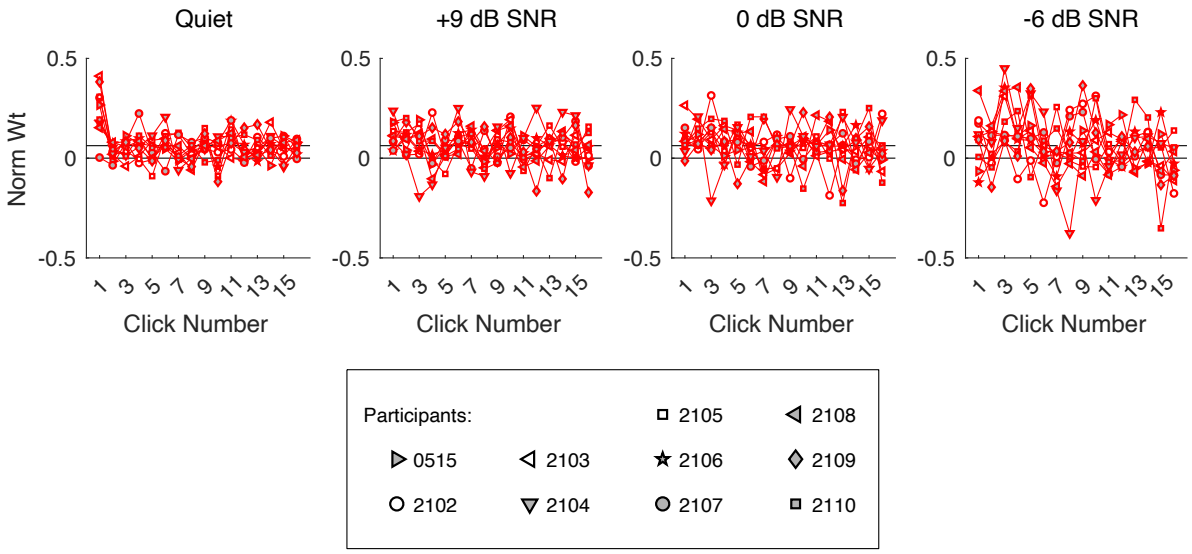

FIG. 3.3. Individual-participant TWFs found quiet (first panel) and in various levels of competing noise (remaining panels: +9 dB SNR, 0 dB SNR, and -6 dB SNR). Individual participant TWFs are plotted as independent symbols (legend at bottom).

3.3.2. Localization Performance in Competing Noise

The RMS error, indicating the errors made outside the 22.5° of spatial jitter, is plotted in the left panel of Fig. 3.4. The RMS error is plotted as a cross-participant mean for the quiet condition and each SNR condition. There were no significant differences in RMS error between conditions. These results are in disagreement with those of Chapter 2, in which the RMS error in the -6 dB SNR condition significantly differed from the +9 and 0 dB SNR condition. The mean RMS errors in the -6 dB SNR condition are similar to those found in Chapter 2 for the same condition. However, the mean RMS errors in the +9 and 0 dB SNR conditions in the current study fall to near 10°, whereas the RMS errors in the same conditions in Chapter 2 fall closer to 5°. The localization of the click stimuli may generally be more difficult for click stimuli than complex tones, even in quiet. Click trains in the current study have a high-rate envelope that can

carry an ITD cue, particularly an ITD envelope cue (Yost, 1976). Transposed tones, stimuli similar to Gabor clicks, have been found to have the same ITD threshold as pure tones (Bernstein and Trahoitis, 2002). Therefore, the ITD sensitivity for the current stimuli with a high-frequency carrier may be reduced for different reasons, such as the duration of click stimuli versus the duration of the tones when presented in competing noise (100 ms; Chapter 2), leading to slightly more localization errors for click trains in competing noise.

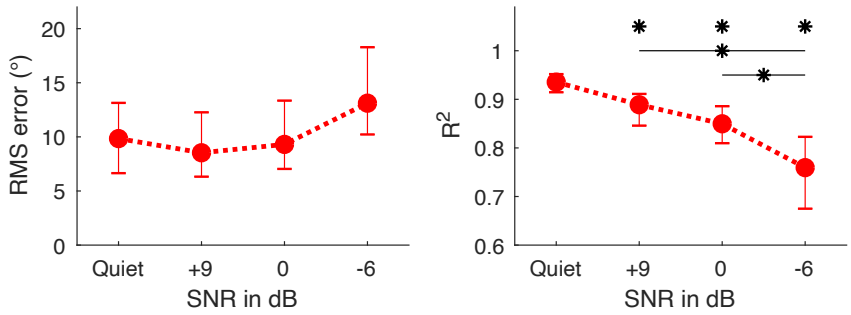

FIG. 3.4. The left panel plots mean RMS error (in degrees) across participants for the quiet and SNR conditions. The right panel plots the mean R^2 value across participants for the quiet and SNR conditions. Error bars indicate bootstrapped ±95% confidence intervals on each mean value (RMS error or R^2). Asterisks (*) indicate bootstrapped, two-tailed, significant differences ($p <$ .05) between (RMS error or R^2) values in quiet versus each SNR condition. Asterisks with lines indicate significant differences across SNR conditions.

The R^2 statistic for each TWF measurement (for each participant in each condition) indicates how well the data are accounted for by the multiple linear regression model (function 1) used to calculate weights. The right panel of Fig. 3.4 plots the mean R^2 value across participants as a function of SNR condition for each frequency stimulus. Bootstrapped difference

tests at each SNR value were calculated between the quiet and SNR conditions and between SNR conditions. Significant differences were found between the quiet condition and each individual SNR condition. Significant differences were also found between SNR conditions +9 dB and -6 dB and 0 dB and -6 dB but not between +9 and 0 dB. These results are similar to those found in Chapter 2, indicating that the level of the competing noise being above the level of the stimulus leads to more localization errors. However, at 0 dB, the mean R^2 value falls below .9, whereas in Chapter 2, the mean R^2 falls above .9. As noted earlier, the localization accuracy of clicks with a high-frequency carrier may be reduced compared to the localization accuracy of complex tones in low levels of noise for reasons such as the duration of the stimuli. The current R^2 data reveals a trend toward a reduction in the localization accuracy of a click train stimulus in competing noise. The data are also consistent with Chapter 2 and Lorenzi et al. (1999), where localization accuracy is significantly degraded in the unfavorable SNR condition (-6 dB SNR).

Five participants exhibited a pulling bias (2102, 2106, 2108, 2109, 2110); that is, the presence of the competing noise pulled the perception of the target click train towards the competing noise stimulus. Among these, only participant 2102 exhibited a pulling bias for all SNR conditions, with little to no responses near 0° for all conditions. Participants 2106, 2109, 2108, and 2110 exhibited a pulling bias only as the SNR unfavorably decreased. Response azimuths as a function of the base loudspeaker are plotted in Fig. 3.5 for participant 2108. In the quiet condition (left panel), participant 2108 had near-perfect localization, as responses were within the 22.5° range (solid grey lines). As the SNR unfavorably decreased, the response density for the lateral angles increased; responses progressively fell below and above the 22.5° range for negative and positive base values, respectively (especially for base values near 0°). For the -6 dB SNR, most responses for base values between -11.25° and 11.25° were closer to lateral

angles with minimal responses near 0°. There were also left/right confusions for negative base values (except for -56.25° and possibly -45°). No participants demonstrated a pushing bias. Participant 2109 had a pushing bias in Chapter 2, which changed to a pulling bias in the current study. This may be due to a change in the stimulus from complex tones to click trains (in the current study). Pulling biases have been reported by Butler and Naunton (1964) for tones presented with competing tones and by Good and Gilkey (1996) for noise bursts presented with competing broadband noise.

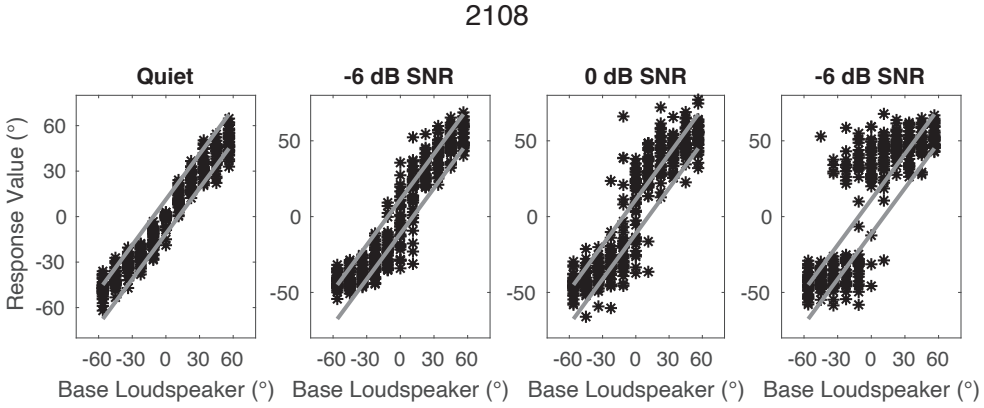

FIG. 3.5. Each panel plots individual response values (in degrees; before rank-transformation) as a function of the base loudspeaker (as asterisks) for participant 2108. Solid grey lines indicate the 22.5° range of responses around the base azimuth. Columns from left to right indicate the quiet and SNR conditions (+9 dB, 0 dB, and -6 dB), respectively.

3.3.3. Suggestions for the Reduction of Onset Dominance in Competing Noise

With the addition of a competing noise at various levels, TWFs in the current study have revealed a reduction in onset dominance. Recall that binaural adaptation, measured by Hafter and colleagues (Hafter and Dye, 1983; Hafter et al., 1983), demonstrates a reduction in the integration of ongoing ITD cue information for high-rate click trains. This phenomenon was

demonstrated with a relatively larger weight for the onset click than the ongoing clicks with observer weighting methods. Houtgast and Plomp (1964) demonstrated a similar phenomenon with a 500-Hz tone. That is, increasing the duration of the tone did not increase the sensitivity to the ITD of the tone as would be expected (i.e., there was reduced integration of ongoing ITD cue information). However, in the presence of competing noise Houtgast and Plomp (1964) found that increasing the duration of the tone led to an increase in the ITD sensitivity, essentially an increased integration of ongoing ITD cue information. The reasoning for this was said to be due to the reduction of an "onset" of the stimulus in the presence of competing noise. For example, if the onset is determined by the rising portion of the tone (or, in the current study, the first click), the competing noise may "mask" such rising portion. The attack time of the rising portion of the stimuli is reduced in the presence of competing noise. It is possible that in the current study, either across some or all trials, participants could not detect the onset portion of the first click.

For SNR conditions +9 and 0 dB, the weight of the second click significantly increased from quiet. One possibility is that, across some trials, the auditory system treated the second click as the first click and the first click was ignored or inaudible. This increase of weights at later clicks in the -6 dB SNR condition would then be due to the first few clicks being ignored or inaudible. One aspect of the stimuli known to reduce or "reset" onset dominance is the irregularity of the temporal envelope. Stecker (2018) found that when trains of noise bursts were identical noise tokens, onset dominance was similar to the current study in quiet. However, whenever the noise token changed, onset dominance occurred at the first noise token change. When noise tokens changed at each burst, no onset dominance occurred. In the current study, competing noise may have added temporal irregularity to the perception of the stimulus, overall reducing onset dominance. If participants could overcome the temporal irregularity of the masker

during later clicks, it is possible that the clicks were grouped, and onset dominance occurred later along the click train. Occurring more than once in the -6 dB SNR condition as evident in the increased weights above the line of equity later in the click train (see Fig. 3.1, right panel). These possible explanations for the reduction of onset dominance follow the reliable envelope-slope-triggered auditory representation theory (RESTART; Stecker et al., 2021), which states that there may be one mechanism in the processing of binaural cues that triggers binaural cue processing with a rising envelope. The current study can be further evaluated with a model that incorporates the RESTART theory, especially because the rising envelope is most likely reduced with the addition of noise. The competing noise can serve as a representation of internal noise or external noise found in real-world conditions.

3.4. Summary and Conclusions

The purpose of the current study was to explore the effects of competing noise on TWFs. The results of this study revealed three main findings:

1) TWFs measured in the presence of competing noise revealed a decrease in onset dominance across all SNRs (+9, 0, and -6 dB), consistent with the results of Akeroyd and Guy (2011). However, no distinct relationship was found between SNR and the amount of onset dominance reduction. Whether participants continue to rely upon the onset of a stimulus when faced with environmental noise is questionable.

2) Compared to TWFs measured in quiet, the second click in the +9 and 0 dB conditions revealed an increase in relative weight, while the third and fourth click revealed an increase in relevant weight in the -6 dB condition. The presence of the competing noise perhaps masked the rising part of the onset leading to onset-like events for later clicks. If so, this would be consistent

with the RESTART theory in that the rising part of the onset is particularly important for binaural integration.

3) The localization performance degraded with the addition of the competing noise, especially as the SNR was -6 dB SNR. A pulling effect of the stimulus toward the location of the masker for almost half of the participants. Pulling and pushing effects may be dependent on the stimulus type and duration.

REFERENCES

Akeroyd, M. A., and Guy, F. H. (**2011**). "The effect of hearing impairment on localization dominance for single-word stimuli," J. Acoust. Soc. Am., **130**, 312–323. doi:10.1121/1.3598466

Bernstein, L. R., and Trahiotis, C. (**2002**). "Enhancing sensitivity to interaural delays at high frequencies by using 'transposed stimuli,'" J. Acoust. Soc. Am., **112**, 1026–1036. doi:10.1121/1.1497620

Brown, A. D., and Stecker, G. C. (**2010**). "Temporal weighting of interaural time and level differences in high-rate click trains," The Journal of the Acoustical Society of America, **128**, 332–341. doi:10.1121/1.3436540

Brown, A. D., Stecker, G. C., and Tollin, D. J. (**2015**). "The Precedence Effect in Sound Localization," J. Assoc. for Res. in Otolaryn., **16**, 1–28.

Brungart, D. S., and Simpson, B. D. (**2009**). "Effects of bandwidth on auditory localization with a noise masker," J. Acoust. Soc. Am., **126**, 3199–3208. doi:10.1121/1.3243309

Chiang, Y.-C., and Freyman, R. L. (**1998**). "The influence of broadband noise on the precedence effect," J. Acoust. Soc. Am., **104**, 3039–3047. doi:10.1121/1.423885

Freyman, R. L., Zurek, P. M., Balakrishnan, U., and Chiang, Y.-C. (**1997**). "Onset dominance in lateralization," J. Acoust. Soc. Am., **101**, 1649–1659. doi:10.1121/1.418149

Gardner, M. B. (**1968**). "Historical Background of the Haas and/or Precedence Effect," J. Acoust. Soc. Am., **43**, 1243–1248. doi:10.1121/1.1910974

Good, M. D., and Gilkey, R. H. (**1996**). "Sound localization in noise: The effect of signal-to-noise ratio," J. Acoust. Soc. Am., **99**, 1108–1117. doi:10.1121/1.415233

Hafter, E. R., and Dye, R. H. (**1983**). "Detection of interaural differences of time in trains of high-frequency clicks as a function of interclick interval and number," J. Acoust. Soc. Am., **73**, 644–651. doi:10.1121/1.388956

Hafter, E. R., Dye, R. H., and Wenzel, E. (**1983**). "Detection of interaural differences of intensity in trains of high-frequency clicks as a function of interclick interval and number," J. Acoust. Soc. Am., **73**, 1708–1713. doi:10.1121/1.389394

Houtgast, T., and Plomp, R. (**1968**). "Lateralization Threshold of a Signal in Noise," J. Acoust. Soc. Am., **44**, 807–812. doi:10.1121/1.1911178

Leakey, D. M., and Cherry, E. C. (**1957**). "Influence of Noise upon the Equivalence of Intensity Differences and Small Time Delays in Two-Loudspeaker Systems," J. Acoust. Soc. Am., **29**, 284–286. doi:10.1121/1.1908858

Litovsky, R. Y., Colburn, H. S., Yost, W. A., and Guzman, S. J. (**1999**). "The precedence effect," J. Acoustic. Soc. Amer., **106**, 1633–1654.

Lorenzi, C., Gatehouse, S., and Lever, C. (**1999**). "Sound localization in noise in normal-hearing listeners," J. Acoust. Soc. Am., **105**, 1810–1820.

P. M. Zurek (**1987**). "The precedence effect," Directional Hearing, Springer, New York, NY, pp. 85–105.

Saberi, K. (**1996**). "Observer weighting of interaural delays in filtered impulses," Percep. and Psycho., **58**, 1037–1046. doi:10.3758/BF03206831

Shinn-Cunningham, B. G., Zurek, P. M., and Durlach, N. I. (**1993**). "Adjustment and discrimination measurements of the precedence effect," J. Acoust. Soc. Am., **93**, 2923–2932. doi:10.1121/1.405812

Stecker, G. C. (**2018**). "Temporal weighting functions for interaural time and level differences. V. Modulated noise carriers," J. Acoust. Soc. Am., **143**, 686–695. doi:10.1121/1.5022785

Stecker, G. C., Bernstein, L. R., and Brown, A. D. (**2012**). "Binaural Hearing with Temporally Complex Signals" In Binaural Hearing, Springer Handbook of Auditory Research, Springer International Publishing, Vol. 73. doi:10.1007/978-3-030-57100-9

Stecker, G. C., and Brown, A. D. (**2012**). "Onset- and offset-specific effects in interaural level difference discrimination," J. Acoust. Soc. Am., **132**, 1573–1580. doi:10.1121/1.4740496

Stecker, G. C., and Hafter, E. R. (**2002**). "Temporal weighting in sound localization," J. Acoust. Soc. Am., **112**, 1046–1057. doi:10.1121/1.1497366

Stecker, G. C., and Moore, T. M. (**2018**). "Reverberation enhances onset dominance in sound localization," J. Acoust. Soc. Am., **143**, 786–793. doi:10.1121/1.5023221

Yost, W. A. (**1976**). "Lateralization of repeated filtered transients," J. Acoust. Soc. Am., **60**, 178–181. doi:10.1121/1.381061

CHAPTER 4

Spectral Weighting Functions for Localization of Complex Sound: The Effect of Hearing Impairment

4.1. Introduction

Adult listeners with bilateral sensorineural hearing loss (SNHL) have a reduced ability to localize sounds relative to listeners with normal hearing, especially when sounds originate at more lateral angles (Noble et al., 1994; Dobreva et al., 2011; Cai et al., 2015). Monaural and binaural spatial hearing cues support a listener's ability to perform sound localization while providing the listener with situational awareness of 360° auditory space not available in the direct visual field. For localization in the horizontal plane, binaural cues are the dominant spatial hearing cues for sound localization (e.g., Wightman and Kistler, 1997). These cues arise from interaural differences between the two ears, including interaural level differences (ILDs) arising from attenuation of the sound by the head, and interaural time differences (ITDs), from the delay between the sound arriving at each ear. However, binaural cues vary in availability and reliability across frequency, and their utility changes across the spectral components of the signal.

For listeners with NH, low-frequency ITD cues tend to dominate during the localization of broadband stimuli (Macpherson and Middlebrooks, 2002; Wightman and Kistler, 1992). The ITD "dominance region" (Bilsen and Raatgever, 1973; Tollin and Henning, 1999) is a specific range of frequencies where ITD cues are particularly influential to the overall spatial percept. Spectral weighting functions (SWFs) measured during lateralization (Ahrens et al., 2020; Baltzell et al., 2020; Folkerts and Stecker, 2022) and localization (Folkerts and Stecker, 2022) display the relative weight (or influence) of each frequency component. For ITD and ILD cues

presented simultaneously (Folkerts and Stecker, 2022), participants place the greatest weight on the 800-Hz ITD component, as opposed to other components, including ILD components (i.e., the 800-Hz ILD component). The 800-Hz component is at the "peak" of the ITD dominance region; however, when components are within the overall range of the ITD dominance region (200-1000 Hz), weights are distributed evenly.

Although the salience of binaural cues across frequency has been established for NH listeners, it is not known if listeners with SNHL continue to give importance to the same specific cues across frequency. It has yet to be determined if listeners with SNHL also rely primarily on the ITD cue at the peak of the dominance region (the 800-Hz component) during localization.

Existing work investigating the localization of broadband stimuli by listeners with SNHL reveals their performance is slightly reduced when compared to listeners with NH (Hausler et al., 1983; Nobel et al., 1994; Van den Bogaert et al., 2006; Keidser et al., 2009; Best et al. 2010; Neher et al., 2011; van Esch et al., 2013; Brungart et al., 2017). The studies of Smith-Olinde et al. (1998), Van den Bogart et al. (2006), and Keidser et al. (2009) measured the localization ability of listeners with SNHL with noise bands centered at a low center frequency (400 or 500 Hz) and separately with noise bands centered at a high center frequency (3000 or 3100 or 4000 Hz). Across studies, listeners with SNHL localized the low-frequency noise bands with better accuracy than the high-frequency noise bands. However, performance was reduced compared to NH listeners, with no trends suggesting that performance was reduced more for low- or high-frequency stimuli (see also van Esch et al., 2013). Assuming the low-frequency noise represents ITD-based localization and high-frequency noise represents ILD-based localization, the data suggests listeners with SNHL have a reduced ability to utilize both the ITD and ILD cues

(however, do note that ITD cues provided by the envelope of high-frequency noise bands are also available).

Listeners with SNHL have also demonstrated a reduction in ITD and ILD lateralization sensitivity compared to listeners with NH (Gabriel et al., 1992; Koehnke et al., 1995; Smith-Olinde et al., 1998). The ITD threshold of listeners with SNHL, measured with a low- and high-frequency centered noise band, is poorer than listeners with NH (Hawkins and Wightman, 1980). A close examination of the results of Hawkins and Wightman (1980) reveals that some listeners with SNHL have sensitivity similar to NH listeners for the low-frequency stimulus; however, thresholds for the high-frequency stimulus were much poorer for all listeners with SNHL. The highest frequency in which an ITD could be detected decreases for listeners with SNHL to about 850-Hz compared to 1230 Hz for listeners with normal hearing (Neher et al., 2011). Although age may be a confound when measuring the sensitivity to binaural cues (e.g., Ross et al., 2007; Strelcyk and Dau, 2009; King et al., 2014).

Combined, these findings suggest that listeners with SNHL have reduced reliability of binaural cues. To explore this hypothesis, Folkerts and Stecker (2022) measured SWFs in listeners with NH using reduced levels of high-frequency components in a broadband signal, partially simulating high-frequency hearing loss by reducing the audibility of high-frequency sounds. If SNHL affects spectral weighting, the level of each frequency component would be expected to change the weighting of cues across frequencies. Their results demonstrated an upweighting of low-frequency components, which were higher in sound level than the high-frequency components. This change in SWF is consistent with the "level dominance" theory, which suggests perceptual weighting depends on each component's level (Berg, 1990; Lutfi and Jesteadt, 2006). These results indicate that adults with typical age-related hearing loss (e.g., mild

sloping to moderately severe sensorineural hearing loss; e.g., Allen and Eddins, 2010) would increase the weight to low-frequency components compared to listeners with NH, which would be perceptually higher in level than the high-frequency components. However, the level adjustment technique used by Folkerts and Stecker (2022) does not account for all of the changes in the auditory system associated with SNHL, such as steep growth of loudness (e.g., Allen et al., 1990)

One way to account for both the loss of audibility and steep growth of loudness is by introducing a threshold elevating noise masker (Steinberg and Gardner, 1937). Masking allows for the presentation of stimuli at equal SPL, resulting in the same sensation level for listeners with NH as would be expected for listeners with SNHL. Therefore, along with SWFs measured in participants with SNHL, the current study measured SWFs in NH participants in the presence of a spectrally shaped noise masker. Based on the preceding review, it was expected that the SWFs would reveal a shift in the "peak" of the dominance region toward lower frequencies for participants with simulated and real SNHL. Any differences between real and simulated SNHL could then be attributed to other consequences of SNHL (e.g., suprathreshold processing deficits; e.g., Plomp, 1978). The localization accuracy of participants with simulated and real SNHL was compared to determine if masking accounts for the known localization degradation of SNHL listeners. The effect of hearing loss and age on SWFs (specifically the weight placed at 800 Hz) was determined for participants with SNHL.

4.2. Methods

SWFs were measured in NH participants in quiet and in the presence of a threshold elevating noise (TEN) masker that was spectrally shaped, following the methods of Desloge et

al. (2010). Unlike the work of Desloge and colleagues, the TEN was implemented in the free field as a diffuse noise, arriving from all available loudspeakers, surrounding the participant 360° in azimuth. For all NH participants, the target hearing level during simulation was that of a typical mild-moderate SNHL in the free field. Free-field detection thresholds were measured and compared across participants with SNHL in quiet and in TEN. SWFs were also measured in participants with a bilateral, mild-moderate SNHL with thresholds similar to those simulated in participants with NH (see Fig. 1). Three complex tone stimulus conditions used by Folkerts and Stecker [2022; octave frequencies from 100 to 6400 Hz (T1), harmonics of 200 Hz spanning 200 to 1400 Hz (T2), and harmonics of 800 Hz spanning 800 to 5600 Hz (T3)] were utilized. SWFs were measured (and analyzed) in a similar manner to Folkerts and Stecker (2022). Comparisons were made between NH SWFs, TEN SWFs, and SNHL SWFs.

4.2.1. Participants

Participants with NH were ten adults (7 females) aged 21 – 32 years that were recruited from the Vanderbilt University community. NH was confirmed with pure tone audiometric thresholds less than 20 dB HL that differed less than 15 dB between left and right ears for octave frequencies from 250 to 8000 Hz. Participants 0515 (author), 2103, 2104, 2105, 2106, 2107, 2108, and 2109 also participated in the studies of Chapters 2 and 3.

Participants with SNHL were fourteen adults (9 females) aged 28 – 83 years (median: 74) that were recruited based on their hearing loss status through the Vanderbilt University Medical Center Audiology Clinic. Participants' pure tone audiometric thresholds were near the mild-moderate range of losses for a symmetrical sloping high-frequency SNHL (Bisgaard et al., 2010). Specifically, participants were recruited if their thresholds at 500 Hz were 20 – 45 dB HL,

at 1000 Hz were 30 – 50 dB HL, and at 4000 Hz were 50 – 70 dB HL, with no greater than a 30-dB difference across all frequencies and no greater than a 20-dB difference across three consecutive frequencies. Pure tone audiometric thresholds were remeasured if the thresholds in record were measured over six months prior to the recruitment date. All participants were monetarily compensated. Approval was obtained for experimental procedures from Vanderbilt University Medical Center Institutional Review Board (IRB #191952).

4.2.2. Target Stimuli

All stimuli were generated in MATLAB (Mathworks, Natick, MA) and synthesized at 48 kHz. Stimuli were presented through the Dante audio-over-ethernet network (Focusrite Rednet, El Segundo, CA) with digital amplification (Ashly ne820PE, Webster, NY) for playback to a 64-loudspeaker array (Meyer MM-4, Berkeley, CA) in in the Vanderbilt Bill Wilkerson Anechoic Chamber Laboratory (ACL; 4.6 x 6.4 x 6.7 m; Eckel Industries, Cambridge, MA). The loudspeakers in the ACL are at ear height, spanning 360° (5.625° of separation) with a 2-meter radius.

Target stimuli for the measurement of free-field thresholds consisted of pure tones. All tones were presented from the loudspeaker directly in front of the participant (at 0° azimuth; see section 4.2.3 for the task). The duration of each tone was 500 ms with 10-ms cos2 onset/offset ramps. Thresholds were measured for the following frequencies: 250, 500, 1000, 2000, 3000, 4000, 6000, and 8000 Hz. The level of the tone was adjusted with a custom MATLAB script using a two-down, one-up procedure to arrive at a 70.1% correct threshold level (Levitt, 1971). A step size of 10 dB was used for the first four reversals, and a step size of 2 dB was used for the last four reversals. The threshold value was calculated from the average of the last four reversals.

Target stimuli for the measurement of SWFs included three stimulus conditions comprised of tone complexes consisting of seven pure-tone components. The duration of the tone complex was 100 ms with 10-ms cos2 onset/offset ramps. The component configuration was octave frequencies from 100 to 6400 Hz for T1, harmonics of 200 Hz spanning 200 to 1400 Hz for T2, and harmonics of 800 Hz spanning 800 to 5600 Hz for T3. Stimuli were presented at a level corresponding to 60 dB, with components presented at equal amplitude. The spatial configuration of each of the seven frequency components was manipulated from trial to trial to introduce spatial jitter. On each trial, a "base" azimuth was chosen from 11 possible locations; -56.26° to +56.26° in 11.25° steps. Five adjacent loudspeakers centered on the base azimuth [-11.25°, -5.625°, 0°, +5.625°, and +11.25° (relative to the base)] constituted the set of source loudspeakers from which individual components of the stimulus were presented on a given trial. Each component was randomly and independently assigned to one of the five source loudspeakers.

4.2.3. Masking Noise for Hearing Loss Simulation

To create the TEN masker, the estimates for hearing thresholds of a mild SNHL (Bisgaard et al., 2010; Table 1) were chosen. The critical ratios from Desloge et al. (2010) were then subtracted from the target hearing levels independently for each frequency (125, 250, 500, 1000, 1500, 2000, 3000, 4000, 6000, and 8000 Hz) to determine the spectrum level sufficient to mask that specific tone (Hawkins and Stevens, 1950). Linear interpolation was used to determine the spectrum level of 22 1/3-octave bands of noise with center frequencies ranging from 79 Hz to 10 000 Hz. A filter was then created from the 22 1/3-octave bands of noise. Independent samples of Gaussian noise were passed through the filter to create 64 TEN noise samples. Each noise

sample was presented randomly (across trials) to one of the 64 loudspeakers in the ACL, resulting in a diffuse TEN masker.

The duration of the TEN was 1100 ms with 10-ms $\cos^2$ onset/offset ramps. During the free-field threshold task, the TEN was presented 300 ms before the tone onset and terminated 300 ms after the tone offset. During the SWF task, the TEN was presented 500 ms before the complex tone onset and terminated 500 ms after the complex tone offset.

4.2.4. Procedure

Following informed consent and monaural threshold measurement, participants completed two tasks, a free-field threshold detection task and the SWF task. Participants were instructed to select the interval that contained the tone during a three interval, forced-choice procedure for the free field threshold task. Responses were made on a touch-sensitive display (Apple iPad Air, Cupertino, CA) which was mounted at a comfortable distance (~0.5 m in front and ~0.5 m below ear level) from the participant. The iPad provided a visual cue to signify each interval and feedback to the participant immediately after each response. Thresholds were measured once per frequency for a total of eight runs per condition (8 total runs for participants with SNHL [quiet only] and 16 total runs for participants with NH [quiet and TEN masker]).

The SWF task was the same task used to measure SWFs in quiet (Folkerts and Stecker, 2022) and in competing noise (Chapter 2). Briefly, participants were instructed to make an eye movement to the perceived location of the target signal and then to record that location on the schematic diagram (180° arc; Fig. 2.1) by touching the iPad screen. The response azimuth was computed from the touch screen response and recorded as the localization judgment.

During data collection, the 180° arc utilized to collect response azimuths had to be switched over to a 360° arc (Fig. 4.1) for four participants with SNHL (2206, 2207, 2209, and 2217). This transformation was necessary because, on each trial, the participant nearly always localized the stimulus presented in front of the participant as originating behind them. To assess if SWFs could be measured in these participants with front-back confusions, responses were mirrored along the frontal (coronal) plane (Middlebrooks and Green, 1991). Figure 4.2 plots each response value as a function of the base loudspeaker for participant 2207 in each stimulus condition (panels). Black asterisks indicate original response values. Blue asterisks indicate response values behind the listener on the left, which were then subtracted from -180°. Red asterisks indicate response values behind the listener on the right, which were then subtracted from 180°. After responses were transformed, localization performance was quite accurate (i.e., response values were within the 22.5°-degree range; indicated by solid grey lines in Fig. 4.2), indicating that participants had front-back errors. Therefore, SWFs were measured in participants who localized stimuli behind them (2206, 2207, 2209, and 2217) with responses transformed before SWF, RMS error, and R^2 calculations (see Analysis section 4.2.5).

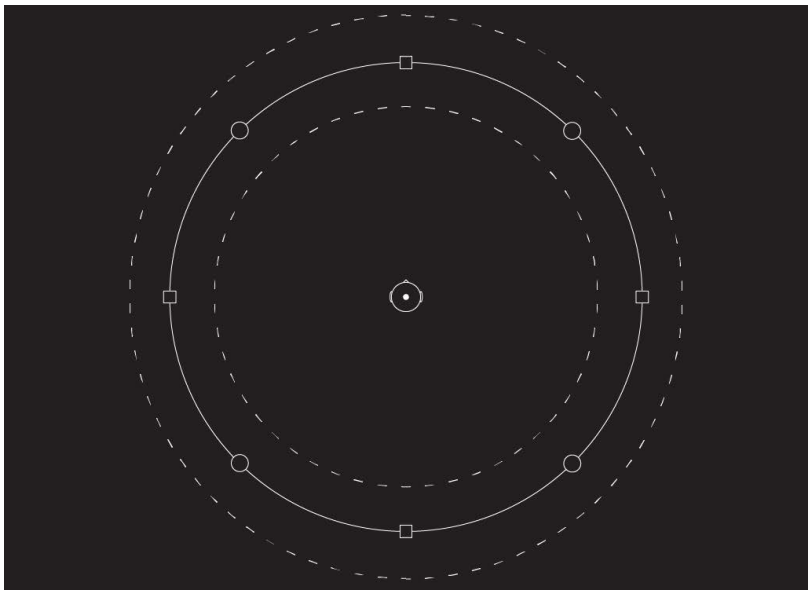

FIG. 4.1. Schematic used to record localization responses. The head marks the participant with a centered white dot at the middle portion of the 360° arc (circle). The solid white line of the circle indicates the loudspeaker array. Landmarks are included along the solid line indicating 0° (empty top square), +180° (empty bottom square), -90° and +90° (empty bottom squares), and -45° and +45° (empty top middle circles) and -135° and +135° (empty bottom circles). In the sound field, -45° and +45° were marked by unused circular loudspeakers. Dashed lines were used to indicate the distance (if necessary), either in front or behind the loudspeaker array.

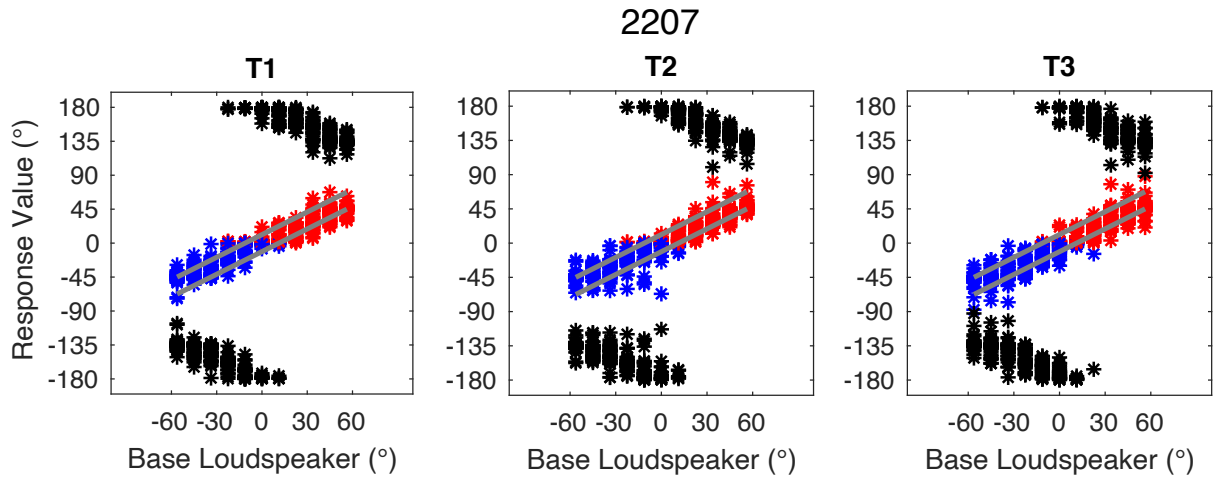

FIG. 4.2. Each panel plots individual response values (in degrees; before rank transformation) as a function of the base loudspeaker (as asterisks) for participant 2207. Black asterisks indicate response values before transforming responses to the frontal horizontal field. Red asterisks indicate response values that were greater than 90° which were then subtracted from 180°. Blue asterisks indicate response values that were less than -90° which were then subtracted from -180°. Solid grey lines indicate the 22.5° range of responses around the base azimuth. Columns from left to right indicate stimulus conditions (T1, T2, and T3).

The base loudspeaker was selected pseudorandomly from 11 possible locations (± 56.25°) across trials, with each base value presented six times per run of 66 trials. Participants completed six runs (396 trials) for each of the three stimulus conditions [octave frequencies from 100 to 6400 Hz (T1), harmonics of 200 Hz spanning 200 to 1400 Hz (T2), and harmonics of 800 Hz spanning 800 to 5600 Hz (T3)]. Participants with NH completed two sets, one in quiet and one in the presence of the TEN in random order, with sets interleaved.

4.2.5. Analysis

Free-field thresholds, initially measured in dB SPL, were converted to dB HL by means of subtracting the RETSPL (ANSI/ASA S3.6-2004, Annex C) from the measured threshold in dB SPL.

SWFs were calculated in the same manner as the SWFs in quiet (Folkerts and Stecker, 2022) and in competing noise (Chapter 2). That is, perceptual weights for each of the seven frequency components were estimated by multiple linear regression of the rank-transformed responses θ_R onto the azimuth values of each component θ_i.

$$\theta_R = \sum_{i=1}^{7} \beta_i \, \theta_i + k \tag{1}$$

Weights were computed by normalizing regression coefficients β_i so that absolute values summed to 1 across weights.

$$w_i = \beta_i \, / \sum_{j=1}^{7} |\beta_j| \tag{2}$$

The normalized weights w_i indicate the relative influence of the frequency component i on participants' localization judgments. Plotted together, the normalized weights constitute the SWF for each participant in each condition. Group average SWFs were calculated by taking the arithmetic mean normalized weight across participants for each component (separately for NH in quiet, NH in TEN, and SNHL in quiet).

Both Folkerts and Stecker (2022) and Chapter 2 computed the "average ratio" (AR) as a univariate measure of non-uniformity, specifically with an emphasis on the 800-Hz component in the ITD dominance region (AR_{800}). The AR_{800} was calculated in the current study to determine

the prevalence of the upweighting of the 800-Hz component between participants with simulated and real SNHL and participants with NH in quiet. The AR_{800} was defined as the ratio of weight on the 800-Hz component to the mean of other weights:

$$AR_{800} = \mathrm{w}_{800Hz} / (\sum_{j \neq 800Hz} w_j / 6) \quad (3)$$

The AR_{800} was calculated for each participant in each stimulus condition, and the group average was the arithmetic mean across participants (separately for NH in quiet, NH in TEN, and SNHL in quiet).

As in Folkerts and Stecker (2022) and Chapter 2, the current study computed the SWF confidence intervals and evaluated planned comparisons of weight and AR_{800} by non-parametric bootstrap tests. Bootstrapped confidence intervals on mean weight values were computed by resampling weights, with replacement, across subjects to generate 2000 bootstrap replicates. The mean weight was computed for each replicate to estimate the sampling distribution of mean weights. Confidence intervals were computed at the 95% level by taking the 2.5 and 97.5 percentile points from this sampling distribution.

Null-hypothesis significance tests used a similar approach. Each measure (e.g., AR_{800}) was resampled across participants to generate 2000 bootstrap replicates. A statistic of interest (e.g., mean or difference between two means) was then computed for each bootstrap replicate to estimate the corresponding sampling distribution. The proportion of bootstrap replicates falling at or below the null-hypothesis prediction (e.g., AR <= 1) defines the (one-sided) p-value, which is expressed to one significant digit. For two-sided statistical tests, the p-value was computed as the minimum of proportions falling on either side of the prediction, doubled. When any

proportion was zero (i.e., the bootstrap sampling distribution did not overlap the null-hypothesis prediction), p-values are listed at the resolution of the bootstrap test itself (i.e., $p < .0005$ for 2000-fold bootstrap).

To evaluate localization performance, the root mean square (RMS) error (indicating errors made outside of the 22.5° range of spatial jitter) and the R^2 (from measured SWFs) were calculated for all participants in each stimulus condition.

4.3. Results and Discussion

4.3.1. Free-field Detection Thresholds

Figure 4.3 plots the free-field detection thresholds (dB HL) of all participants separately (symbols) for participants with NH in quiet (grey), participants with NH in TEN (orange), and participants with SNHL in quiet (light blue). The target hearing level for the TEN is marked by a solid black line. Average thresholds across frequency reveal that participants with SNHL have threshold improvements (by 6 dB) in the free field, more so than participants with NH (3 dB) when thresholds are compared to better ear monaural headphone thresholds. The improvement in thresholds, or decrease in dB HL, was most apparent at 250 Hz, where the decrease in dB HL was 12.7 for participants with NH and 13.8 dB. The decrease in dB HL was least apparent at 4000 Hz (-1.3 dB) for participants with NH and 8000 Hz (-0.3 dB) for participants with SNHL. For the remaining frequencies, the decrease in dB HL ranged from .4 to 3.3 dB for participants with NH and 2.1 to 7.6 for participants with SNHL.

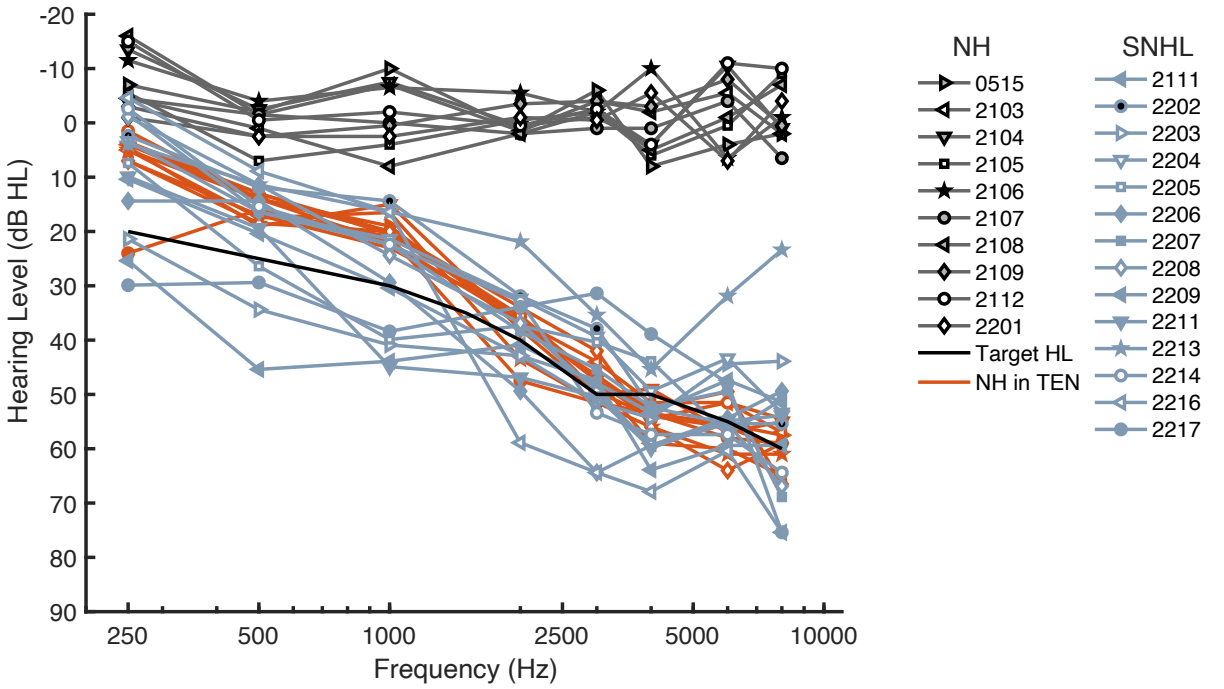

FIG. 4.3. Individual-participant free-field hearing thresholds (in dB HL) are plotted as a function of test tone frequency. The quiet thresholds of NH participants are plotted as grey lines with symbols (left side of legend). The quiet thresholds of SNHL participants are plotted as light blue lines with symbols (right side of legend). The TEN thresholds of NH participants are plotted as orange lines with symbols (left side of legend). The solid black line represents the target threshold levels of the TEN.

Compared to the literature, these results from participants with NH are similar on average to the expected 3 dB binaural advantage (Hirsh, 1948); however, participants with SNHL demonstrated an average benefit twice that size. Early threshold differences between free-field and monaural headphone thresholds revealed a 6-dB difference, with free-field thresholds being "better" by 6 dB (Sivian and White, 1933). Killion (1978), however, found that when accounting for the binaural advantage, a correction for eardrum pressure in the free field (being higher if

calibration is done with the listener absent; as done in the current study) and physiological noise (which reduces thresholds measured with headphones at low frequencies) thresholds in the free field are the same as monaural headphone thresholds. However, correcting these discrepancies in the current data would continue to result in an additional 3-dB advantage found in SNHL participants. Somewhat related are results from studies on the binaural loudness summation, which reveal no significant differences between listeners with NH and SNHL except for at levels above 60 dB SPL (e.g., Hawkins et al., 1987, Oetting et al., 2016).

Other methodological factors in the current study can be driving this free-field advantage. Threshold measurements in the free field and over headphones in the current study were derived using different psychophysical procedures, and the monaural thresholds were measured with the standard clinical method (modified Hughson-Westlake; Hughson and Westlake, 1944). The forced-choice procedure of the current study is reported to result in lower thresholds (Hesse, 1986). Step sizes between the two methods (5 dB for monaural headphones and 2 dB for binaural thresholds) should also be considered, and the tone presentation (pulsed for monaural headphones and steady-state for binaural thresholds). Free field and monaural headphone thresholds should be closely examined and remeasured, with minimal methodological differences, to find if there is a difference in binaural advantage between NH and SNHL participants.

These results also reveal the simulation of SNHL (Fig. 4.3; orange lines) for all participants falls near the target threshold (solid black line), although the match is closer for high frequencies (2000 Hz and above) than for lower frequencies (1000 Hz and below). At 1000 Hz and below, the overall level of the TEN was below 30 dB SPL. Confirmation of these target levels with a sound level meter proved difficult as the target levels were near the noise floor of

the sound level meter. Even with these lower-than-expected threshold levels, the threshold level at 250 Hz for 9/14 participants with SNHL fell at or below the threshold range of NH TEN thresholds (not including participant 2107, who had a higher threshold). Threshold levels at 500 and 100 Hz for 7/14 and 6/14 participants with SNHL, respectively, fell at or below the threshold range of NH TEN thresholds. At and above 2000 Hz, most of the SNHL participants' thresholds fell at or below the threshold range of NH TEN thresholds. The TEN was capable of representing the free-field hearing level of most participants with SNHL (Fig 4.3, light blue lines versus orange lines). Although it is known that TEN can accurately represent SNHL thresholds over headphones (e.g., Dubno and Schaefer 1992; Desloge et al., 2010), the current study is the first to implement the TEN in the free field as a diffuse masker.

4.3.2. Spectral Weighting Functions

Figure 4.4 plots cross-participant mean SWFs for NH participants in quiet (left column) and in the presence of the TEN (middle column) and for SNHL participants in quiet (right column). For stimulus condition T1 (octave tones 100-6400 Hz), in Folkerts and Stecker (2022; see Fig. 1.1), maximum weight was placed on the 800-Hz component with a lower weight placed on the 400-Hz component with a difference of .08. In the current study for participants with NH in quiet (T1; top left panel), the difference between component weights at 800 Hz and 400 Hz was markedly less (.02), revealing a "broadening" of the peak in the dominance region. Across studies, no other differences of this magnitude were found for stimulus condition T2 (harmonic tones 200-1400 Hz; middle panels) or T3 (harmonic tones 800-5600 Hz; top panels).

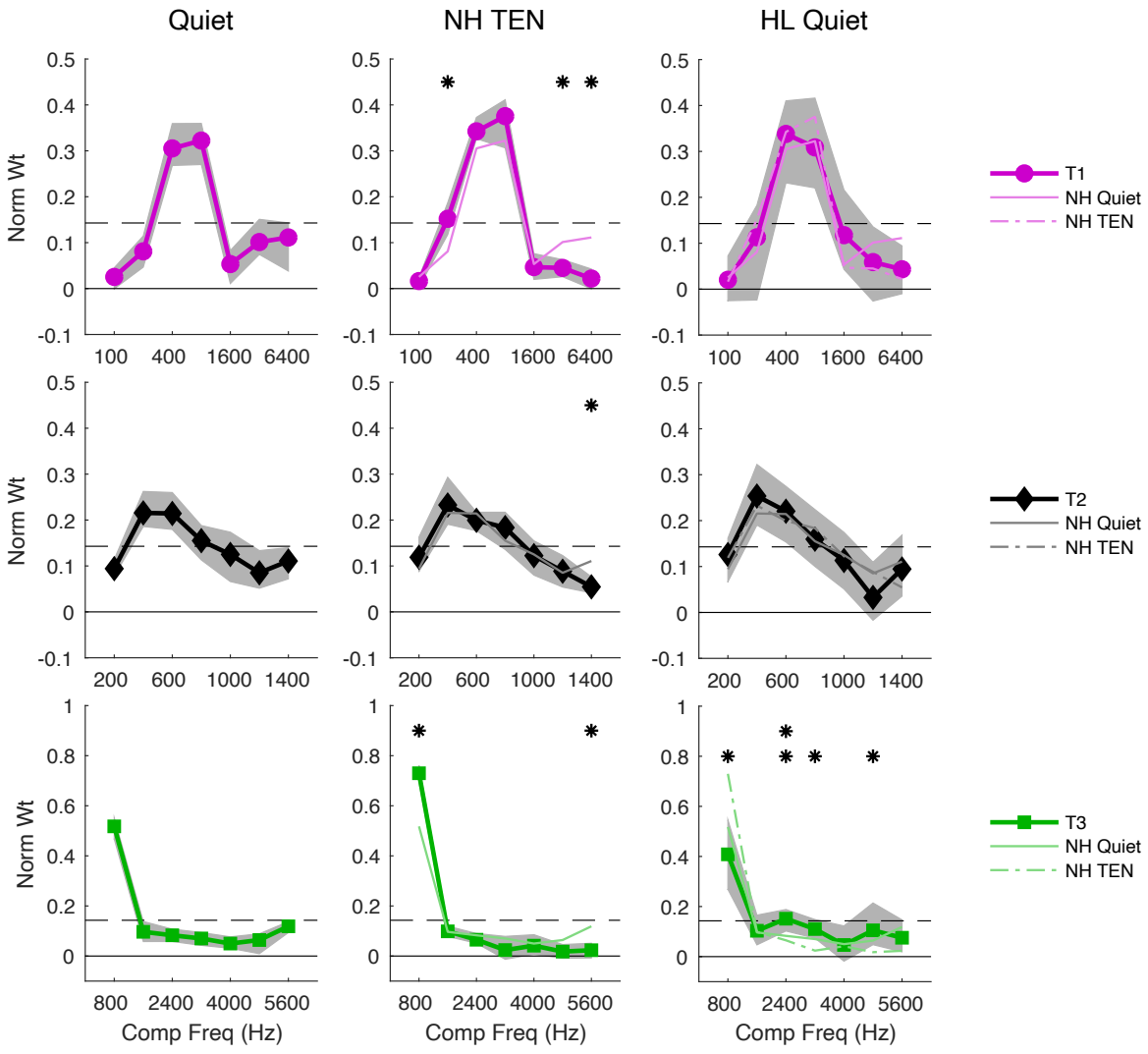

FIG. 4.4. Mean SWFs obtained across participants with NH in quiet (left column), NH in TEN (middle column), and SNHL in quiet (right column). The rows plot SWF data for stimulus conditions T1 (magenta circles; top row), T2 (black diamonds), and T3 (green squares). Symbols and thick lines plot cross-participant mean normalized weight as a function of component frequency. Shaded regions indicate bootstrapped ±95% confidence intervals on each mean weight. Dashed lines indicate the expected value (1/7) for uniform weighting across components. NH quiet SWFs are replotted as thin colored lines in NH TEN and SNHL quiet panels for purposes of comparison. NH TEN SWFs are replotted as thin colored dashed-dot lines in and

SNHL quiet panels also, for purposes of comparison. Bootstrapped, two-tailed, significant differences ($p < .05$) between weights for NH quiet and NH TEN or SNHL quiet weights are indicated with asterisks (*) at the top of each panel. Significant differences between weights for NH TEN and SNHL quiet weights are indicated with asterisks below the top asterisks.

Finding a shift of the peak of the dominance region was expected for NH in TEN and SNHL in quiet. However, for stimulus condition T1 (Fig. 4.4; magenta circles), this shift was apparent for NH in quiet, NH in TEN, and for SNHL in quiet when compared with SWFs measured by Folkerts and Stecker (2022). Leading to no significant differences in the 400 Hz weight across for NH in quiet, NH in TEN, and for SNHL in quiet. One possibility is that participants with NH changed their localization strategy (i.e., using both the 400- and 800-Hz component) during blocks of runs with the TEN which generalized to blocks of runs in quiet since quiet and TEN blocks were interleaved. However, there still were significant differences between weights in quiet and in the presence of the TEN for NH participants. That is, an increase in the 200-Hz component weight in TEN and a decrease in the highest frequency component weights (4800 and 5600 Hz). Significant differences were also found in stimulus conditions T2 and T3 between weights for participants with NH in quiet and in the presence of the TEN (Fig. 4.4; thin colored line). Namely, in stimulus conditions T2 and T3, the highest frequency component weight (1400 and 5600 Hz, respectively) was reduced in TEN, and in stimulus condition T3, the 800-Hz component weight increased. Therefore, even with the increase in the 400-Hz component in quiet (relative to our previous study), there was still an increase in relative weight to lower frequency components and a decrease in higher frequency components in the presence of the TEN. However, with the exception of stimulus condition T2 (which continues to

reveal relatively flat weights; see Folkerts and Stecker, 2022), the ITD dominance region (with a peak around 400-800 Hz) continues to be the salient frequency region for localization.

SWFs measured in participants with SNHL, when compared to SWFs for NH participants in quiet and in the presence of the TEN, only revealed significant differences in weights for stimulus condition T3 (Fig. 4.4; bottom right). The 2400-Hz component weight was significantly larger in SNHL participants in quiet when compared to NH participants in quiet (Fig. 4.4; thin green line). The 2400-Hz component weight, as well as the 3200- and 4800-Hz component weights, were significantly larger in SNHL participants in quiet compared to NH participants in TEN (Fig. 4.4; dashed green line). These differences signify that participants with SNHL have slightly greater utilization of higher-frequency component weights than participants with NH, especially in the presence of the TEN. The TEN may have led participants with NH to ignore the influence of high-frequency components more so than participants with SNHL. Masking caused the firing of the auditory nerve to be increased compared to participants with SNHL (see Reed et al., 2009), especially at high-frequency levels. It is possible that the TEN masked the binaural cues available at high frequencies (see Chapter 2), reducing the influence of cues in that region. Participants with SNHL could have still utilized the high-frequency components (if they were audible), leading to a slight increase in weight (about .05) even if it is not the dominant weight. A significantly lower weight was found at the 800-Hz component for SNHL participants compared to NH participants in the presence of the TEN. Again, masking of high-frequency binaural cues in the presence of the TEN may have led NH participants to overemphasize the 800-Hz component. However, for SNHL participants, the maximum weight remained for the 800-Hz component in stimulus condition T3.

SWFs measured in participants with SNHL followed the general trend of weighting functions found in participants with NH (in quiet and TEN). Except for stimulus condition T2, the dominance region continued to be the salient frequency region for localization. However, SNHL participants' confidence intervals (Fig. 4.4; right column) were markedly larger across stimulus conditions (when compared to NH Quiet and NH TEN). There are two possible reasons for such an increase. First, it was expected that participants with SNHL would have a reduced ability to localize sounds compared to participants with NH (Abel et al., 2000; Van den Bogaert et al., 2006; Otte et al., 2013). The localization ability of all participants will be addressed in the next section. Second, with the wide range of free-field thresholds found in participants with SNHL (Fig. 4.3), it is possible that weighting strategies differed across participants due to their hearing thresholds. These differences can be more easily seen when plotting individual participant SWFs (Fig. 4.5 and 4.6) and individual participant AR_{800} values (Fig. 4.7).

Figure 4.5 displays individual-participant SWFs with panels arranged in the same manner as Fig. 4.4. For participants with NH, in quiet and in TEN, the overall trend of SWF shapes is consistent with the results found in the mean data (Fig. 4.4). That is, overall, SWFs were quite similar across participants. However, for participants with SNHL, there was a wide range of SWF shapes across stimulus conditions. Focusing on the 800-Hz component across stimulus conditions, participants with SNHL ranged from placing no weight (0; or negative weight) on the component to a weight as high as .62 for T1 (octave tones 100-6400 Hz), .39 for T2 (harmonic tones 200-1400 Hz), and .88 for T3 (harmonic tones 800-5600 Hz).

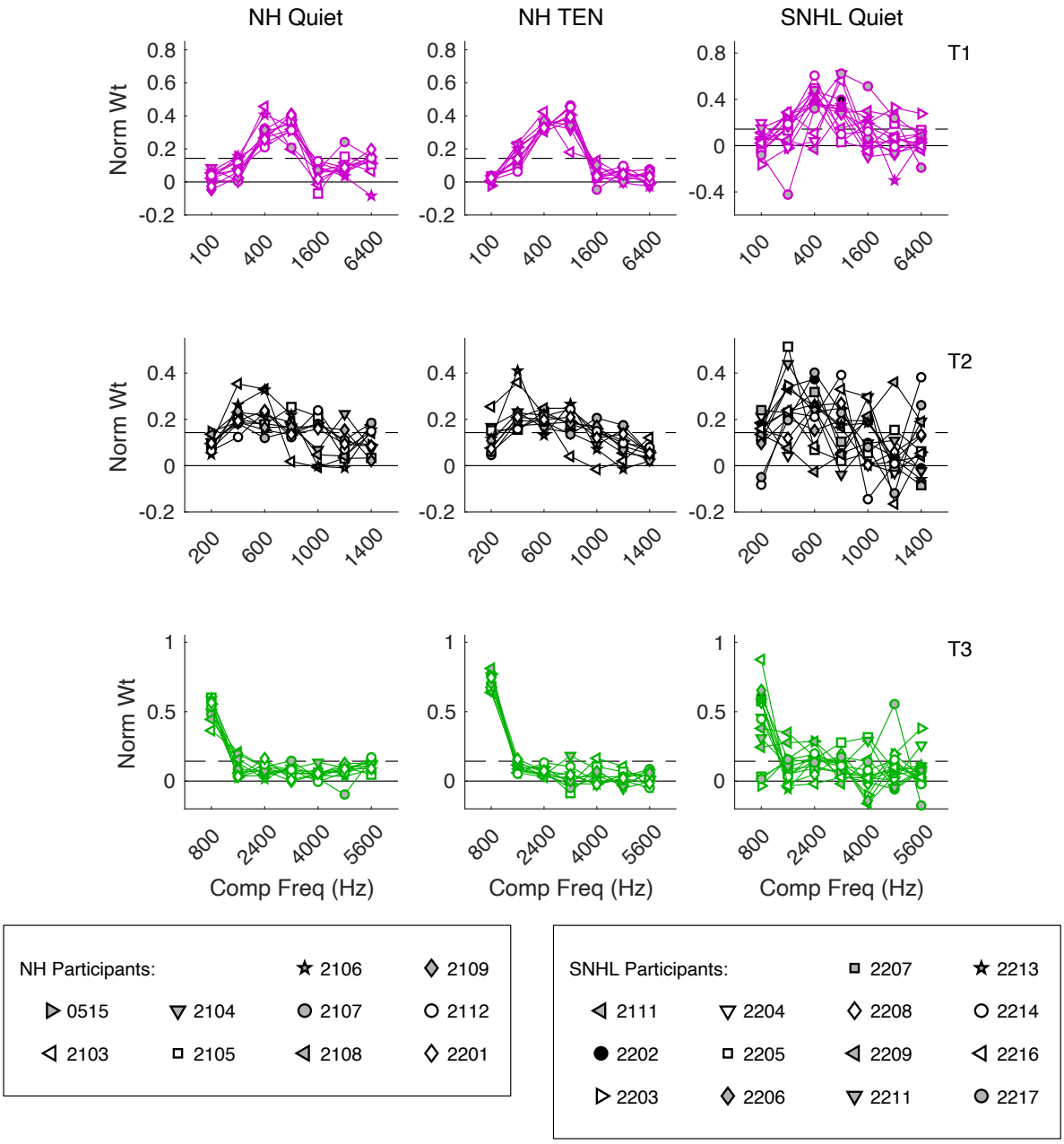

FIG. 4.5. Individual-participant SWFs found in participants with NH in quiet (left column), NH in TEN (middle column), and SNHL in quiet (right column). The rows plot SWF data for stimulus conditions T1 (magenta; top row), T2 (black; middle row), and T3 (green; bottom row). Each panel plots SWFs obtained for individual participants (symbols; legend at bottom).

Figure 4.6 replots the individual-participant SWFs of Fig. 4.5 for participants with SNHL to show if SWFs are dependent on hearing thresholds. The data are arranged in a manner to view the SWFs across stimulus conditions for each individual participant (panels). Each panel also displays the free-field threshold (right vertical axis; thick, light blue line). Visual inspection of the data suggests many participants with SNHL continue to place the largest weight on the 400- and 800-Hz components when localizing tone complexes. These participants (i.e., participants 2202, 2204, 2206, 2207, 2208, 2213, and 2216) all have good thresholds at low frequencies compared to the remaining participants. Some participants with poor thresholds at low frequencies (i.e., participants 2111, 2203, 2205, and 2211) place the greatest weight on the 400-Hz component for stimulus conditions T1 (octave tones 100-6400 Hz) and T2 (harmonic tones 200-1400 Hz) while other participants with poor thresholds at low frequencies (i.e., participant 2209 and 2217) have elevated weights for high-frequency components. The utilization of the 800-Hz component in stimulus condition T3 (harmonic tones 800-5600 Hz) seems to be reduced for participants with poor thresholds at low frequencies. The differences in the salience of the 800-Hz component across participants with SNHL and the possible relationship with free-field thresholds will be assessed in section 4.3.5.

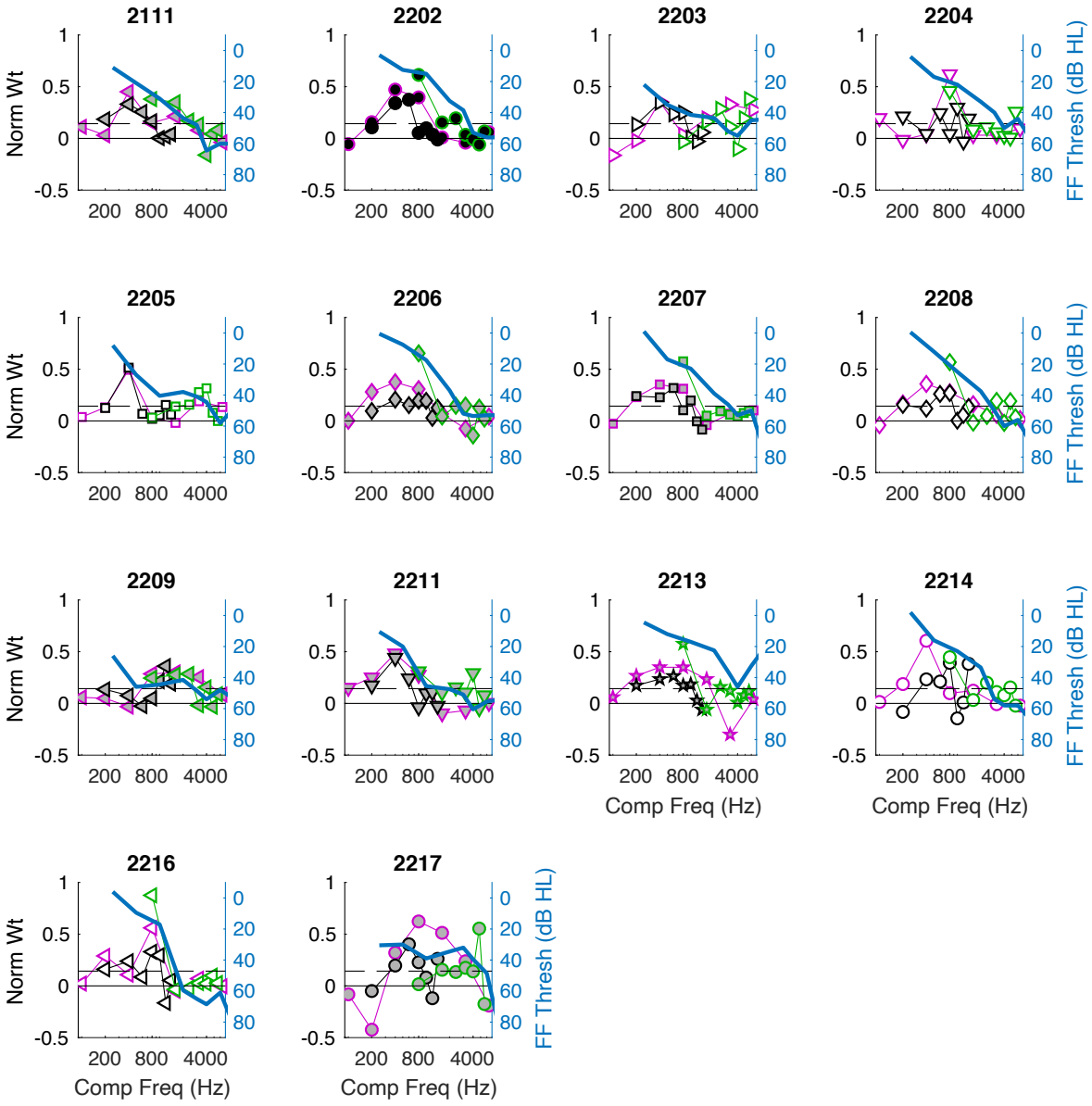

FIG. 4.6. Individual-participant SWFs found in participants with SNHL in quiet (Fig. 4.5; right column) are plotted as a function of component frequency (Hz; horizontal axis). Each panel plots the individual SWF data for stimulus conditions T1 (magenta), T2 (black), and T3 (green; legend on right). Dashed lines indicate the expected value (1/7) for uniform weighting across components. Each panel also plots free-field pure tone thresholds (dB HL; solid light blue line;

right vertical axis) as a function of frequency (Hz; horizontal axis) obtained for respective individual participants (panels).

Recall participants 2206, 2207, 2209, and 2217 had prevalent front-back errors. Within these participants, weighting functions were not similar. Participants 2206 and 2207 gave the maximum weight to the 400-Hz component and a relatively slightly reduced weight to the 800-Hz component for stimulus condition T1 (octave tones 100-6400 Hz) and a maximum weight at 800 Hz for stimulus condition T3 (harmonic tones 800-5600 Hz). These SWFs for participants 2206 and 2207 are similar to average weighting functions found in participants with NH in quiet and in TEN (Fig. 4.4). Participants 2209 and 2217, however, had a different pattern of SWFs, with components at high frequencies (> 800 Hz) receiving larger relative weights.

At times, participant 2209 could localize some stimuli in front of them, and participant 2217 indicated some responses correctly near 60°. This only occurred in condition T3 (harmonic tones 800-5600 Hz). More tonal components available in the range of high frequencies could have helped these participants resolve front-back confusions. Front-back confusions are known to be resolved with the monaural spectral cue (Musicant and Butler, 1984), which is primarily available in the high-frequency range (e.g., Wightman and Kistler 1997). To understand if front-back confusions were more prevalent due to a higher degree of SNHL, free-field thresholds for participants who localized stimuli behind them (2206, 2207, 2209, and 2217) were averaged across 4000, 6000, and 8000 Hz and compared to the average of the remaining participants. The averages were nearly identical (near 54 dB HL), indicating the front-back confusions were not dependent on the degree of SNHL, consistent with the results of Best et al. (2010) for speech. The average of low-frequency free-field thresholds (250, 500, and 1000 Hz) were slightly larger

for participants who experienced front-back confusions (23.4 dB HL) than for the remaining participants (17.2 dB HL); indicating a possible relationship between the degree of low-frequency hearing loss and prevalence of front-back confusions (Noble et al., 1998).

Figure 4.7 plots the average and individual participant AR_{800} values as violin plots (Hintze and Nelson, 1998; Bechtold, 2016). For participants with NH in quiet, NH in TEN, and SNHL in quiet, AR_{800} values were significantly greater than 1 ($p < .0005$) for stimulus conditions T1 (octave tones 100-6400 Hz) and T3 (harmonic tones 800-5600 Hz). Stimulus condition T2 (harmonic tones 200-1400 Hz) revealed a mean AR_{800} near 1 for all participants (NH in quiet: 1.13, NH in TEN: 1.04, and SNHL in quiet: 1.38), corroborating mean SWFs (Fig. 4.4; middle panels) where relatively equal weighting across components was found. Significant differences in AR_{800} were found between NH participants in quiet and in the presence of the TEN for stimulus conditions T1 and T3. In both instances, AR_{800} is larger when NH participants are in the presence of the TEN. As expressed earlier, the TEN masker may have caused participants to overemphasize lower frequency components. The significant difference in AR_{800} for stimulus condition T3 between participants with NH in TEN and SNHL in quiet substantiates this overemphasis. Most NH participants' AR_{800} (in TEN) was larger than most SNHL participants' AR_{800} (in quiet; Fig. 4.7 green circles). However, one participant with SNHL (2216) had a considerably larger AR_{800} (22.77) in that condition (T3) compared to all participants. That same participant (2216) also had one of the largest AR_{800} (6.22) in stimulus condition T1, but not as large as participant 2204, who had the largest AR_{800} (9.11) in that condition. The density of AR_{800} for the remaining participants with SNHL is only slightly larger than participants with NH (in quiet and TEN) across all stimulus conditions. Despite density similarities, there is a divide in

AR_{800}. For example, in stimulus condition T3, some participants have an AR_{800} closer to 6, while some participants have an AR_{800} closer to 0.

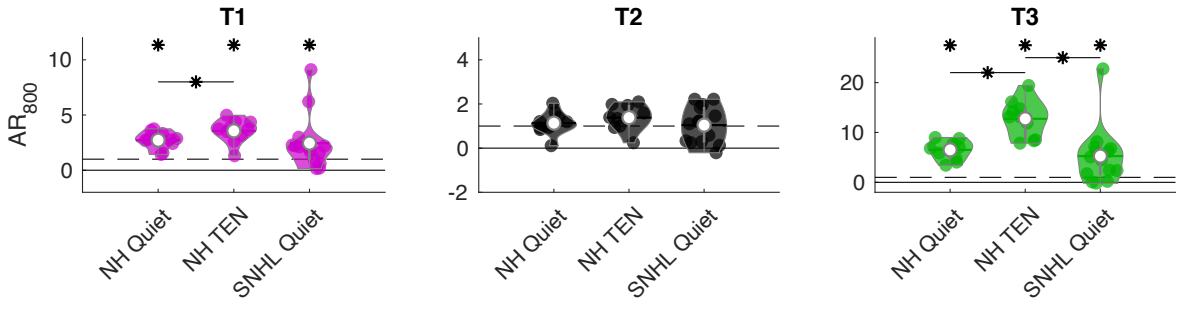

FIG. 4.7. Violin plots of AR_{800} values (vertical axis) are shown for each stimulus condition (panels), plotted for participants with NH in quiet, NH in TEN, and SNHL in quiet (horizontal axis). Colored circles in each panel plot AR_{800} for individual participants; violin plots indicate the density (width of each violin) and mean (white circle) of obtained values. Dashed lines indicate the expectation for uniform spectral weighting AR = 1. Asterisks (*) indicate conditions in which AR_{800} significantly exceeded this value ($AR_{800} > 1$, $p < .0005$ by 2000-fold bootstrap test). Asterisks with a line indicate bootstrapped significant differences between conditions ($p < .05$, two-tailed).

4.3.3. Localization Performance

The localization performance of participants with SNHL was compared to participants with NH in quiet and in the presence of the TEN as a secondary analysis of the SWF response data. This served two main purposes. First, to determine if SWFs were confidently measured in participants with SNHL (focusing on the R^2 statistic). Second, to determine if the TEN masker reduced the localization performance of participants with NH to the level of participants with SNHL.

The left panel of Fig. 4.8 plots the RMS error (in degrees), indicating errors made outside the 22.5° range of spatial jitter. The mean RMS error is plotted across participants with NH in quiet, NH in TEN, and SNHL in quiet (horizontal axis) separately for each stimulus condition (legend). Analysis revealed there were no significant differences across stimulus conditions for each group of participants. For participants with NH, the RMS error (for all stimulus conditions) was not different when they were in quiet than when they were in the presence of the TEN. Participants with SNHL, however, did significantly differ from participants with NH in all three stimulus conditions, resulting in an increase of responses outside of the spatial jitter.

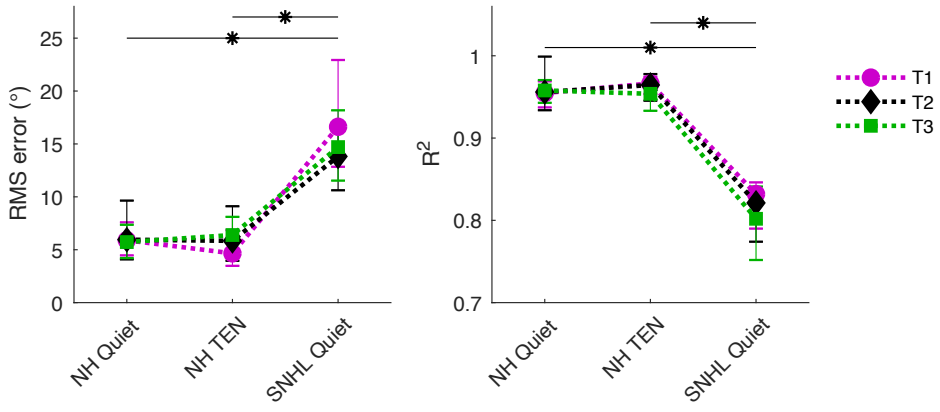

FIG. 4.8. The left panel plots mean RMS error (in degrees) across groups of participants with NH in quiet, NH in TEN, and SNHL in quiet for stimulus conditions T1 (magenta circles), T2 (black diamonds), and T3 (green squares; legend to the right of panels). The right panel plots the mean R^2 value across participants for stimulus conditions T1, T2, and T3. Error bars indicate bootstrapped ±95% confidence intervals on each mean value (RMS error or R^2). Asterisks (*) indicate bootstrapped, two-tailed, significant differences ($p < .05$) between (RMS error or R^2)

values in stimulus condition T1 versus T3. Asterisks with lines indicate significant differences across participant groups (for all three stimulus conditions, calculated separately).

The right panel of Fig. 4.8 plots the R^2 statistic, indicating how well the response data were accounted for by the multiple linear regression model (function 1) used to calculate weights. The mean R^2 value is plotted across participants with NH in quiet, NH in TEN, and SNHL in quiet (horizontal axis) separately for each stimulus condition (legend). Results were similar to the results for the RMS error, with significant differences found in all stimulus conditions across participants with NH and participants with SNHL. Both methods used to calculate localization error (RMS error and R^2) reveal that 1) participants with SNHL have a reduced ability to localize tone complexes, 2) the average R^2 revealed that the regression model (function 1) accounted for 80% of the variability for participants with SNHL, and 3) the TEN masker did not reduce the localization ability of NH participants.

Consistent with the results of Keidser et al. (2009), Best et al. (2010), Neher et al. (2011), and Brungart et al. (2017), participants with SNHL in the current study had an average increase in RMS error of about 10°. No significant differences were found between stimulus conditions; however, the error bar of condition T1 (octave tones 100-6400 Hz) demonstrates that some participants may have had more trouble localizing broadband stimuli. Examining the RMS errors for individual participants with SNHL reveals that two participants had RMS errors close to 40°. These participants were two of the participants that experienced many front-back errors (2206 and 2217). Surprisingly, these participants did not have large RMS values for stimulus conditions T2 (harmonic tones 200-1400 Hz) or T3 (harmonic tones 800-5600 Hz). There is no obvious reason why these participants' localization performance differed across stimulus

conditions since more tones providing low-frequency ITD cues are available in stimulus condition T1 than in stimulus condition T3.

Overall, many participants with SNHL continue to utilize the ITD dominance region even when their localization accuracy is degraded. For example, participants 2213 and 2214 had R^2 values below .72 and RMS errors of about 15° for stimulus condition T1 (octave tones 100-6400 Hz). Participant 2213 placed the greatest weights on both the 400- and 800-Hz components (.35). Participant 2213 placed the greatest weight on the 400-Hz component (.61). The same participants, 2213 and 2214, had R^2 values below .7 and RMS errors of about 23° for stimulus condition T3 (harmonic tones 800-5600 Hz). Both participants placed the greatest weight on the 800-Hz component (.58 and .45, respectively).

4.3.4. Measured Interaural Cues

The localization performance of participants with SNHL degraded compared to participants with NH in the presence of the TEN, signifying that although the TEN provided similar audibility of components to participants with NH, the TEN did not simulate the localization accuracy of participants with SNHL. This may be attributed to the availability of binaural cues across components when the TEN was present. To inspect the binaural cues available when the TEN was present, recordings of stimulus condition T1 (octave tones 100-6400 Hz) in quiet and in TEN were made and analyzed in a similar manner as Chapter 2. Briefly, with a Knowles Electronics Manikin for Acoustic Research (KEMAR; Burkhard and Sachs, 1975), recordings were made of all stimulus components presented at each base loudspeaker (-56.26° to +56.26° in 11.25° steps) in quiet and in the presence of the TEN. A 50-ms sliding window beginning at the stimulus onset was shifted by 10 ms for a total of 6 windows

encompassing the 100-ms duration of the signal. For each window, the Binaural Toolbox (Akeroyd, 2001) was utilized to calculate the average ITD, interaural correlation (IAC), and ILD across windows (for more details, see Chapter 2, including the diagram in Fig. 4.9).

Figure 4.9 displays average cue values (across windows) as color plots for ITD (top row), IAC (middle row), and ILD (bottom row) for stimuli presented in quiet (left column) and in the presence of the TEN masker (right column). Within each panel, the cue value (see legend to the right of panels) is plotted as a function of the base loudspeaker (location of components). In the quiet condition, ITD cues systematically and reliably changed with azimuth for the 200-, 400-, and 800-Hz tone components, as depicted by the cue values of the components from left (-56.25°) to right (56.25°) monotonically increasing in μs ITD. In TEN, the ITD cue becomes less reliable at some base locations, and the ITD becomes erratic at high frequencies. However, for the 200- and 400-Hz components, the ITD cues remain reliable. The IAC in TEN compared to the IAC in quiet, approaching 1 for most components in each location, is reduced, especially for high-frequency components. The ILD cue in quiet is reliable for component frequencies up to 800 Hz, as depicted by the cue values of the components from left (-56.25°) to right (56.25°) monotonically increasing in dB ILD (albeit with a larger range of cue values for the 1600 and 5600-Hz components). In TEN, the ILD cue becomes less reliable for high-frequency components (3600 and 5600 Hz).

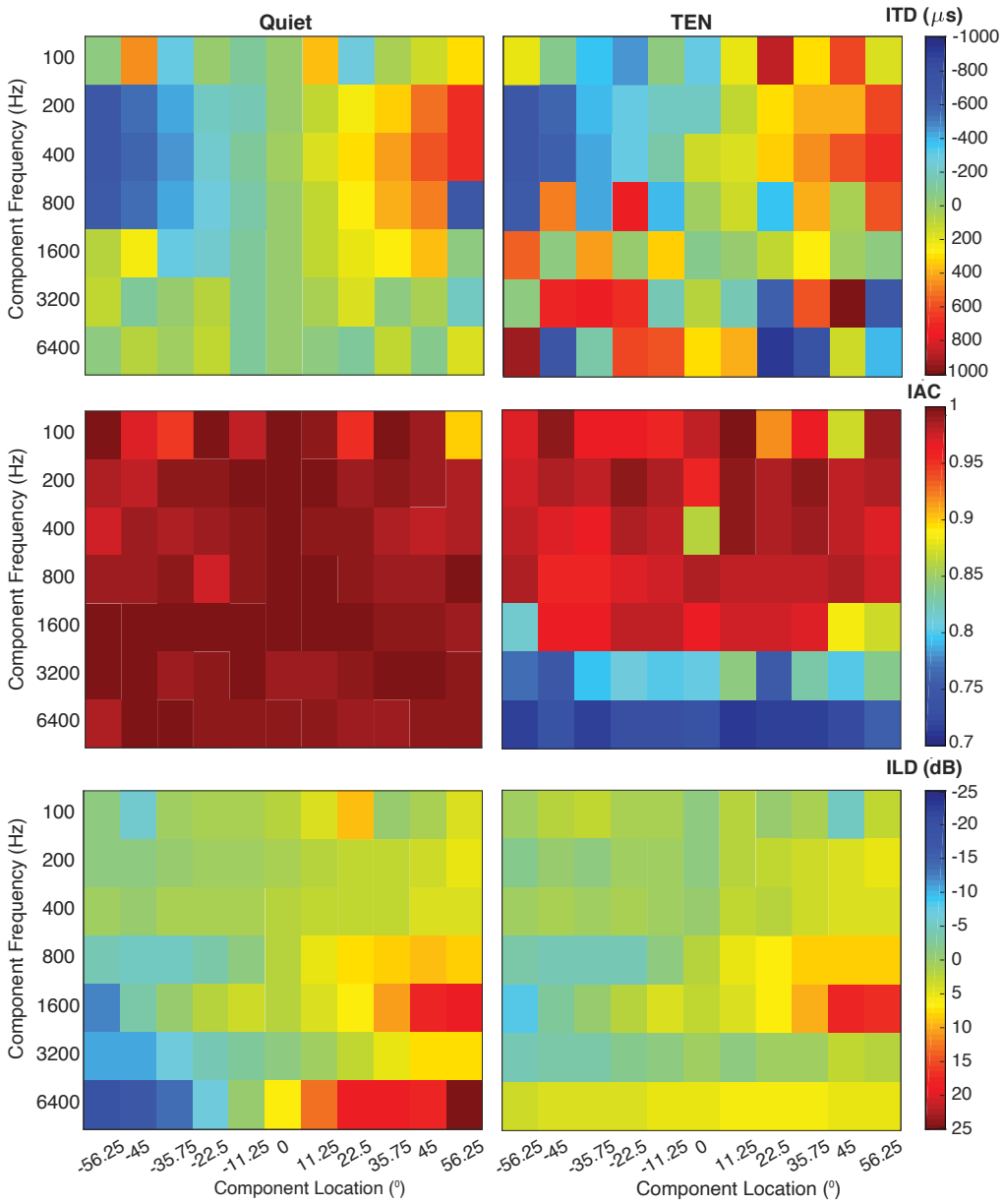

FIG. 4.9. Average ITD, IAC, and ITD cues (rows) calculated across 50-ms windows shifted by 10 ms for a total duration of the stimulus (100 ms) for quiet (left column) and TEN (right column). Each panel plots the cue values for each ERB centered at the component (Hz; x-axis) as a function of component location (°; y-axis). The cue values are plotted as colored values indicated by the color bar to the right of the last column for each row. The ITD values range from blue, indicating a -1000-μs ITD, to red, indicating a 1000-μs ITD. The IAC values range

from blue, indicating an IAC value of 1, to red, indicating an IAC value of .7. The ILD values range from blue, indicating a -25 dB ILD to red, indicating a 25 dB ILD.

Due to the availability of the ITD cue and ILD cue at component frequencies that were highly weighted by participants with NH in TEN (400 and 800 Hz), it is no surprise these participants were able to localize stimuli in the presence of the TEN accurately. With that and the results of localization accuracy of participants with SNHL, it can be concluded that the TEN does not accurately represent the cues available to participants with SNHL. Instead, the sensitivity to binaural cues is degraded for participants with SNHL (e.g., Gabriel et al., 1992) even though they are available acoustically (Fig. 4.9; Quiet). It is still unclear if binaural cues are degraded in a frequency-specific manner. The results of Hawkins and Wightman (1980) suggest the ITD cue is degraded for high frequencies more so than for low frequencies. However, their stimuli utilized bands of noise (where ITD cues in the envelope are available), while the current study used tones. Localization studies suggest cues are degraded for both low and high-frequency stimuli (Smith-Olinde et al., 1998; Van den Bogart et al., 2006; Kediser et al., 2009; van Esch et al., 2013). However, all these studies utilized only two frequencies, representing low and high frequencies. Using investigations of binaural cue sensitivity across frequency (see Fullgrabe and Moore, 2018) would allow for the development of a more accurate TEN to mask binaural cues, with the goal of simulating the degradation in localization performance.

4.3.5. The Effect of Free-field Threshold and Age

To understand the effects of both hearing threshold and age, Pearson correlations were conducted between the weight placed on the 800-Hz component by participants with SNHL and

average free-field thresholds for low frequencies (250, 500, and 1000 Hz), average free-field thresholds for high frequencies (3000, 4000, 6000 and 8000 Hz), and age (in years). Figure 4.10 plots each individual participant's weight placed on the 800-Hz component as a function of their average low-frequency free-field threshold (left panel), average high-frequency free-field threshold (middle panel), and age (right panel) for each stimulus condition (legend). For each stimulus condition, the least-squares regression line is also plotted in each panel. The correlation value is displayed to the right of each regression line, with significant correlations indicated in bold with an asterisk. A Bonferroni correction for three tests (low- and high-frequency free-field thresholds and age) per three individual dependent variables (i.e., the 800-Hz weight for each stimulus condition) gave a p-value of .0056 (for nine tests in total).

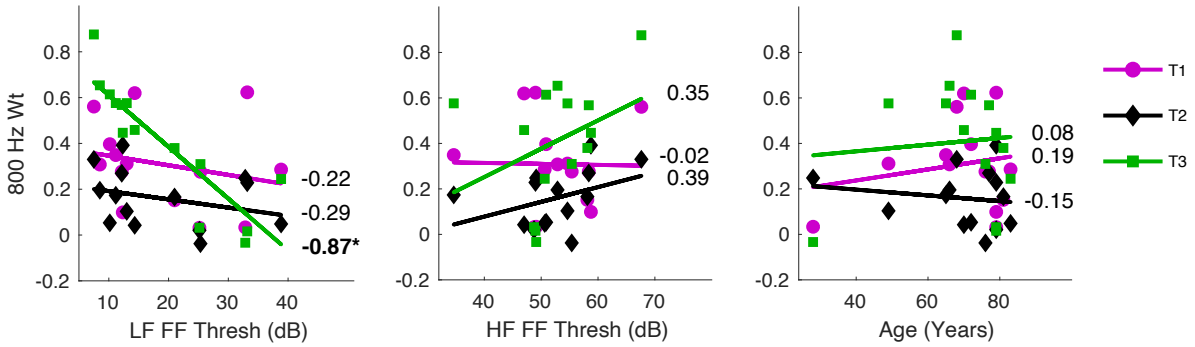

FIG. 4.10. Scatter plots for each individual SNHL participant's 800-Hz weight are plotted as a function of their average low-frequency free-field threshold (left panel), average high-frequency free-field threshold (right panel), and age (right panel) for each stimulus condition (legend). Each panel plots the least-squares regression line for each stimulus condition (by color; see legend). The correlation values (r) are displayed to the right of each regression line. Bold correlation values indicate significant correlations ($p < .05$) while bold with asterisks indicate a significant correlation $p < .0056$ after Bonferroni correction (n = 9).

Only one significant correlation was found between average low-frequency free-field thresholds and the weight placed on the 800-Hz component in condition T3 (harmonic tones 800-5600 Hz). The negative correlation indicates that as low-frequency thresholds increased, the weight placed on the 800-Hz component (in condition T3) decreased. The distribution of the 800-Hz weight raged from .89 to values below 0. Participant 2216, who placed the greatest weight on the 800-Hz component, had a steeply sloping hearing loss (as indicated by the free-field threshold) between 1000 and 2000 Hz (17 and 59.5 dB, respectively). Their weight placed on the 800-Hz component was more similar to the average weight placed on that component by participants with NH in the TEN (.73) than in quiet (.52). The average free-field threshold for participants with NH in the TEN at 1000 Hz was 23 dB, and at 2000 Hz was 43.5 dB HL. As for participants with SNHL who placed the lowest weight on the 800-Hz component (2203 and 2217), their hearing threshold profiles are flatter, with the loss at low frequencies being similar to the loss at high frequencies. With this, it should be considered that it is not just the loss at low frequencies affecting the weight placed at 800-Hz, but possibly the shape of the hearing loss.

These results suggest that age and degree (and possibly shape) of hearing loss can only partially explain weights for participants with SNHL. One additional possibility not explored that could contribute to the decrease in weight of the 800-Hz component is sensitivity to the ITD cue at that frequency. There is some evidence that ITD sensitivity varies with age and hearing loss. The studies of Neher et al. (2011 and 2012), compare both age and average low-frequency monaural thresholds (125, 250, 500, and 750 Hz) to the highest frequency an ITD could be detected and the average sensitivity to ITD cues (250, 500, and 700 Hz), particularly in the fine structure. A significant correlation was found between the two ITD measures and age; however, no correlation was found between the ITD measures and low-frequency thresholds. Similar

results were found by Whitmer et al. (2014) when thresholds were averaged across 500, 1000, 200, and 4000 Hz at the better ear, and the effects of age were removed. When a meta-analysis was performed by Fullgrabe and Moore (2018) on fine structure ITD sensitivity, significant correlations were found between ITD sensitivity and both age and the monaural threshold at the test frequency, although correlations were larger for age. These results are consistent with the results of King et al. (2014), who found that ITD sensitivity (at 500 Hz) was significantly correlated with the monaural threshold for low frequencies (250 and 500 Hz).

Although the current study does not specifically measure ITD sensitivity in the form of threshold measures, ITD sensitivity has been shown to be inversely proportional to SWFs (Folkerts and Stecker, 2022). It may be possible that with the increase in free-field thresholds at low frequencies, participants with SNHL had a decline in sensitivity to the 800-Hz ITD. However, in the current study, the correlation between the 800-Hz weight and low-frequency hearing loss is not significant for stimulus conditions T1 (octave tones 100-6400 Hz) and T2 (harmonic tones 100-6400 Hz). This is most likely due to the greatest weight being placed on another component. For example, for stimulus condition T1, the average SWF had peak weights at 400 and 800 Hz. It is not believed that using the AR_{800} would have helped this because if 400- and 800-Hz were equally weighted, the ratio's denominator would have caused the AR_{800} to decrease. Measuring correlations for the 800-Hz component weight instead accounted for at least "part" of the peak. A closer examination of individual SWFs (Fig. 4.5 or 4.6) reveals that some participants placed more weight on the 400- or 800-Hz component while others placed similar weight on 400- and 800-Hz. As mentioned earlier, a more thorough investigation relating SWF shapes and hearing threshold profiles is warranted and may help parse out correlation calculations.

4.4. Summary and Conclusions

The purpose of the current study was to explore the effects of hearing loss on SWFs by evaluating participants with NH with simulated hearing loss (TEN) and participants with SNHL. The SWFs of these participants were compared to participants with NH tested in quiet. The results of this study revealed six main findings:

1) The TEN masker was successfully implemented in the free field. Target threshold values matched measured threshold values, although masking was more effective in the high frequencies than the low frequencies. Overall, thresholds for participants with NH with TEN were within the range of thresholds measured in participants with SNHL.

2) SWFs measured in participants with NH in quiet compared to SWFs also measured in the quiet with different participants (Folkerts and Stecker, 2022) revealed changes to the SWF shape. Namely, for stimulus condition T1 (octave tones 100-6400 Hz), the 400-Hz component revealed an elevated weight in the current study compared to the previous study, resulting in a widening of the ITD dominance region peak. This may be attributed to interleaved blocks of trials in quiet and in the presence of the TEN masker.

3) SWFs measured in participants with NH in TEN compared to SWFs measured in quiet also revealed changes to the SWF shape. Some low-frequency components received greater weights, while the highest frequency component in all stimulus conditions received a lower weight. However, overall the 400 Hz and 800-Hz components tended to dominate SWFs, especially with the T1 (octave tones 100-6400 Hz) and T3 stimuli (harmonic tones 800-5600 Hz).

4) SWFs measured in participants with SNHL also revealed a broader dominance region peak (400-800 Hz) relative to previous work with participants with NH (Folkerts and Stecker, 2022). In addition, compared to participants with NH in quiet and TEN, confidence intervals are wider

for participants with SNHL. Individual SNHL participant SWFs reveal a variety of shapes across stimulus conditions. On average, the 400 and 800-Hz components received the highest weight for many—but not all—participants with SNHL.

5) The localization performance of participants with SNHL was reduced compared to participants with NH in quiet and in the presence of the TEN masker. The masker did not drive participants with NH to have reduced localization accuracy, most likely due to the binaural cues that remained available when the masker was present. Although participants with SNHL had reduced localization ability and an increased prevalence of front-back errors, SWFs measured were reliable and depict the use of the ITD dominance region even for participants with a reduced localization ability.

6) The amount of weight placed on the 800-Hz component by participants with SNHL was negatively correlated with average low-frequency free-field thresholds; participants with higher thresholds placed less relative weight on 800 Hz with the T3 stimulus (harmonic tones 800 – 5600 Hz). The 800-Hz component weight was not correlated with high-frequency free-field thresholds or age, or with the other stimulus conditions.

REFERENCES

Abel, S. M., Giguère, C., Consoli, A., and Papsin, B. C. (**2000**). "The effect of aging on horizontal plane sound localization," J. Acoust. Soc. Am., **108**, 743–752. doi:10.1121/1.429607

Ahrens, A., Joshi, S. N., and Epp, B. (**2020**). "Perceptual Weighting of Binaural Lateralization Cues across Frequency Bands," J. Assoc. for Res. in Otolaryn., **21**, 485–496. doi:10.1007/s10162-020-00770-3

Allen, P. D., and Eddins, D. A. (2010). Presbycusis phenotypes form a heterogeneous continuum when ordered by degree and configuration of hearing loss. Hear. Res. **264**, 10-20. doi: 10.1016/j.heares.2010.02.001

Allen, J. B., Hall, J. L., and Jeng, P. S. (**1990**). "Loudness growth in 1/2-octave bands (LGOB)—A procedure for the assessment of loudness," J. Acoust. Soc. Am., **88**, 745–753. doi:10.1121/1.399778

Baltzell, L. S., Cho, A. Y., Swaminathan, J., and Best, V. (**2020**). "Spectro-temporal weighting of interaural time differences in speech," J. Acoust. Soc. Am., **147**, 3883–3894. doi:10.1121/10.0001418

Berg, B. G. (**1990**). "Observer efficiency and weights in a multiple observation task," J. Acoust. Soc. Am., **88**, 149–158. doi:10.1121/1.399962

Bernstein, L. R., and Trahiotis, C. (**2019**). "No more than 'slight' hearing loss and degradations in binaural processing," J. Acoust. Soc. Am., **145**, 2094–2102. doi:10.1121/1.5096652

Best, V., Kalluri, S., McLachlan, S., Valentine, S., Edwards, B., and Carlile, S. (**2010**). "A comparison of CIC and BTE hearing aids for three-dimensional localization of speech," Intern. J. Aud., **49**, 723–732. doi:10.3109/14992027.2010.484827

Bilsen, F. A., and Raatgever, J. (**1973**). "Spectral Dominance in Binaural Lateralization," Acoustica, **28**, 131–132.

Bronkhorst, A. W., and Plomp, R. (**1988**). "The effect of head-induced interaural time and level differences on speech intelligibility in noise," J. Acoust. Soc. Am., **83**, 1508–1516. doi:10.1121/1.395906

Bronkhorst, A. W., and Plomp, R. (**1989**). "Binaural speech intelligibility in noise for hearing-impaired listeners," J. Acoust. Soc. Am., **86**, 1374–1383. doi:10.1121/1.398697

Bronkhorst, A. W., and Plomp, R. (**1992**). "Effect of multiple speechlike maskers on binaural speech recognition in normal and impaired hearing," J. Acoust. Soc. Am., **92**, 3132–3139. doi:10.1121/1.404209

Brungart, D. S., Cohen, J. I., Zion, D., and Romigh, G. (**2017**). "The localization of non-individualized virtual sounds by hearing impaired listeners," J. Acoust. Soc. Am., **141**, 2870–2881. doi:10.1121/1.4979462

Cai, Y., Zheng, Y., Liang, M., Zhao, F., Yu, G., Liu, Y., Chen, Y., et al. (**2015**). "Auditory Spatial Discrimination and the Mismatch Negativity Response in Hearing-Impaired Individuals," (H. Lin, Ed.) PLoS ONE, **10**, e0136299. doi:10.1371/journal.pone.0136299

Desloge, J. G., Reed, C. M., Braida, L. D., Perez, Z. D., and Delhorne, L. A. (**2010**). "Speech reception by listeners with real and simulated hearing impairment: Effects of continuous and interrupted noise," J. Acoust. Soc. Am., **128**, 342–359. doi:10.1121/1.3436522

Dobreva, M. S., O'Neill, W. E., and Paige, G. D. (**2011**). "Influence of aging on human sound localization," J. Neuro., **105**, 2471–2486. doi:10.1152/jn.00951.2010

Dubno, J. R., and Schaefer, A. B. (**1992**). "Comparison of frequency selectivity and consonant recognition among hearing-impaired and masked normal-hearing listeners," J. Acoust. Soc. Am., **91**, 2110–2121. doi:10.1121/1.403697

van Esch, T. E. M., Kollmeier, B., Vormann, M., Lyzenga, J., Houtgast, T., Hällgren, M., Larsby, B., et al. (**2013**). "Evaluation of the preliminary auditory profile test battery in an international multi-centre study," Intern. J. Aud., **52**, 305–321. doi:10.3109/14992027.2012.759665

Folkerts, M.L., and Stecker, G. C. (**2022**). "Spectral weighting functions for lateralization and localization of complex," J. Acoust. Soc. Am., **151**, 3409–3425. doi:10.1121/10.00011469

Füllgrabe, C., and Moore, B. C. J. (**2018**). "The Association Between the Processing of Binaural Temporal-Fine-Structure Information and Audiometric Threshold and Age: A Meta-Analysis," Tren. Hear., **22**, 233121651879725. doi:10.1177/2331216518797259

Gabriel, K. J., Koehnke, J., and Colburn, H. S. (**1992**). "Frequency dependence of binaural performance in listeners with impaired binaural hearing," J. Acoust. Soc. Am.**91**, 336–347. doi:10.1121/1.402776

Häusler, R., Colburn, S., and Marr, E. (**1983**). "Sound Localization in Subjects with Impaired Hearing: Spatial-Discrimination and Interaural-Discrimination Tests," Acta Oto-Laryn., **96**, 1–62. doi:10.3109/00016488309105590

Hawkins, D. B., and Wightman, F. L. (**1980**). "Interaural Time Discrimination Ability of Listeners with Sensorineural Hearing Loss," Int. J. Audiol., **19**, 495–507. doi:10.3109/00206098009070081

Hawkins, J. E., and Stevens, S. S. (**1950**). "The Masking of Pure Tones and of Speech by White Noise," J. Acoust. Soc. Am., **22**, 6–13. doi:10.1121/1.1906581

Hirsh, I. J. (**1948**). "Binaural summation- a century of investigation.," Psych. Bull., **45**, 193–206. doi:10.1037/h0059461

Hughson, W., & Westlake, H. (**1944**). Manual for program outline for rehabilitation of aural casualties both military and civilian. Trans Am Acad Ophthalmol Otolaryngol, **48**(Suppl), 1-15.

Keidser, G., O'Brien, A., Hain, J.-U., McLelland, M., and Yeend, I. (**2009**). "The effect of frequency-dependent microphone directionality on horizontal localization performance in hearing-aid users," Intern. J. Audiol., **48**, 789–803. doi:10.3109/14992020903036357

Killion, M. C. (**1978**). "Revised estimate of minimum audible pressure: Where is the ''missing 6 dB''?," J. Acoust. Soc. Am., **63**, 1501–1508. doi:10.1121/1.381844

King, A., Hopkins, K., and Plack, C. J. (**2014**). "The effects of age and hearing loss on interaural phase difference discrimination," J. Acoust. Soc. Am., **135**, 342–351. doi:10.1121/1.4838995

Lutfi, R. A., and Jesteadt, W. (**2006**). "Molecular analysis of the effect of relative tone level on multitone pattern discrimination," J. Acoust. Soc. Am., **120**, 3853–3860. doi:10.1121/1.2361184

Macpherson, E. A., and Middlebrooks, J. C. (**2002**). "Listener weighting of cues for lateral angle: The duplex theory of sound localization revisited," J. Acoust. Soc. Am., **111**, 2219. doi:10.1121/1.1471898

Musicant, A. D., and Butler, R. A. (**1984**). "The influence of pinnae-based spectral cues on sound localization," J. Acoust. Soc. Am., **75**, 1195–1200. doi:10.1121/1.390770

Neher, T., Laugesen, S., Søgaard Jensen, N., and Kragelund, L. (**2011**). "Can basic auditory and cognitive measures predict hearing-impaired listeners' localization and spatial speech recognition abilities?," J. Acoust. Soc. Am., **130**, 1542–1558. doi:10.1121/1.3608122

Neher, T., Lunner, T., Hopkins, K., and Moore, B. C. J. (**2012**). "Binaural temporal fine structure sensitivity, cognitive function, and spatial speech recognition of hearing-impaired listeners (L)," J. Acoust. Soc. Am., **131**, 2561–2564. doi:10.1121/1.3689850

Noble, W., Byrne, D., and Lepage, B. (**1994**). "Effects on sound localization of configuration and type of hearing impairment," J. Acoust. Soc. Am., **95**, 992–1005. doi:10.1121/1.408404

Noble, W., Sinclair, S., and Byrnet, D. (**1998**). "Improvement in Aided Sound Localization with Open Earmolds: Observations in People with High-Frequency Hearing Loss," J. Amer. Acad. Audiol., **9**, 10.

Otte, R. J., Agterberg, M. J. H., Van Wanrooij, M. M., Snik, A. F. M., and Van Opstal, A. J. (**2013**). "Age-related Hearing Loss and Ear Morphology Affect Vertical but not Horizontal Sound-Localization Performance," J. Assoc. for Res. in Otolaryn., **14**, 261–273. doi:10.1007/s10162-012-0367-7

Plomp, R. (**1978**). "Auditory handicap of hearing impairment and the limited benefit of hearing aids," J. Acoust. Soc. Am., **63**, 18. doi: 10.1121/1.381753

Reed, C. M., Braida, L. D., and Zurek, P. M. (**2009**). "Review Article: Review of the Literature on Temporal Resolution in Listeners With Cochlear Hearing Impairment: A Critical Assessment of the Role of Suprathreshold Deficits," Trends Amp., **13**, 4–43. doi:10.1177/1084713808325412

Ross, B., Fujioka, T., Tremblay, K. L., and Picton, T. W. (**2007**). "Aging in Binaural Hearing Begins in Mid-Life: Evidence from Cortical Auditory-Evoked Responses to Changes in Interaural Phase," J. Neuro., **27**, 11172–11178. doi:10.1523/JNEUROSCI.1813-07.2007

Sivian, L. J., and White, S. D. (**1933**). "On Minimum Audible Sound Fields," **4**, 288–321.

Smith-Olinde, L., Koehnke, J., and Besing, J. (**1998**). "Effects of sensorineural hearing loss on interaural discrimination and virtual localization," J. Acoust. Soc. Am., **103**, 2084–2099. doi:10.1121/1.421355

Steinberg, J. C., and Gardner, M. B. (**1937**). "The Dependence of Hearing Impairment on Sound Intensity," J. Acoust. Soc. Am., **9**, 11–23.

Strelcyk, O., and Dau, T. (**2009**). "Relations between frequency selectivity, temporal fine-structure processing, and speech reception in impaired hearing," J. Acoust. Soc. Am., **125**, 3328. doi:10.1121/1.3097469

Tollin, D. J., and Henning, G. B. (**1999**). "Some aspects of the lateralization of echoed sound in man. II. The role of the stimulus spectrum," J. Acoust. Soc. Am., **105**, 838–849. doi:10.1121/1.426273

Van den Bogaert, T., Klasen, T. J., Moonen, M., Van Deun, L., and Wouters, J. (**2006**). "Horizontal localization with bilateral hearing aids: Without is better than with," J. Acoust. Soc. Am., **119**, 515–526. doi:10.1121/1.2139653

Whitmer, W. M., Seeber, B. U., and Akeroyd, M. A. (**2014**). "The perception of apparent auditory source width in hearing-impaired adults," J. Acoust. Soc. Am., **135**, 3548–3559. doi:10.1121/1.4875575

Wightman, F. L., and Kistler, D. J. (**1992**). “The dominant role of low-frequency interaural time differences in sound localization,” J. Acoust. Soc. Am., **91**, 1648–1661. doi:10.1121/1.402445

Wightman, F. L., and Kistler, D. J. (**1997**). “Monaural sound localization revisited,” J. Acoust. Soc. Am., **101**, 1050–1063. doi:10.1121/1.418029

CHAPTER 5

Temporal weighting functions for localization of complex sound: The effect of hearing impairment

5.1. Introduction

The binaural cues listeners utilize to localize sounds in space can vary over time and frequency. Across time, stimuli onsets are particularly important. For example, Stecker and Hafter (2002) presented click trains with small perturbations in the spatial location. The perceived location of the click train is fused and dependent on the location of the onset, similar to the precedence effect when pairs of stimuli are presented with a short-inter-stimulus-intervals (ISI; Gardner, 1968, Zurek, 1987, Litovsky et al., 1999; Brown et al., 2015). The perceptual influence, or weight, of each click in the click train was determined by linear regression (Ahumada and Lovell, 1971) of the response location on the spatial location of each click. When plotted as a function of click number, the weights constitute the temporal weighting function (TWF). Onset dominance, a relatively large weight for the first click, was apparent for inter-click-intervals (ICI) below 5 ms. At longer ICIs, the onset and ongoing clicks received similar weights; that is, all clicks similarly contributed to the perceived location of the click train. This limitation of onset dominance to longer ICIs for click trains is similar to the precedence effect echo threshold for click pairs (e.g., Babkoff and Sutton, 1966). The echo threshold is the ISI limit for onset dominance and the number of images perceived.

The binaural cues attributed to onset dominance of 4000-Hz (high-frequency) Gaussian click trains by Stecker and Hafter (2002) include the interaural time difference of the envelope (ITD_{env}; the delay of the sound wave envelope between the two ears) and the interaural level

difference (ILD; the amplitude difference of the sound wave between the two ears). Lateralization TWFs confirm onset dominance (Freyman et al., 1997) specifically for the ITD_{env} cue (e.g., Saberi 1996; Brown and Stecker, 2010; Stecker et al., 2013) and ILD cue (e.g., Brown and Stecker, 2010; Stecker et al., 2013) with the same ICI limitation found in the free field (i.e., onset dominance was eliminated for ICIs > 5ms). Diedesch and Stecker (2015) confirmed onset dominance for low-frequency stimuli carrying an interaural difference in the fine structure (ITD_{fs}; the delay of the sound wave amplitude fluctuations between the two ears). Stecker (2018) applied amplitude modulation to click trains resulting in the rising portion of the envelope receiving the greatest weight and constituting the onset. Therefore, this work (and studies of the precedent effect and binaural adaptation; e.g., Hafter and Dye, 1983) demonstrate that listeners with normal hearing process binaural cues at the rising portion of the onset of grouped stimuli.

Less, however, is known about how listeners with typical age-related hearing loss [e.g., mild sloping to moderately-severe sensorineural hearing loss (SNHL); e.g., Allen and Eddins, 2010] process binaural cues across time. The primary consequences of SNHL are reduced audibility of low-level sounds and a loss of cochlear compression, causing a smaller dynamic range of sound levels and a greater rate of growth of loudness (Hellman and Meiselman, 1990, 1993; Oxenham and Plack, 1998; Moore, 2004). The loss of compressive non-linearity can increase the perception of the fluctuations (Moore et al., 1992, 1996; Fullgrabe et al., 2003), potentially resulting in increased amplitude modulation sensitivity for listeners with SNHL compared to listeners with NH (Bacon and Gleitman, 1992; Moore et al., 1992, 1996; Moore and Glasberg, 2001; Fullgrabe et al., 2003). In addition, the temporal integration of amplitude modulation cues improves for listeners with SNHL compared to listeners with NH (Wallaert et al., 2017), possibly due to taking advantage of "multiple looks" at the amplitude modulation

cycle (Viemeister and Wakefield, 1991). As a result of the potential changes in amplitude modulation sensitivity, each click in a click train might be treated as an independent source during auditory localization, leading to a flat TWF for listeners with age-related SNHL.

Consistent with this hypothesis, studies on the effect of SNHL on the precedence effect reveal a trend towards reduced onset dominance for adults with SNHL compared to those with NH. Cranford et al. (1998) presented two successive click stimuli with opposing ITD values. At ISIs below 1 to 2 ms, older listeners with SNHL had reduced lateralization towards the first click, similar to the results of Goverts et al. (2002) with low pass filtered noise. Akeroyd and Guy (2011) presented speech stimuli in the free field with a 4-ms ISI within the stimulus. Regression analysis used to determine onset dominance revealed a wide variety of weights for listeners with SNHL, which correlated with their hearing thresholds (i.e., as thresholds increased, onset dominance decreased).

This study aims to evaluate the effects of SNHL on TWFs. TWFs were measured for adults with SNHL and adults with NH with and without the presence of a threshold elevating noise (TEN) masker. The purpose of the TEN masker was to account for loss of audibility and a greater rate of growth of loudness found in listeners with SNHL (Steinberg and Gardner, 1937). Differences between listeners with NH in TEN and SNHL could then be attributed to suprathreshold processing changes such as the increase in temporal integration in listeners with SNHL. Because Roberts et al. (2002) found an increase in the echo threshold that leads to the fusion of two successive stimuli in listeners with SNHL as a single stimulus, onset dominance in participants with SNHL may only be apparent for longer ICIs. Therefore, TWFs were measured for a 2-ms ICI and a 5-ms ICI. The current study predicts that TWFs will reveal a reduction in

onset dominance for participants with SNHL and participants with NH with the TEN masker. Onset dominance may, however, be apparent at longer ICIs (i.e., 5-ms ICI).

5.2. Methods

TWFs were measured in NH participants in quiet and in the presence of a threshold elevating noise (TEN) masker implemented in Chapter 4 during the measurement of spectral weighting functions (SWFs). For a full description of the generation of the TEN and the threshold task, the reader is referred to Chapter 4. In brief, the TEN was presented in the free field as a diffuse noise, arriving from all available loudspeakers, surrounding the participant 360° in azimuth. For all NH participants, the target hearing level during simulation was that of a typical mild SNHL in the free field. Free-field detection threshold testing confirmed similar threshold levels between participants with NH in TEN and participants with mild-moderate SNHL (Fig. 4.3). TWFs were also measured in participants with a bilateral, mild-moderate SNHL. Two ICIs were utilized (2 ms and 5 ms) for 4000 Hz Gabor click trains (the same click train implemented by Stecker and Hafter, 2002; 2009). TWFs were measured (and analyzed) as in Stecker and Moore (2018). Comparisons were made between NH TWFs, TEN TWFs, and SNHL TWFs.

5.2.1. Participants

The participants in the current study are the same participants from Chapter 4 (NH and SNHL), including the author (0515). Participants with NH were ten adults (7 females) aged 21 – 32 years that were recruited from the Vanderbilt University community. NH was confirmed with

pure tone audiometric thresholds less than 20 dB HL that differed less than 15 dB between left and right ears for octave frequencies from 250 to 8000 Hz.

Participants with SNHL were fourteen adults (9 females) aged 28 – 83 years (median: 74) that were recruited based on their hearing loss status through the Vanderbilt University Medical Center Audiology Clinic. Participants' pure tone audiometric thresholds were near the mild-moderate range of losses for a symmetrical sloping high-frequency SNHL (Bisgaard et al., 2010). Specifically, participants were recruited if their thresholds at 500 Hz were 20 – 45 dB HL, at 1000 Hz were 30 – 50 dB HL, and at 4000 Hz were 50 – 70 dB HL, with no greater than a 30-dB difference across all frequencies and no greater than a 20-dB difference across three consecutive frequencies. Pure tone audiometric thresholds were remeasured if the thresholds in record were measured over six months prior to the recruitment date. All participants were monetarily compensated. Approval was obtained for experimental procedures from Vanderbilt University Medical Center Institutional Review Board (IRB #191952).

5.2.2. Target Stimuli

All stimuli were generated in MATLAB (Mathworks, Natick, MA) and synthesized at 48 kHz. Stimuli were presented through the Dante audio-over-ethernet network (Focusrite Rednet, El Segundo, CA) with digital amplification (Ashly ne820PE, Webster, NY) for playback to a 64-loudspeaker array (Meyer MM-4, Berkeley, CA) in in the Vanderbilt Bill Wilkerson Anechoic Chamber Laboratory (ACL; 4.6 x 6.4 x 6.7 m; Eckel Industries, Cambridge, MA). The loudspeakers in the ACL are at ear height, spanning 360° (5.625° of separation) with a 2-meter radius.

Target signals were trains of 16 4-kHz Gabor clicks (with a nominal duration of 2 ms) as in Stecker and Hafter (2002; 2009) and Stecker and Moore (2018). Two stimulus conditions, 2-ms ICI and 5-ms ICI, were utilized. The overall level of the target signal was 60 dB SPL, except for one participant with SNHL, 2216, who could not hear the stimulus, so it was set to 70 dB SPL. The spatial configuration of each of the clicks in the click train were manipulated from trial to trial to introduce spatial jitter. On each trial, a "base" azimuth was chosen from 11 possible locations; -56.26° to +56.26° in 11.25° steps. Five adjacent loudspeakers centered on the base azimuth [-11.25°, -5.625°, 0°, +5.625°, and +11.25° (relative to the base)] constituted the set of source loudspeakers from which individual components of the stimulus were presented on a given trial. Each click was randomly and independently assigned to one of the five source loudspeakers.

5.2.3. Procedure

A touch-sensitive display (Apple iPad Air, Cupertino, CA) was mounted at a comfortable distance (~0.5 m in front and ~0.5 m below ear level) from the listener. This was used to record localization responses aligned to a top-down schematic of the room and loudspeaker array displayed on the screen (i.e., a 180° arc; Fig. 2.1). During data collection, the 180° arc utilized to collect response azimuths had to be switched over to a 360° arc (Fig. 4.1) for three participants with SNHL (2207, 2209, and 2217). This transformation was necessary because, on each trial, the participant nearly always localized the stimulus presented in front of them as originating behind them. These front-back confusions are evidenced to be more prevalent in listeners with SNHL than listeners with NH (e.g., Keidser et al., 2006).

On each trial, participants were instructed to sit upright and face directly forward (toward the loudspeaker at 0°) before and during each stimulus presentation. These instructions helped to ensure participants received expected spatial cues. Immediately following each single presentation of the stimulus, listeners were instructed to make an eye movement to the target signal's perceived location and then record that location on the schematic diagram by touching the iPad screen.

Participants were asked to indicate the leftmost edge or leftmost image on any trial in which the lateral percept appeared "wide" or "split." The response azimuth was computed from the touch screen response and recorded as the localization judgment. The base loudspeaker was selected pseudorandomly from 11 possible locations (± 56.25°) across trials, with each base value presented six times per run of 66 trials. Participants completed six runs (66 trials each) for each of the four conditions (quiet and three SNR conditions). Participants completed six runs (396 trials) for each of the two stimulus conditions (2-ms ICI and 5-ms ICI). Participants with NH completed two sets, one in quiet and one in the presence of the TEN in random order, with sets interleaved.

5.2.4. Analysis

TWFs were calculated separately for each listener and condition. Within each 66-trial run, the localization judgment was normalized by rank transform across each 66-trial run. Perceptual weights for each of the 16 clicks were estimated by multiple linear regression of the rank-transformed responses θ_R onto the azimuth values of each component θ_i. For the participants with front-back errors, the responses on the left and right were transformed by subtraction of -180° and 180°, respectively.

$$\theta_R = \sum_{i=1}^{16} \beta_i \, \theta_i + k \quad (1)$$

Weights were computed by normalizing regression coefficients β_i so that absolute values summed to 1 across weights.

$$w_i = \beta_i \, / \sum_{j=1}^{16} |\beta_j| \quad (2)$$

The normalized weights w_i indicate the relative influence of the click i on listeners' localization judgments. Plotted together, the normalized weights constitute the TWF for each listener in each condition. Group average TWFs were calculated by taking the arithmetic mean normalized weight across listeners, for each click.

Stecker and Moore (2018) and Chapter 3 computed the "average ratio" (AR) as a univariate measure of non-uniformity, specifically with an emphasis on the first click (onset). The AR_{onset} was used to interpret prominence of onset dominance in participants with real and simulated SNHL. The AR_{onset} was defined as the ratio of weight on the first click to the mean of the remaining clicks:

$$AR_{\text{onset}} = \mathrm{w}_{\text{click 1}} \, / (\sum_{j \neq \text{click 1}} w_j / 15) \quad (3)$$

As in Stecker and Moore (2018), the current study computed the TWF confidence intervals and evaluated planned comparisons of weight and AR_{onset} by non-parametric bootstrap tests. Bootstrapped confidence intervals on mean weight values were computed by resampling

weights, with replacement, across subjects to generate 2000 bootstrap replicates. The mean weight was computed for each replicate to estimate the sampling distribution of mean weights. Confidence intervals were computed at the 95% level by taking the 2.5 and 97.5 percentile points from this sampling distribution.

Null-hypothesis significance tests used a similar approach. Each measure (e.g., AR_{onset}) was resampled across participants to generate 2000 bootstrap replicates. A statistic of interest (e.g., mean, or difference between two means) was then computed for each bootstrap replicate to estimate the corresponding sampling distribution. The proportion of bootstrap replicates falling at or below the null-hypothesis prediction (e.g., AR <= 1) defines the (one-sided) p-value, which is expressed to one significant digit. For two-sided statistical tests, the p-value was computed as the minimum of proportions falling on either side of the prediction, doubled. When any proportion was zero (i.e., the bootstrap sampling distribution did not overlap the null-hypothesis prediction), p-values are listed at the resolution of the bootstrap test itself (i.e., $p < .0005$ for 2000-fold bootstrap).

As a secondary analysis of localization performance, the root mean square (RMS) error (indicating errors made outside of the 22.5° range of spatial jitter) and the R^2 [from measured TWFs, indicating the variability in response data accounted for by the multiple linear regression model (function 1)] were calculated for all participants in each stimulus condition.

5.3. Results and Discussion

5.3.1. Temporal Weighting Functions

Figure 5.1 plots cross-participant mean TWFs for NH participants in quiet (left column) and in the presence of the TEN (middle column) and for SNHL participants in quiet (right

column). For NH participants in quiet, the largest weight was found for the first click for both the 2- and 5-ms ICI stimulus conditions, resulting in onset dominance. The weight for the first click in the 2-ms ICI stimulus condition was higher (.23) than in the 5-ms ICI stimulus condition (.13). These results are consistent with the results of Stecker and Hafter (2002; 2009) and Stecker and Moore (2018) for the 5-ms ICI. The lowest ICI Stecker and Hafter (2002) measured was 3 ms. The current study reveals a slightly larger weight for the 2-ms ICI (by about .05). Stecker and Hafter (2002; 2009) also found that for the 5-ms ICI, the weights at the offset of the stimulus (last clicks) gradually increased until the last click was larger than the first click.

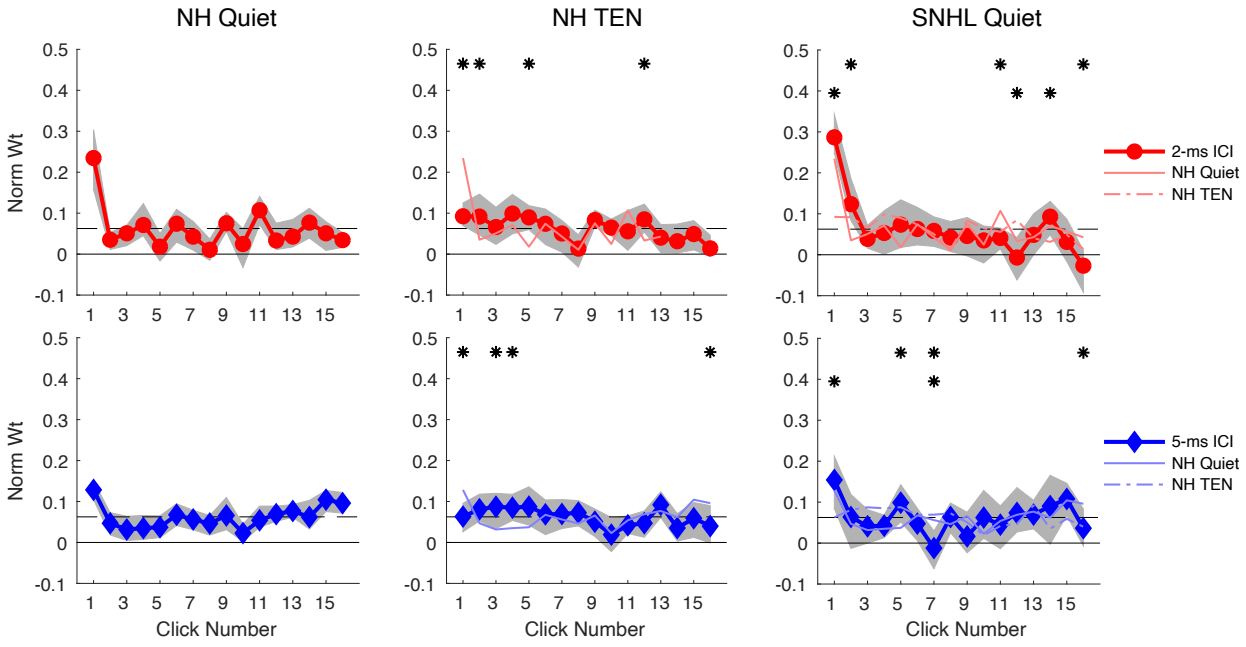

FIG. 5.1. Mean TWFs obtained across participants with NH in quiet (left column), NH in TEN (middle column), and SNHL in quiet (right column). The rows plot TWF data for 2-ms ICI (red circles; top row) and 5-ms ICI (blue diamonds). Symbols and solid lines plot cross-participant mean normalized weight as a function of click number. Shaded regions indicate bootstrapped ±95% confidence intervals on each mean weight. Dashed lines indicate the expected value (1/16)

for uniform weighting across components. NH quiet TWFs are replotted as thin colored lines in NH TEN and SNHL quiet panels for purposes of comparison. NH TEN TWFs are replotted as thin colored dashed-dot lines in and SNHL quiet panels also, for purposes of comparison. Bootstrapped, two-tailed, significant differences ($p < .05$) between weights for NH quiet and NH TEN or SNHL quiet weights are indicated with asterisks (*) at the top of each panel. Significant differences between weights for NH TEN and SNHL quiet weights are indicated with asterisks below the top asterisks.

When participants with NH were tested in the presence of the TEN masker, onset dominance was significantly reduced. That is, the weight for the first click was significantly smaller in TEN than in quiet for both the 2-ms ICI (Fig. 5.1; top middle panel) and 5-ms ICI (bottom middle panel), as indicated by asterisks at the top of the panels. This is consistent with the results of Akeroyd and Guy (2011) and Goverts et al. (2002), who found a decrease in onset dominance in the presence of interfering noise for precedence effect tasks. Some clicks for the ongoing portion of the stimulus (clicks 2-13) received significantly greater weight in TEN than in quiet. The offset, or last click, was reduced for the 5-ms ICI. These results can be attributed to the reduction in the weight of the onset leading to continuous integration of binaural cue information over time. Most weights are along the dashed line (Fig. 5.1), indicating uniform weighting.

Unlike participants with NH in the TEN masker, participants with SNHL exhibit onset dominance for both the 2- and 5-ms ICI stimulus conditions, consistent with the prevalence of onset dominance during a precedence effect task when the ISI between clicks was above 1 ms (Cranford et al., 1998). When compared to listeners with NH in quiet, the amount of weight

placed on the first click was not significantly different for either ICI. However, the mean weights on the first clicks were slightly higher for listeners with SNHL by .06 (2-ms ICI) and .02 (5-ms ICI). Surprisingly, the weight for the second click for the 2-ms ICI stimulus was significantly larger than it was for participants with NH (in quiet). A gradual drop in weight between clicks 1 and 2 for the 2-ms ICI condition may indicate that listeners with SNHL combine the binaural cues provided by both clicks. Some clicks within the ongoing portion of the stimulus received significantly larger and smaller weights. Weights close to zero were found for listeners with SNHL but not for participants with NH. Indicating some clicks did not contribute to the overall localization response.

The individual-participant TWFs depicted in Fig. 5.2 (arranged in the same manner as Fig. 5.1) demonstrate a large variability in weights in participants with SNHL compared to listeners with NH. Within these differences, many participants (such as 2214; white circles) demonstrate onset dominance but also demonstrate large increases and decreases in weight as if weighting is dramatic and "restarts" within the stimulus. It is easier to see these fluctuations across individual participants in Fig. 5.3, which replots their TWFs in separate panels, along with their free-field detection thresholds measured in Chapter 4. Large fluctuations of the individual TWFs are most likely the cause of significant differences in weight across participants with NH and SNHL during the ongoing portions of the stimulus. The hypothesis of the current study stated that due to the changes in amplitude modulation sensitivity with SNHL (Moore et al., 1992, 1996; Fullgrabe et al., 2003), onset dominance would decrease (i.e., each click would be treated independently, resulting in a flat TWF). However, TWFs revealed onset dominance as well as fluctuations of weight values for the ongoing portion of the stimulus. The sensitivity to amplitude modulation may have instead increased the prevalence of onset dominance, especially

for the 5-ms ICI stimulus. Fluctuations in the weighting pattern for some participants may have been caused by increased amplitude modulation integration (Wallaert et al., 2017). It is possible that if monaural temporal integration is increased, so is binaural integration.

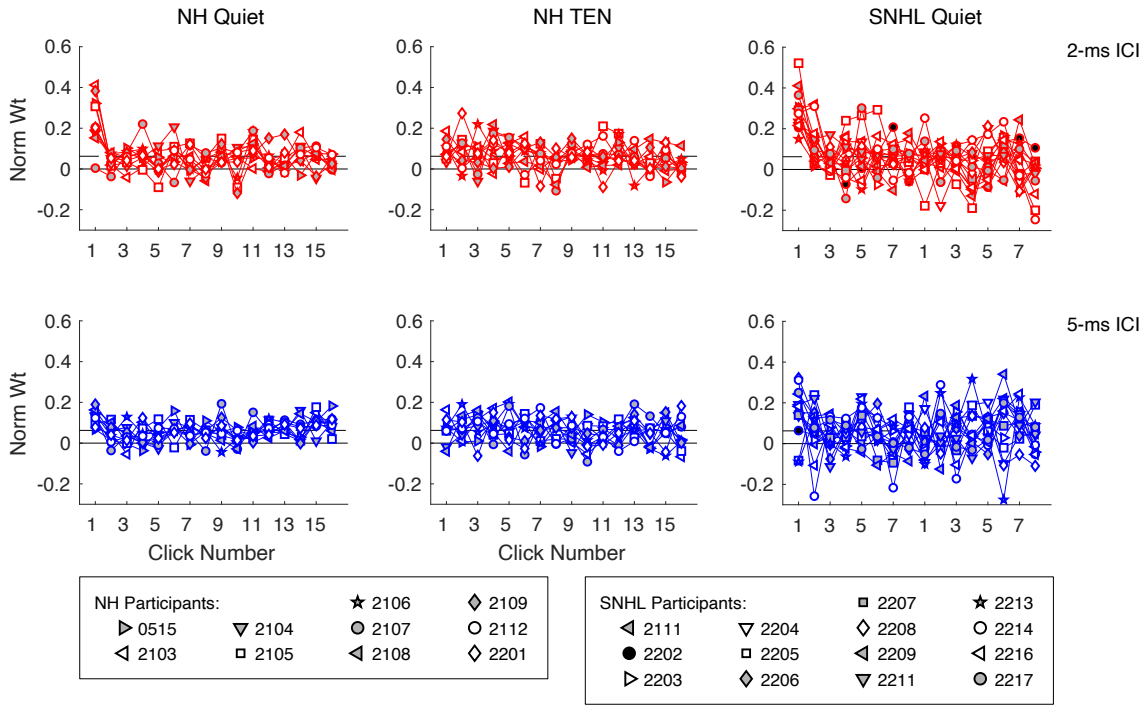

FIG. 5.2. Individual-participant TWFs found in participants with NH in quiet (left column), NH in TEN (middle column), and SNHL in quiet (right column). The rows plot TWF data for 2-ms ICI (red) and 5-ms ICI (blue) stimulus condition. Each panel plots TWFs obtained for individual participants (symbols; legend at bottom).

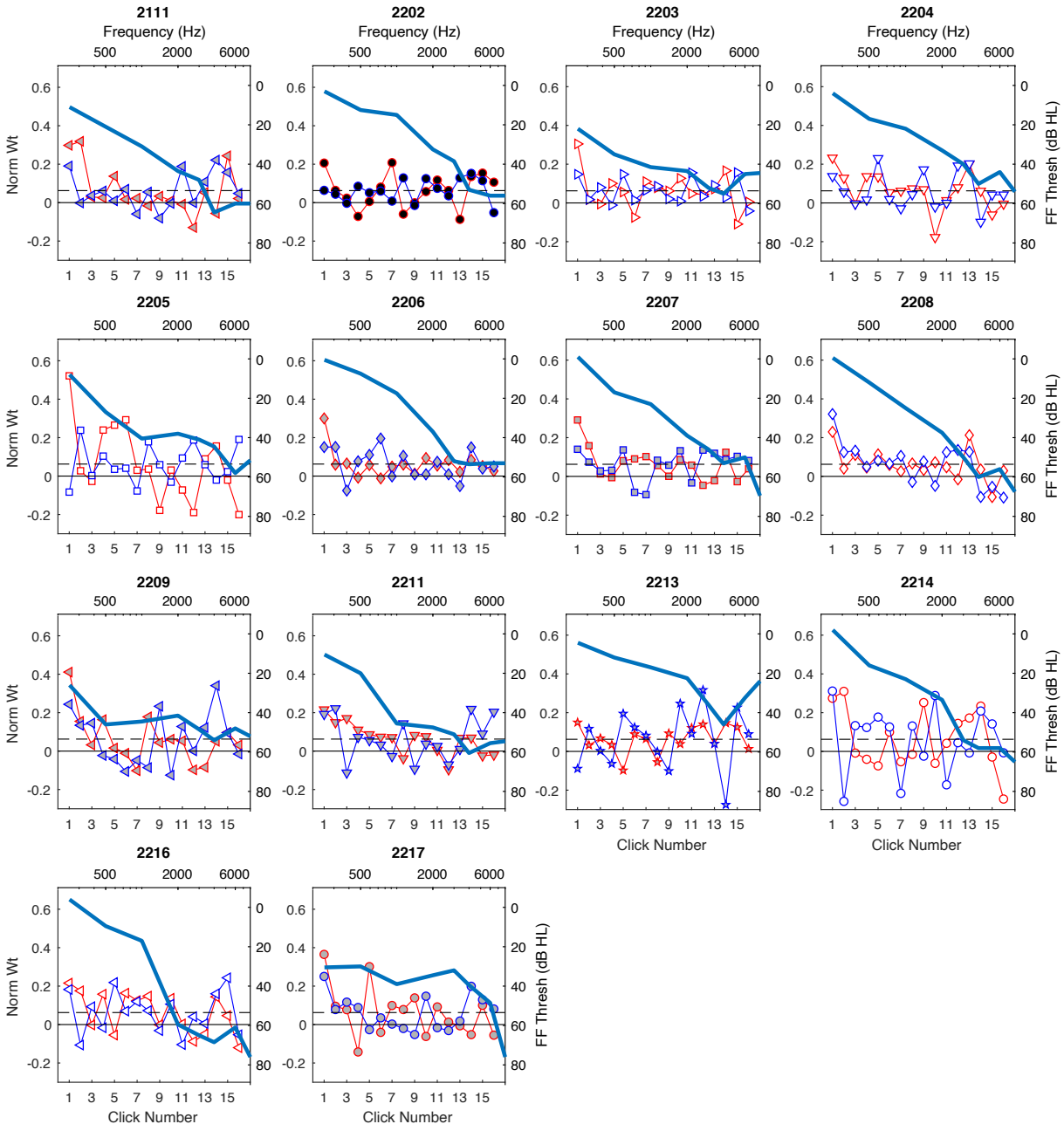

FIG. 5.3. Individual-participant TWFs found in participants with SNHL in quiet (Fig. 5.2; right column) are plotted as a function of click number (horizontal axis). Each panel plots the individual TWF data for 2-ms ICI (red) and 5-ms ICI (blue) stimulus conditions. Dashed lines indicate the expected value (1/16) for uniform weighting across components. Each panel also plots free-field pure tone thresholds (dB HL; solid light blue line; right vertical axis) as a

function of frequency (Hz; top horizontal axis) obtained for respective individual participants (panels).

The offset or last click (16) was significantly smaller for participants with SNHL compared to participants with NH. This is surprising, especially since for the 5-ms ICI, there is a gradual increase in weight up until the last click for participants with NH. It is possible that this too is due to the fluctuations. An increase in amplitude modulation integration of monaural information may be able to explain these fluctuations; however, it is interesting that participants do not integrate each click, which should lead to equal weighting. Instead, it seems as if the binaural system "restarts," which in NH listeners occurs due to a change in the stimulus (Hafter and Buell, 1990). Stecker and Hafter (2002) found that a brief interval within the click stimulus leads to an onset occurring for the first click after the quiet interval. It may be that participants with SNHL are not integrating binaural information evenly due to the reduction in ITD_{env} and ILD processing or even ITD_{fs} (e.g., Fullgrabe and Moore, 2018) and monaural temporal fine structure processing (e.g., Strelcyk and Dau, 2009).

The TWF patterns of listeners with SNHL were not replicated by participants with NH in the TEN masker. Consistent with Goverts et al. (2002) and Akeroyd and Guy (2011), onset dominance was reduced with the addition of noise. However, this did not result in a replication of the participants with SNHL data. Onset dominance was prevalent across many listeners with SNHL (Fig. 5.2 and 5.3). Participants with SNHL placed a significantly larger weight on the first click when compared to participants with NH in TEN; for both 2- and 5-ms ICI stimulus conditions (as indicated by second-level asterisks in Fig. 5.1; right panels). Because of the large fluctuations across TWFs measured in participants with SNHL (Fig. 5.2 and 5.3), it may not be

easy to visually inspect the onset dominance's strength. The AR_{onset} values depict a single value, the ratio between the first click and the remaining clicks. AR_{onset} values are depicted as violin plots in Fig. 5.4. For participants with SNHL, AR_{onset} values are similar to NH participants. Although, their variability does increase to larger AR_{onset} values and smaller values for the 5-ms ICI stimulus condition (right panel). AR_{onset} values for participants with NH in TEN had little individual variability and were significantly smaller than AR_{onset} values for participants with SNHL and NH in quiet. The mean AR_{onset} values for participants with NH in TEN were 1.57 for the 2-ms ICI and 1.07 for the 5-ms ICI. The reduction in onset weights is most likely due to masking by the TEN. When Chapter 3 presented independent Gaussian noise maskers at lateral angles (-90° and +90°), onset dominance was reduced, even for a 6 dB SNR. In that study, the reduction was attributed to the masking of the rising envelope of the click. It is now apparent that the TEN masker did not simulate TWFs for participants with SNHL. This is most likely because participants have demonstrated an enhanced sensitivity to sound envelopes and the TEN masker caused the envelopes to be less detectable for participants with NH.

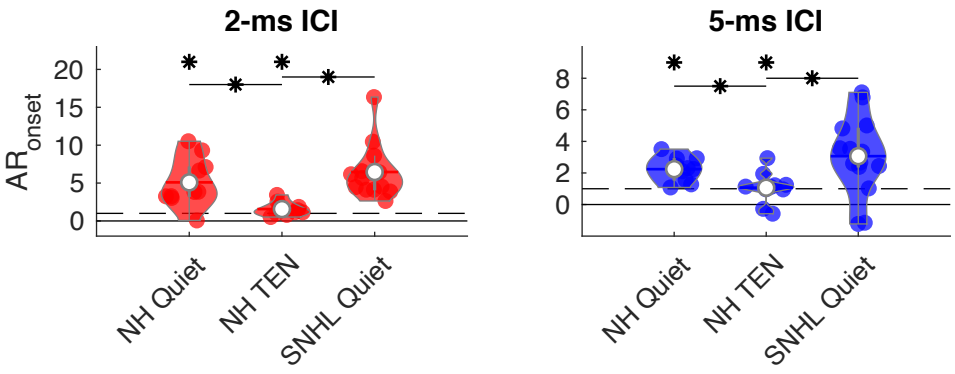

FIG. 5.4. Violin plots of AR_{onset} values (vertical axis) are shown for each stimulus condition (panels), plotted for participants with NH in quiet, NH in TEN, and SNHL in quiet (horizontal

axis). Colored circles in each panel plot AR_{onset} for individual participants; violin plots indicate the density (width of each violin) and mean (white circle) of obtained values. Dashed lines indicate the expectation for uniform spectral weighting AR = 1. Asterisks (*) indicate conditions in which AR_{onset} significantly exceeded this value ($AR_{onset} > 1$, $p < .0005$ by 2000-fold bootstrap test). Asterisks with a line indicate bootstrapped significant differences between conditions ($p < .05$, two-tailed).

5.3.2. Localization Performance

The localization performance of participants with SNHL was compared to participants with NH in quiet and in the presence of the TEN as a secondary analysis of the TWF response data. Two metrics were used, the RMS error and the R^2 statistic. The RMS errors and the R^2 values are depicted in Fig. 5.5 (left and right panels, respectively) for the 2-ms ICI (red circles) and the 5-ms ICI (blue circles). As in Chapter 4, RMS errors and R^2 values did not significantly increase when NH participants were in the presence of the TEN. In the current study, the TEN seemed to slightly reduce the number of errors made for the 2-ms ICI. The error bars for listeners with NH in quiet (Fig. 5.5; left panel) are larger than the error bars when the same participants were in the presence of the TEN. Figure 5.6 plots the response values as a function of the base loudspeaker for participant 2107, who had larger errors outside of the 22.5° range of loudspeakers (solid grey lines) when they were in quiet and not so much when they were in TEN. These errors are mainly due to the spread of responses outside the 22.5° range, especially for more lateral angles. When in the presence of the TEN, participant 2107 condensed their responses. It is possible that the TEN, which is a diffuse noise, caused this perception as "pushing" of the responses towards lateral competing noises occurred in Chapter 3 for a 2-ms

ICI click train, where the competing noise provided a somewhat diffuse perception (Blauert, 1997).

The effect of rank-transforming the responses is clearly depicted when comparing the RMS errors for participants with NH in TEN with their R^2 values (Fig. 5.5 right panel). That is, the linear regression model (function 1) accounted for most of the responses due to normalization providing a uniform distribution of responses (i.e., the most lateral response, which can be 80° or 50°, is transformed to 1; with the remaining responses falling between 0 and 1).

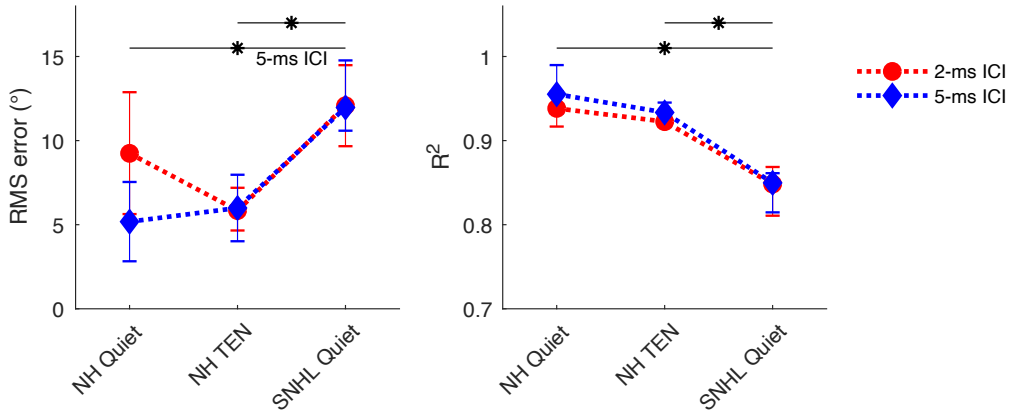

FIG. 5.5. Mean RMS error (in degrees; left panel) and mean or R^2 (right panel) across groups of participants with NH in quiet, NH in TEN, and SNHL in quiet for the 2-ms ICI (red circles) and 5-ms ICI (blue diamonds) stimulus conditions. Error bars indicate bootstrapped ±95% confidence intervals on each mean value (RMS error or R^2). Asterisks with lines indicate significant differences across participant groups for the two stimulus conditions, calculated separately (unless indicated below the line; i.e., the RMS error was only significant for the 5-ms ICI between participants with NH and SNHL in quiet).

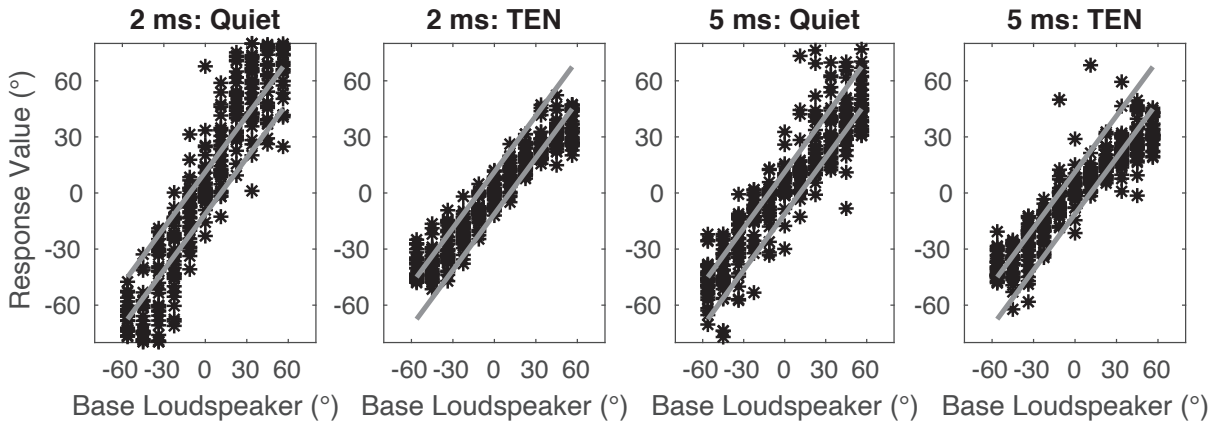

FIG. 5.6. Each panel plots individual response values (in degrees; before rank-transformation) as a function of the base loudspeaker (as asterisks) for participant 2107. Solid grey lines indicate the 22.5° range of loudspeakers (where the components were distributed) around the base azimuth. Panels from left to right indicate the 2-ms ICI stimulus condition in quiet then TEN (first two panels) and the 5-ms ICI stimulus condition in quiet then TEN (last two panels).

To determine if TWFs were confidently measured in participants with SNHL, the R^2 statistic was evaluated. As depicted in Fig. 5.5 (right panel), the average R^2 value was .83 for the 2-ms ICI and .82 for the 5-ms ICI; that is, the linear regression model used to calculate TWFs accounted for more than 80% of the response data. Even the smallest R^2 values were above .7. Thus, response accuracy was sufficiently high to calculate TWFs accurately. However, when comparing the R^2 values between participants with SNHL and NH (in quiet and TEN), there are significant differences (Fig. 5.5 left panel); 95% variability in the response data for participants with NH could be accounted for. This is most likely due to the increase in localization errors

which were significantly more prevalent for participants with SNHL than participants with NH (Fig. 5.5 right panel).

Significant differences were found between participants with SNHL and NH (in quiet and TEN), as the average RMS error for participants with SNHL was about 13° for both stimulus conditions. The average RMS error for participants with NH was about 5° in quiet and TEN, except for the 2-ms ICI condition in quiet. Figure 5.7 plots the response values as a function of the base loudspeaker for participant 2216, who had the largest RMS errors (across participants) of about 20° for both stimulus conditions. Many of their responses for lateral base loudspeakers reveal errors in responses. Specifically, for base loudspeakers between 22.5° to 56.25° on the left and right (negative and positive degrees), responses ranged between 30° and 80° separately for the left and right sides. Rank transformation would reveal the same pattern because all of the responses were spread within this range, revealing a reduction of a distinct pattern of responses, unlike participant 2107 (Fig. 5.6), who had a strict pattern of responses that were monotonic as a function of the base loudspeaker. The R^2 values for participant 2216 were .82 for the 2-ms ICI and .78 for the 5-ms ICI. Therefore, TWFs accounted for about 80% of participant 2216's data, even with errors at lateral angles.

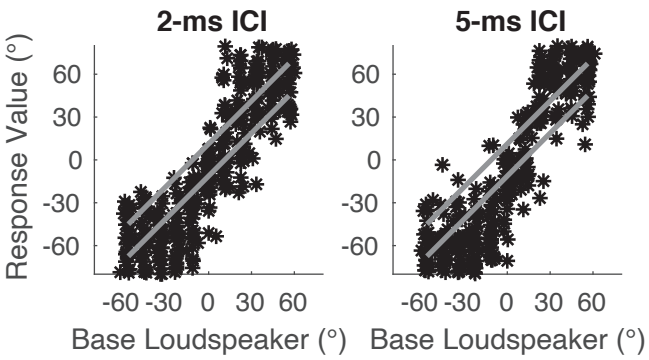

FIG. 5.7. Similar to Fig. 5.6, each panel plots individual response values (in degrees; before rank-transformation) as a function of base loudspeaker (as asterisks) for participant 2216. Solid grey lines indicate the 22.5° range of loudspeakers (where the components were distributed) around the base azimuth. The panel on the left indicates the 2-ms ICI stimulus condition, and the panel on the right indicates the 5-ms ICI stimulus condition.

It is not surprising that participants with SNHL had a slight increase in localization errors. Errors in localization of wideband stimuli centered at high frequencies providing ITD_{env} and ILD cues have been found (Van den Bogaert et al., 2006; Keidser et al., 2009; van Esch et al., 2013). Investigations of ITD_{env} cue encoding in listeners with SNHL reveal a reduced sensitivity to such cues compared to listeners with NH (Hawkins and Wightman, 1980; Buus et al., 1984; Lacher-Fougere and Demany, 2005). However, King et al. (2014) found that the sensitivity to the ITD_{env} cue was more positively correlated with age than hearing threshold. This is consistent with the findings of amplitude modulation encoding, where older listeners had a reduced sensitivity compared to younger listeners (Wallaert et al., 2016). For the encoding of the ILD cue, early results concluded no change in sensitivity for listeners with SNHL compared to

listeners with NH (Hausler et al., 1983). Other studies have found that although this is true for many listeners with SNHL, some listeners demonstrate a reduction of encoding of the ILD cue (Gabriel et al., 1992; Koehnke et al., 1995; Smith-Olinde et al., 1998). The effects of age and hearing loss on ILD sensitivity have not been established.

5.3.3. The Effect of Free-field Threshold and Age

To understand the effect of both hearing threshold and age on the degree of onset dominance, Pearson correlations were conducted between the AR_{onset} measured participants with SNHL and average free-field thresholds for low frequencies (250, 500, and 1000 Hz), average free-field thresholds for high frequencies (3000, 4000, 6000 and 8000 Hz), and age (in years). The AR_{onset}, rather than the amount of weight placed on the first click, was chosen because it accounted for the fluctuations of the TWFs found for some participants (see section 5.3.1). Large weights were averaged within the denominator (however do note that for some participants, these fluctuations also include negative weights, which would drive the average toward 0). Figure 5.9 displays each individual participant's AR_{onset} value as a function of their average low-frequency free-field threshold (left panel), average high-frequency free-field threshold (middle panel), and age (right panel) for each stimulus condition (legend). In each panel, for each stimulus condition, the least-squares regression line is also plotted. The correlation value is displayed to the right of each regression line (except for the 2 ms, with significant correlations indicated in bold with an asterisk after correcting for family-wise errors using a Bonferroni correction (n = 6; $p < .0083$).

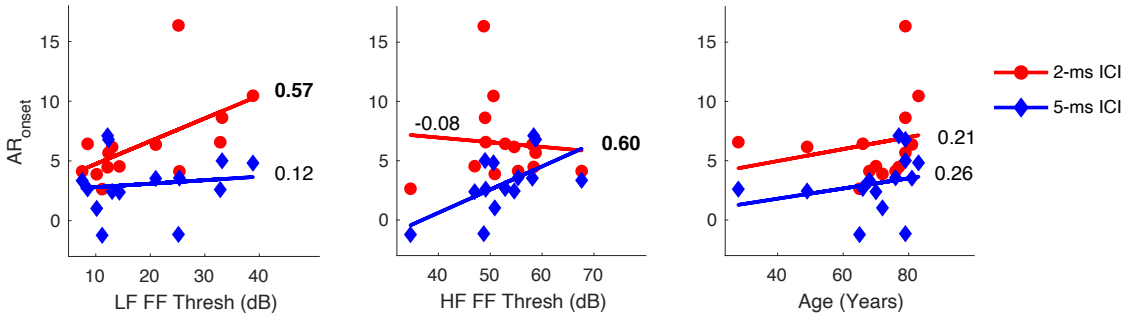

FIG. 5.8. Scatter plots for each individual SNHL participant's AR_{onset} value as a function of their average low-frequency free-field threshold (left panel), average high-frequency free-field threshold (right panel), and age (right panel) for each stimulus condition (legend). Each panel plots the least-squares regression line for each stimulus condition (by color; see legend). The correlation values (r) are displayed to the right of each regression line. Bold correlation values indicate significant correlations ($p < .05$) while bold with asterisks indicate a significant correlation $p < .0083$ after Bonferroni correction (n = 6).

After correcting for family-wise errors, no significant correlations were found. There were, however, two correlations that were moderately correlated ($p < .05$). The AR_{onset} for the 2-ms ICI stimulus condition was positively correlated with low-frequency free-field thresholds, and the AR_{onset} for the 5-ms ICI stimulus condition was positively correlated with high-frequency free-field thresholds. These results do not align with Akeroyd and Guy (2011), who found the weight of the first portion of a precedence stimulus to be negatively correlated with monaural hearing thresholds. It is unknown why the current study shows a trend for onset dominance increasing with decreasing hearing thresholds, while Akeroyd and Guy (2011) found onset dominance to be reduced with increasing thresholds. One key in the current data might be in the divide of these correlations between stimulus conditions. The 2-ms ICI AR_{onset} seems to be in the

range of participants with NH (Fig. 5.4; left panel), a value of about 5, for listeners with low low-frequency loss. With increasing low-frequency hearing loss, participants have quite large AR_{onset} values. The 5-ms ICI AR_{onset} seems to be in the range of participants with NH (Fig. 5.4; right panel), a value of about 1, for listeners with low high-frequency hearing loss. With increasing high-frequency hearing loss, participants have larger AR_{onset} values. These results then indicate that onset dominance may be enhanced for participants with SNHL when their thresholds increase.

What's intriguing is, hearing loss for low frequencies and high frequencies had different effects on onset dominance. It has been found that low-frequency monaural thresholds are correlated with degradation in ITD_{fs} cue sensitivity (King et al., 2014; Fullgrabe and Moore, 2018). Although the ITD_{env} cue was available in the stimulus for the current study, with a similar type of stimulus (transposed tones), evidence has suggested that the encoding of this cue may stem from the same binaural mechanism as used to encode the ITD_{fs} cue (Colburn and Esquissaud, 1976; Bernstein and Trahiotis, 2002; 2003). Lacher-Fougere and Demany (2005) found that listeners with SNHL have a reduction in ITD_{env} sensitivity which was dependent on their overall hearing thresholds. However, it is unclear how either a reduction in ITD_{fs} or ITD_{env} sensitivity relates to the rate limitation or strength of onset dominance. The rate limitation of ITD_{env} cues has been ascribed to a central rather than peripheral mechanism (e.g., Bernstein and Trahiotis, 2014). With this and the results of the current study, the central mechanism may be affected in listeners with SNHL differently for low-frequency and high-frequency losses, leading to an increased strength of onset dominance for different ITD_{env} cue rates. However, the reader is suggested to proceed with caution as fluctuations in the TWFs of many participants with SNHL (see Fig. 5.5) may not have been captured by the AR_{onset} due to the negative weights. These

fluctuations are ascribed to multiple onsets occurring for the participant within the stimulus, most likely due to an increase in the perception of the envelope slope, which would be due to changes in peripheral processing.

5.4. Summary and Conclusions

The purpose of the current study was to explore the effects of hearing loss on onset dominance by evaluating TWFs measured in participants with NH with simulated hearing loss (TEN) and participants with SNHL. The TWFs of these participants were compared to participants with NH tested in quiet. The results of this study revealed four main findings:

1) The simulation of SNHL reduced onset dominance for participants with NH; however, TWFs of participants with SNHL revealed onset dominance similar to participants with NH. TWFs for listeners with SNHL were not well modeled by threshold elevation in participants with NH. TWFs measured in participants with NH (in quiet) were consistent with previous TWF measures for the same or similar stimuli (Stecker and Hafter 2002; 2009; Stecker and Moore, 2018).

2) Individual SNHL participant TWFs reveal a variety of shapes across stimulus conditions. Instead of just the first click receiving the largest relative weight, many participants revealed fluctuations in weighting within TWFs. This is possibly due to combinatory effects of increased amplitude modulation integration and decreased binaural sensitivity. Multiple onset-like events within the stimulus, leading to the restarting of binaural processing, may have occurred for these listeners.

3) The localization performance of participants with SNHL was reduced compared to participants with NH in quiet and in the presence of the TEN masker. The masker did not drive participants with NH to have reduced localization accuracy, even though the masker reduced the

onset dominance. Like TWFs, the localization performance of participants with SNHL was not well modeled by threshold elevation of participants with NH. Although participants with SNHL had reduced localization ability, they demonstrated strong onset dominance.

REFERENCES

Ahumada, A., and Lovell, J. (**1971**). "Stimulus Features in Signal Detection," J. Acoust. Soc. Am., **49**, 1751–1756. doi:10.1121/1.1912577

Akeroyd, M. A., and Guy, F. H. (**2011**). "The effect of hearing impairment on localization dominance for single-word stimuli," J. Acoust. Soc. Am., **130**, 312–323. doi:10.1121/1.3598466

Babkoff, H., and Sutton, S. (**1969**). "Binaural Interaction of Transients: Interaural Intensity Asymmetry," J. Acoust. Soc. Am., **46**, 887–892. doi:10.1121/1.1911805

Bacon, S. P., and Gleitman, R. M. (**1992**). "Modulation Detection in Subjects With Relatively Flat Hearing Losses," J. Speech Lang. Hear. Res., **35**, 642–653. doi:10.1044/jshr.3503.642

Berg, B. G. (**1989**). "Analysis of weights in multiple observation tasks," J. Acoust. Soc. Am., **86**, 1743–1746. doi:10.1121/1.398605

Bernstein, L. R., and Trahiotis, C. (**2002**). "Enhancing sensitivity to interaural delays at high frequencies by using 'transposed stimuli,'" J. Acoust. Soc. Am., **112**, 1026–1036. doi:10.1121/1.1497620

Bernstein, L. R., and Trahiotis, C. (**2003**). "Enhancing interaural-delay-based extents of laterality at high frequencies by using 'transposed stimuli,'" J. Acoust. Soc. Am., **113**, 3335. doi:10.1121/1.1570431

Bernstein, L. R., and Trahiotis, C. (**2014**). "Sensitivity to envelope-based interaural delays at high frequencies: Center frequency affects the envelope rate-limitation," J. Acoust. Soc. Am., **135**, 808–816. doi:10.1121/1.4861251

Bisgaard, N., Vlaming, M. S. M. G., and Dahlquist, M. (**2010**). "Standard Audiograms for the IEC 60118-15 Measurement Procedure," Trends Amp., **14**, 113–120. doi:10.1177/1084713810379609

Blauert, J. (**1997**). *Spatial Hearing: The Psychophysics of Human Sound Localization*, MIT Press, 514 pages.

Brown, A. D., and Stecker, G. C. (**2010**). "Temporal weighting of interaural time and level differences in high-rate click trains," J. Acoust. Soc. Am., **128**, 332–341. doi:10.1121/1.3436540

Brown, A. D., Stecker, G. C., and Tollin, D. J. (**2015**). "The Precedence Effect in Sound Localization," J. Assoc. Res. Otolaryn., **16**, 1–28.

Buus, S., Scharf, B., and Florentine, M. (**1984**). "Lateralization and frequency selectivity in normal and impaired hearing," J. Acoust. Soc. Am., **76**, 77–86. doi:10.1121/1.391010

Colburn, H. S., and Esquissaud, P. (**1976**). "An auditory-nerve model for interaural time discrimination of high-frequency complex stimuli," J. Acoust. Soc. Am., **59**, S23–S23. doi:10.1121/1.2002503

Cranford, J. L., Andres, M. A., Piatz, K. K., and Reissig, K. L. (**1993**). "Influences of Age and Hearing Loss on the Precedence Effect in Sound Localization," J. Speech Lang. Hear. Res., **36**, 437–441. doi:10.1044/jshr.3602.437

Diedesch, A. C., and Stecker, G. C. (**2015**). "Temporal weighting of binaural information at low frequencies: Discrimination of dynamic interaural time and level differences," J. Acoust. Soc. Am., **138**, 125–133. doi:10.1121/1.4922327

van Esch, T. E. M., Kollmeier, B., Vormann, M., Lyzenga, J., Houtgast, T., Hällgren, M., Larsby, B., et al. (**2013**). "Evaluation of the preliminary auditory profile test battery in an

international multi-centre study," Intern. J. Aud., **52**, 305–321. doi:10.3109/14992027.2012.759665

Freyman, R. L., Zurek, P. M., Balakrishnan, U., and Chiang, Y.-C. (**1997**). "Onset dominance in lateralization," J. Acoust. Soc. Am., **101**, 1649–1659. doi:10.1121/1.418149

Füllgrabe, C., Meyer, B., and Lorenzi, C. (**2003**). "Effect of cochlear damage on the detection of complex temporal envelopes," Hear. Res., **178**, 35–43. doi:10.1016/S0378-5955(03)00027-3

Füllgrabe, C., and Moore, B. C. J. (**2018**). "The Association Between the Processing of Binaural Temporal-Fine-Structure Information and Audiometric Threshold and Age: A Meta-Analysis," Trends Hear., **22**, 233121651879725. doi:10.1177/2331216518797259

Gabriel, K. J., Koehnke, J., and Colburn, H. S. (**1992**). "Frequency dependence of binaural performance in listeners with impaired binaural hearing," J. Acoust. Soc. Am., **91**, 336–347. doi:10.1121/1.402776

Gardner, M. B. (**1968**). "Historical Background of the Haas and/or Precedence Effect," The Journal of the Acoustical Society of America, **43**, 1243–1248. doi:10.1121/1.1910974

Goverts, S. T., Houtgast, T., and van Beek, H. H. M. (**2002**). "The precedence effect for lateralization for the mild sensory neural hearing impaired," Hear. Res., **163**, 82–92.

Hafter, E. R., and Buell, T. N. (**1990**). "Restarting the adapted binaural system," J. Acoust. Soc. Am., **88**, 806–812. doi:10.1121/1.399730

Hafter, E. R., and Dye, R. H. (**1983**). "Detection of interaural differences of time in trains of high-frequency clicks as a function of interclick interval and number," J. Acoust. Soc. Am., **73**, 644–651. doi:10.1121/1.388956

Häusler, R., Colburn, S., and Marr, E. (**1983**). "Sound Localization in Subjects with Impaired Hearing: Spatial-Discrimination and Interaural-Discrimination Tests," Acta Oto-Laryn., **96**, 1–62. doi:10.3109/00016488309105590

Hawkins, D. B., and Wightman, F. L. (**1980**). "Interaural Time Discrimination Ability of Listeners with Sensorineural Hearing Loss," Int. J. Aud., **19**, 495–507. doi:10.3109/00206098009070081

Hellman, R. P., and Meiselman, C. H. (**1990**). "Loudness relations for individuals and groups in normal and impaired hearing," J. Acoust. Soc. Am., **88**, 2596–2606. doi:10.1121/1.399979

Hellman, R. P., and Meiselman, C. H. (**1993**). "Rate of loudness growth for pure tones in normal and impaired hearing," J. Acoust. Soc. Am., **93**, 966–975. doi:10.1121/1.405402

Keidser, G., O'Brien, A., Hain, J.-U., McLelland, M., and Yeend, I. (**2009**). "The effect of frequency-dependent microphone directionality on horizontal localization performance in hearing-aid users," Int. J. Aud., **48**, 789–803. doi:10.3109/14992020903036357

Keidser, G., Rohrseitz, K., Dillon, H., Hamacher, V., Carter, L., Rass, U., and Convery, E. (**2006**). "The effect of multi-channel wide dynamic range compression, noise reduction, and the directional microphone on horizontal localization performance in hearing aid wearers," Int. J. Aud., **45**, 563–579. doi:10.1080/14992020600920804

King, A., Hopkins, K., and Plack, C. J. (**2014**). "The effects of age and hearing loss on interaural phase difference discrimination," J. Acoust. Soc. Am., **135**, 342–351. doi:10.1121/1.4838995

Koehnke, J., Culotta, C. P., Hawley, M. L., and Colburn, H. S. (**1995**). "Effects of Reference Interaural Time and Intensity Differences on Binaural Performance in Listeners with

Normal and Impaired Hearing" Ear Hear., **16**, 331–353. doi:10.1097/00003446-199508000-00001

Lacher-Fougère, S., and Demany, L. (**2005**). "Consequences of cochlear damage for the detection of interaural phase differences," J. Acoust. Soc. Am., **118**, 2519–2526. doi:10.1121/1.2032747

Litovsky, R. Y., Colburn, H. S., Yost, W. A., and Guzman, S. J. (**1999**). "The precedence effect," J. Acoustic. Soc. Am., **106**, 1633–1654.

Moore, B. C. J. (**2004**). "Testing the concept of softness imperception: Loudness near threshold for hearing-impaired ears," J. Acoust. Soc. Am., **115**, 3103–3111. doi:10.1121/1.1738839

Moore, B. C. J., and Glasberg, B. R. (**2001**). "Temporal modulation transfer functions obtained using sinusoidal carriers with normally hearing and hearing-impaired listeners," J. Acoust. Soc. Am., **110**, 1067–1073. doi:10.1121/1.1385177

Moore, B. C. J., Shailer, M. J., and Schooneveldt, G. P. (**1992**). "Temporal modulation transfer functions for band-limited noise in subjects with cochlear hearing loss," Brit. J. Aud., **26**, 229–237. doi:10.3109/03005369209076641

Oxenham, A. J., and Plack, C. J. (**1997**). "A Behavrioral measure of basilar-membrane nonlinearity in listeners with normal and impaired hearing," J. Acoust. Soc. Am., **101**, 3666–3675.

P. M. Zurek (**1987**). "The precedence effect," Directional Hearing, Springer, New York, NY, pp. 85–105.

Rakerd, B., and Hartmann, W. M. (**1985**). "Localization of sound in rooms, II: The effects of a single reflecting surface," J. Acoust. Soc. Am., **78**, 524–533. doi:10.1121/1.392474

Reed, C. M., Braida, L. D., and Zurek, P. M. (**2009**). "Review Article: Review of the Literature on Temporal Resolution in Listeners with Cochlear Hearing Impairment: A Critical Assessment of the Role of Suprathreshold Deficits," Trends Amp.**13**, 4–43. doi:10.1177/1084713808325412

Roberts, R. A., Besing, J., and Koehnke, J. (**2002**). "Effects of Hearing Loss on Echo Thresholds" Ear Hear., **23**, 349–357. doi:10.1097/00003446-200208000-00010

Saberi, K. (**1996**). "Observer weighting of interaural delays in filtered impulses," Percep. Psycho., **58**, 1037–1046. doi:10.3758/BF03206831

Shinn-Cunningham, B. G., Kopco, N., and Martin, T. J. (**2005**). "Localizing nearby sound sources in a classroom: Binaural room impulse responses," J. Acoust. Soc. Am., **117**, 3100–3115. doi:10.1121/1.1872572

Smith-Olinde, L., Koehnke, J., and Besing, J. (**1998**). "Effects of sensorineural hearing loss on interaural discrimination and virtual localization," J. Acoust. Soc. Am., **103**, 2084–2099. doi:10.1121/1.421355

Stecker, G. C. (**2018**). "Temporal weighting functions for interaural time and level differences. V. Modulated noise carriers," J. Acoust. Soc. Am., **143**, 686–695. doi:10.1121/1.5022785

Stecker, G. C., and Moore, T. M. (**2018**). "Reverberation enhances onset dominance in sound localization," J. Acoust. Soc. Am., **143**, 786–793. doi:10.1121/1.5023221

Stecker, G. C., Ostreicher, J. D., and Brown, A. D. (**2013**). "Temporal weighting functions for interaural time and level differences. III. Temporal weighting for lateral position judgments," J. Acoust. Soc. Am., **134**, 1242–1252. doi:10.1121/1.4812857

Steinberg, J. C., and Gardner, M. B. (**1937**). "The Dependence of Hearing Impairment on Sound Intensity," J. Acoust. Soc. Am., **9**, 11–23.

Strelcyk, O., and Dau, T. (**2009**). "Relations between frequency selectivity, temporal fine-structure processing, and speech reception in impaired hearing," J. Acoust. Soc. Am., **125**, 3328. doi:10.1121/1.3097469

Van den Bogaert, T., Klasen, T. J., Moonen, M., Van Deun, L., and Wouters, J. (**2006**). "Horizontal localization with bilateral hearing aids: Without is better than with," J. Acoust. Soc. Am., **119**, 515–526. doi:10.1121/1.2139653

Viemeister, N. F., and Wakefield, G. H. (**1991**). "Temporal integration and multiple looks," J. Acoust. Soc. Am., **90**, 858–865. doi:10.1121/1.401953

Wallaert, N., Moore, B. C. J., Ewert, S. D., and Lorenzi, C. (**2017**). "Sensorineural hearing loss enhances auditory sensitivity and temporal integration for amplitude modulation," J. Acoust. Soc. Am., **141**, 971–980. doi:10.1121/1.4976080

Wallaert, N., Moore, B. C. J., and Lorenzi, C. (**2016**). "Comparing the effects of age on amplitude modulation and frequency modulation detection," J. Acoust. Soc. Am., **139**, 3088–3096. doi:10.1121/1.4953019

CHAPTER 6

Concluding Remarks

6.1. Chapter 2: Spectral Weighting in Competing Noise

Spectral weighting functions (SWFs) measured in the presence of competing noise for participants with NH revealed upweighting for components within the ITD dominance region. This means that, in noise, listeners with normal hearing (NH) continue to localize sounds based on binaural cues provided in the 400-1000 Hz frequency region, as listeners do in quiet. These results disagree with previous literature, where it was assumed that listeners localized sounds based on binaural cues provided by high frequencies when in the presence of competing noise. These assumptions were based on the reduction of localization performance when high-frequency cues were not available (Abel and Hay, 1996; Lorenzi et al., 1999; Brungart and Simpson, 2009). Also, in the current study, localization performance revealed an increased number of errors for stimuli that contained high-frequency components when compared to stimuli that contained broader band components. Overall, the current study advances the field due to the direct measurement of the relative influence of each frequency component during localization in noise, especially since data on localization in noise is limited. This study also demonstrates the stability of the ITD dominance region, although the peak of the dominance region may be dependent on the environment (i.e., across participants, the peak of the dominance region was 400 to 800 Hz in noise, whereas the peak was 800 Hz in quiet).

As discussed in Chapter 2, using more similar methods to those used in previous localization in noise studies, such as by 1) removing one of the competing noise sources and 2) using the same target stimuli as previous studies (e.g., bursts of Gaussian noise; Abel and Hay,

1996; Lorenzi et al., 1999; Brungart and Simpson, 2009), could further confirm the dominance region. Lateralization SWFs (as in Folkerts and Stecker, 2022) could also be measured in noise to determine if the ITD cue remains the dominant cue since, with the increase in the interaural correlation, Rakerd and Hartmann (2010) found an increase in the relative weight for the ILD cue.

Future studies may also want to include more realistic stimuli. The competing noise in the current study may not depict the noise spectrum found in everyday environments; future studies could use utilizing multi-talker babble or recorded cafeteria noises. Furthermore, Gaussian noises with spectral notches could be used to test the integrity of the ITD dominance region, which has been demonstrated to be affected by the relative level of components (Folkerts and Stecker, 2022). Alternative target stimuli, such as the speech used by Baltzell et al. (2020), might also be a relevant target stimulus for competing babble. In these realistic environmental conditions, it may be of interest to measure SWFs for listeners with sensorineural hearing loss (SNHL), especially since these listeners report trouble detecting speech in noise-filled environments (Nobel and Gatehouse, 2004). This would hopefully elucidate the binaural cues listeners rely on when listening to speech in noise.

One limitation of the current data set is the reliability of the SWF measurements across participants and SNR conditions. One measure of reliability presented in the current study was the R^2 statistic, which is the proportion of variance accounted for by the data. In Chapter 2, this measure was mainly used to measure variabilities in responses (or errors). Across SNR conditions, localization errors increased, and so did the differences in SWF weighting patterns across participants (i.e., Fig. 2.3). The current data set cannot answer whether this is due to changes in perceptual dominance of the cues for each listener or if it was due to changes in the

model reliability. Future work is warranted to disentangle the effects of noise and localization performance on SWFs by adjusting or accounting for sensitivity or threshold measurements when measuring observer weights (e.g., Bremen and Middlebrooks, 2013).

6.2. Chapter 3: Temporal Weighting in Competing Noise

Temporal weighting functions measured in the presence of competing noise for participants with NH revealed a reduction (or elimination) of the upweighting found for the first click in quiet. The reduction in onset dominance agrees with previous literature, where onset dominance for speech stimuli in babble was reduced (Akeroyd and Guy, 2011). Meaning, during localization in the presence of noise, listeners do not rely on the binaural cues provided by the target signal onset.

An unexpected feature of the TWFs in noise was the upweighting of clicks after the first click. This was especially evident when the SNR was -6 dB. This may be due to the competing noise masking the rising envelope of the clicks. The addition of competing noise when measuring TWFs could advance the field by providing data for a model that seeks to characterize the nature of onset dominance within the auditory system. With that, this study raises the questions: Do the TWFs measured in this study display a different form of binaural integration not previously known? Did competing noise change the rate limitation of onset dominance?

In addition to addressing these questions, the same future directions mention relative to Chapter 2 (e.g., measuring TWFs for binaural cues in noise, decreasing the competing noise source to one, or using environment or notched noise). One of the first thoughts when seeing the upweighting of the ongoing clicks was that there must be fluctuations within the envelope of the competing noise. However, since each iteration of the competing noise was generated

independently, this was not expected. A future study may want to determine if upweighting could be driven by competing noise with a fixed envelope (it would be expected that the click at the lower portions of the envelope would be upweighted). Along with testing other ICIs to determine if the rate limitation was increased to a 5-ms ICI, reverberation could be added as a factor of interest. Stecker and Moore (2018) found an enhancement of onset dominance in reverberation for a 5-ms ICI; it would be interesting to understand the effects of the competing noise on this enhancement (i.e., measuring TWFs in a reverberant environment with competing noise).

As in Chapter 2, the R^2 value decreased, and the variability in TWF shapes increased with unfavorably decreasing SNR. One way to address this may be to use a measure of accuracy as the dependent variable when measuring TWFs (instead of localization response in degrees as in the current study). Brown and Stecker (2010) did this to measure lateralization TWFs. The receiver operating characteristic was used to measure hits versus false alarms (probability of responding to the correct location) for each spatially varied click (component). The area under the curve was then used to determine the weight of the particular component. Weights were computed separately for each independent variable.

6.3. Chapter 4: Spectral Weighting for Simulated and Real SNHL

The simulation of hearing loss by a threshold elevating noise masker was successfully implemented in the free field, as audibility decreased for participants with NH in the free field near target threshold values. Threshold elevation in the free field may be useful for localization studies and beyond (such as free field speech reception studies). The key seems to be that the masker is diffuse. However, the masker may not necessarily need to arise from a 64-channel

array (even an 8-channel array may suffice and should be tested). Also, as noted in Chapter 4, the masker does not lead to a similar localization degradation as found in participants with SNHL. Despite similar free-field thresholds of audibility, participants with simulated hearing loss and NH outperformed their peers with SNHL. This may reveal that localization degradation in listeners with SNHL is not dependent on audibility and may actually be due to suprathreshold processing deficits. Future work is warranted to determine the auditory skills that are important for auditory localization in the horizontal plane.

Another area for future investigation is the difference between SWFs in quiet in the current study and in a previous study under nearly identical conditions. Recall that average SWFs measures in listeners with NH in quiet in this current study displayed a broadening of the ITD dominance region compared to previous measures in the same condition (i.e., Folkerts and Stecker, 2022). The only difference between the two studies (besides the participants) was the interleaving of blocks of trails in quiet with blocks of trials in which the masker was present in the current study. There were no noise conditions in the previous study. It is possible the presence of noise in some conditions created aftereffects that generalized to the conditions without noise. Aftereffects pertaining to the localization of stimuli have been found after long exposure to preceding stimuli. Carlile et al. (2001) presented listeners with 4 minutes of a broadband noise stimulus presented either at 0° or 30°. After exposure, listeners were asked to localize a target stimulus, which on average, was localized away from the pre-exposed noise source. Moore et al. (2020) found that auditory localization aftereffects do not change the perceptual weighting between ITD and ILD cues. The current study suggests an aftereffect in weighting strategy adjusted due to experience localizing sounds competing noise; where the weighting strategy remains the same even when the environment becomes quiet.

Average SWFs measured in participants with SNHL reveal a similar pattern in perceptual weighting as participants with NH in the presence of the masker. Overall, participants with SNHL continued to rely on the ITD dominance region during localization. This is an exciting advancement in the field as it was unknown if listeners relied on the "right" cues and if using the "wrong" cues was the cause of localization degradation. Interestingly while remaining to rely on the cues normal listeners do, localization performance was poorer than participants with NH. Therefore, the current study affirms the recent work identifying sensitivity to ITD cues for listeners with SNHL. The next step in SWFs would be to measure lateralization SWFs in listeners with SNHL to confirm that it is indeed the ITD cue that is relied upon.

Individual SWFs revealed that some listeners placed a greater relative weight on higher frequency components (> 800 Hz). Correlation measures suggest that this "misuse" of binaural cues across frequency may be due to poor low-frequency thresholds. Visual inspection of individual SWFs and hearing thresholds does indeed reveal this. However, one question from this may be, does localization performance degrade when the ITD dominance region is not relied upon? The current data do not suggest this. In fact, some participants with low weights in the ITD dominance region localized stimuli better than some participants who relied upon the ITD dominance region. However, recall that the localization error measurements in the current study were estimated since frequency components were presented from five adjacent loudspeakers. Future studies may want to separately assess localization performance to confirm that not using the ITD dominance region does not result in poorer localization performance. Also, the most intriguing result of participants relying on high-frequency components is the binaural cues available at these frequencies. Since the stimuli were composed of tones, it is most likely the ILD cue that is available at high frequencies, as suggested by the binaural cue measurements of the

stimuli in quiet. Lateralization SWFs may be able to confirm this. One suggestion is to include listeners with flat SNHLs in the recruitment. As suggested for SWF and TWF measurements in competing noise, it may be beneficial to use accuracy as the dependent variable during SWF measurements.

6.4. Chapter 5: Temporal Weighting for Simulated and Real SNHL

The masker reduced onset dominance in participants with NH compared to the onset dominance that was prevalent in participants with NH in quiet. As assumed to have occurred during SWF measurements, aftereffects of the masker were not apparent in this study. This may be due to differences in adaptation across weighting strategies (time versus frequency). One possibility is that temporal weighting is quicker to adapt than spectral weighting. Future studies aiming to reproduce the aftereffects of SWFs should also consider measuring TWFs.

Average TWFs measured in participants with SNHL reveal a similar pattern in perceptual weighting as participants with NH in quiet but not in the presence of the masker. As for SWFs, this is an exciting advancement of the field, corroborating precedence effect studies. It may then be assumed that listeners with SNHL are not relying on binaural cues corrupted by echoes in reverberant environments. However, some individual-participant SWFs reveal fluctuations within the weighting functions. This suggests that some listeners with SNHL may rely on cues that would be reduced toward zero in reverberant environments. However, for many of these participants, it seems as if the onset is relied upon along with some portions of the ongoing portions of the stimulus. Many listeners also placed similar weight on the first two components. The integration of binaural temporal information seems to be enhanced in these participants. It

may be beneficial to understand if these fluctuations in TWFs are dependent on monaural envelope temporal integration.

Visual inspection of the data suggests that fluctuations may be the cause of increased localization errors. A meaningful identification of these fluctuations would be necessary to 1) address if fluctuations in TWFs result in a decrease in localization performance and 2) determine if fluctuations are dependent on hearing thresholds. However, as mentioned earlier, it is unclear if degradation in localization performance leads to variability in weighting function shapes. Again, the suggestion is to measure TWFs with accuracy as the dependent variable. This is a crucial next step before weighting function measurements are made in listeners with SNHL with the use of hearing aids, as hearing aids have been demonstrated to further decrease the localization performance of listeners with SNHL (Van den Bogaert et al., 2006).

6.5. Conclusion

When listeners with NH localize a sound in azimuth, they rely primarily on the binaural cues provided by a small portion of the spectrotemporal components of a complex signal. Across frequency, listeners rely upon cues within the ITD dominance region (400-1000 Hz) which peaks near 800 Hz.

If the signal is degraded in the presence of competing noise, listeners with NH continue to rely upon cues within the ITD dominance region. However, the peak in the dominance region broadens to encompass both 400 and 800 Hz. The same is true when listeners are in the presence of a threshold elevating noise masker used to simulate SNHL. Listeners with real SNHL also rely upon cues within the ITD dominance region with a broad peak. However, a small set of listeners rely upon cues provided by high frequencies.

Across time, listeners with NH rely upon cues within the onset of the stimulus. In competing noise, listeners no longer rely upon cues within the onset and may rely upon cues within the ongoing portion of the stimulus. When listeners are in the presence of a threshold elevating noise masker, they no longer rely upon cues provided by the onset. However, unlike listeners with simulated SNHL, listeners with real SNHL rely upon cues provided by the onset (similar to listeners with NH). Some listeners with SNHL may rely upon cues within the ongoing portion of the stimulus as well as the onset.

REFERENCES

Abel, S. M., and Hay, V. H. (**1996**). "Sound Localization the Interaction of Aging, Hearing Loss and Hearing Protection," Scand. Aud., **25**, 3–12. doi:10.3109/01050399609047549

Akeroyd, M. A., and Guy, F. H. (**2011**). "The effect of hearing impairment on localization dominance for single-word stimuli," J. Acoust. Soc. Am., **130**, 312–323. doi:10.1121/1.3598466

Baltzell, L. S., Cho, A. Y., Swaminathan, J., and Best, V. (**2020**). "Spectro-temporal weighting of interaural time differences in speech," J. Acoust. Soc. Am., **147**, 3883–3894. doi:10.1121/10.0001418

Bremen, P., and Middlebrooks, J. C. (**2013**). "Weighting of Spatial and Spectro-Temporal Cues for Auditory Scene Analysis by Human Listeners," (M. S. Malmierca, Ed.) PLoS ONE, **8**, e59815. doi:10.1371/journal.pone.0059815

Brown, A. D., and Stecker, G. C. (**2010**). "Temporal weighting of interaural time and level differences in high-rate click trains," J. Acoust. Soc. Am., **128**, 332–341. doi:10.1121/1.3436540

Brungart, D. S., and Simpson, B. D. (**2009**). "Effects of bandwidth on auditory localization with a noise masker," J. Acoust. Soc. Am., **126**, 3199–3208. doi:10.1121/1.3243309

Carlile, S., Hyams, S., and Delaney, S. (**2001**). "Systematic distortions of auditory space perception following prolonged exposure to broadband noise," J. Acoust. Soc. Am., **110**, 416–424. doi:10.1121/1.1375843

Folkerts, M.L., and Stecker, G. C. (**2022**). "Spectral weighting functions for lateralization and localization of complex," J. Acoust. Soc. Am., **151**, 3409–3425. doi:10.1121/10.00011469

Lorenzi, C., Gatehouse, S., and Lever, C. (**1999**). "Sound localization in noise in normal-hearing listeners," J. Acoust. Soc. Am., **105**, 1810–1820.

Moore, T. M., Picou, E. M., Hornsby, B. W. Y., Gallun, F. J., and Stecker, G. C. (2020). "Binaural spatial adaptation as a mechanism for asymmetric trading of interaural time and level differences," J. Acoust. Soc. Am., 148, 526–541. doi:10.1121/10.0001622

Noble, W., and Gatehouse, S. (**2004**). "Interaural asymmetry of hearing loss, Speech, Spatial and Qualities of Hearing Scale (SSQ) disabilities, and handicap," Intern. J. of Aud., **43**, 100–114. doi:10.1080/14992020400050015

Rakerd, B., and Hartmann, W. M. (**2010**). "Localization of sound in rooms. V. Binaural coherence and human sensitivity to interaural time differences in noise," J. Acoust. Soc. Am., **128**, 3052–3063. doi:10.1121/1.3493447

Stecker, G. C., and Moore, T. M. (**2018**). "Reverberation enhances onset dominance in sound localization," J. Acoust. Soc. Am., **143**, 786–793. doi:10.1121/1.5023221

Van den Bogaert, T., Klasen, T. J., Moonen, M., Van Deun, L., and Wouters, J. (**2006**). "Horizontal localization with bilateral hearing aids: Without is better than with," J. Acoust. Soc. Am., **119**, 515–526. doi:10.1121/1.2139653